Dissertation

submitted to the

Combined Faculties for the Natural Sciences and for Mathematics

of the Ruperto-Carola University of Heidelberg, Germany

for the degree of

Doctor of Natural Sciences

presented by

Linhan Zhuang (M.Med.)

born in Wenzhou, China

Oral examination: 17.02.2020

Regulation of tumor suppressor p53 under hypoxia in human papillomavirus type 16 (HPV16)-positive cervical cancer cells

Referees:

PD Dr. Karin Müller-Decker

Prof. Dr. Frank Rösl

Eidesstattliche Erklärung

Ich erkläre hiermit, dass ich die vorliegende Dissertation selbst verfasst und mich keiner anderen als der von mir ausdrücklich bezeichneten Quellen und Hilfsmittel bedient habe. Diese Dissertation wurde in dieser oder anderer Form weder bereits als Prüfungsarbeit verwendet, noch einer anderen Fakultät als Dissertation vorgelegt. An keiner anderen Stelle ist ein Prüfungsverfahren beantragt.

Heidelberg, den 04.12.2019

Linhan Zhuang

Table of Contents

Summary

The tumor suppressor p53 primarily functions as a transcription factor responding to a myriad of cellular stresses. It is a pivotal and pleiotropic regulator in the stress-induced cellular response networks. Diverse activities of p53 are important not only in DNA repair, induction of cell cycle arrest and apoptosis, but also in senescence, autophagy and metabolism. In cells infected with human papillomaviruses (HPVs), the viral oncoproteins E6 and E7 target the tumor suppressors p53 and pRb, respectively, for degradation and inactivation. HPV E6 and E7 synergistically act to promote uncontrolled cell divisions and inhibit apoptosis. Persistent infections with high-risk HPVs are closely linked to cervical cancer as well as other malignancies in the anogenital and oropharyngeal region. Our previous lab results found that HPV *E6/E7* oncogenes are repressed under hypoxia, a condition that is frequently detected in solid tumors. Unlike the reactivation of pRb, p53 protein levels did not increase in *E6/E7*-repressed hypoxic HPV16-positive cancer cells, but even decreased further. The present study aimed to delineate the dynamics of p53 under hypoxic conditions as well as the mechanisms underlying this regulation and elucidate the role of p53 regulation for downstream responses and cellular outcomes/fates in hypoxic HPV16-positive cancer cells. It was revealed that despite a continuous repression of *E6/E7* oncogenes, p53 did not immediately recover, but instead showed a biphasic regulation (rapid and strong depletion, then marked recovery). The initial hypoxic reduction of p53 was predominantly mediated via a lysosome-dependent mechanism. The biphasic regulation of p53 appears to serve as a survival and protective strategy of hypoxic HPV16-positive cancer cells under stress conditions. The modulation on p53 downstream target genes that coincides with p53 protein dynamics may contribute to enhance cellular adaptation to hypoxia. p53 target genes associated with terminal fates such as cell death (apoptosis) and permanent cell cycle arrest (senescence) are inactivated through p53 depletion by hypoxia, protecting cells from committing to an irreversible fate. After prolonged hypoxia, the restored p53 might be required by HPV16-positive cancer cells to maintain cellular homeostasis and select cells resistant to cell death by induction of apoptotic genes. Hypoxia-associated initial reduction of p53 facilitates the induction of autophagy, which is critical for the evasion of senescence by hypoxic HPV16-positive cancer cells. Collectively, these findings reveal a new regulation pattern of p53 by hypoxia and provide new insights into the role of p53 regulation in downstream responses and cellular adaptation to hypoxia in HPV16-positive cancer cells. This study further has implications for the development of new treatment strategies.

Zusammenfassung

Der Tumorsuppressor p53 fungiert hauptsächlich als Transkriptionsfaktor, der auf zahlreiche zelluläre Belastungen reagiert. Er ist ein zentraler und pleiotroper Regulator in stressinduzierten zellulären Antwortnetzwerken. Die verschiedenen Aktivitäten von p53 sind nicht nur für die DNA-Reparatur, die Induktion des Zellzyklusstillstands und die Apoptose wichtig, sondern auch für die Seneszenz, die Autophagie und den Metabolismus. In mit humanen Papillomviren (HPVs) infizierten Zellen vermitteln die viralen Onkoproteine E6 und E7 den Abbau bzw. die Inaktivierung der Tumorsuppressoren p53 und pRb. HPV E6 und E7 fördern synergistisch die unkontrollierte Zellteilung und hemmen gleichzeitig die Apoptose. Anhaltende Infektionen mit Hochrisiko-HPVs stehen in engem Zusammenhang mit Gebärmutterhalskrebs sowie anderen bösartigen Erkrankungen im Anogenital- und Hals-/Rachenbereich. Unsere früheren Laborergebnisse zeigten, dass HPV-*E6/E7*-Onkogene unter Hypoxie, einem Zustand, der häufig bei soliden Tumoren festgestellt wird, unterdrückt werden. Anders als bei der Reaktivierung von pRb stiegen die p53-Proteinspiegel in *E6/E7*-reprimierten hypoxischen HPV16-positiven Krebszellen nicht an, sondern sanken sogar weiter. Die vorliegende Studie zielte darauf ab, die Dynamik von p53 unter hypoxischen Bedingungen sowie die dieser Regulation zugrundeliegenden Mechanismen zu beschreiben und die Rolle der p53-Regulation für Downstream-Reaktionen und zelluläre Schicksale in hypoxischen HPV16-positiven Krebszellen zu klären. Es wurde gezeigt, dass sich p53 trotz kontinuierlicher Repression von *E6/E7*-Onkogenen nicht sofort erholte, sondern eine biphasische Regulation (schnelle und starke Reduktion, dann deutlicher Anstieg) stattfand. Die anfängliche hypoxische Reduktion von p53 wurde überwiegend über einen lysosomenabhängigen Mechanismus vermittelt. Die biphasische Regulation von p53 dient vermutlich als Überlebens- und Schutzstrategie für hypoxische HPV16-positive Krebszellen unter Stressbedingungen. Die Modulation von p53-Zielgenen, die mit der Dynamik von p53-Proteinleveln übereinstimmt, kann dazu beitragen, die zelluläre Anpassung an Hypoxie zu verbessern. p53-Zielgene, die mit terminalen Schicksalen wie Zelltod (Apoptose) und permanentem Zellzyklusstillstand (Seneszenz) assoziiert sind, werden durch p53-Depletion durch Hypoxie inaktiviert und schützen die Zellen vor einem irreversiblen Schicksal. Nach längerer Hypoxie könnte das wiederhergestellte p53 von HPV16-positiven Krebszellen verwendet werden, um die zelluläre Homöostase aufrechtzuerhalten und Zellen auszuwählen, die gegen Zelltod durch Induktion apoptotischer Gene resistent sind. Die Hypoxie-assoziierte anfängliche Reduktion von p53 erleichtert die Induktion der Autophagie, die für die Umgehung der Seneszenz durch

hypoxische HPV16-positive Krebszellen von entscheidender Bedeutung ist. Zusammengenommen offenbaren diese Ergebnisse ein neues Regulationsmuster von p53 durch Hypoxie und liefern neue Erkenntnisse über die Rolle der p53-Regulation bei Downstream-Reaktionen und der zellulären Anpassung an Hypoxie in HPV16-positiven Krebszellen. Diese Studie hat weiterhin Auswirkungen auf die Entwicklung neuer Behandlungsstrategien.

1. Introduction

1.1 Infection and Cancer

1.1.1 Cancer statistics 2018

Cancer is a major global health burden, with approximately 18.1 million new cases and an estimated 9.6 million cancer deaths in 2018 worldwide (**Figure 1.1)** (source: Globocan 2018) [2]. Of these, 9,456,418 cases (52.31%) were male and 8,622,539 (47.79%) were female. Globally, about 1 in 6 deaths is due to cancer, making it the second leading cause of death following cardiovascular diseases. The most commonly diagnosed cancer worldwide was lung cancer (11.58% of the total cases), followed by female breast cancer (11.55%), colorectal cancer (10.23%), and prostate cancer (7.06%) (**Figure 1.1**). In 2018, lung cancer was responsible for most deaths (18.43% of the total cancer deaths). The second on the list of cancer mortality was colorectal cancer (9.22%). Stomach cancer was the number three cause of cancer death (8.19%), closely followed by liver cancer (8.18%) (**Figure 1.1**).
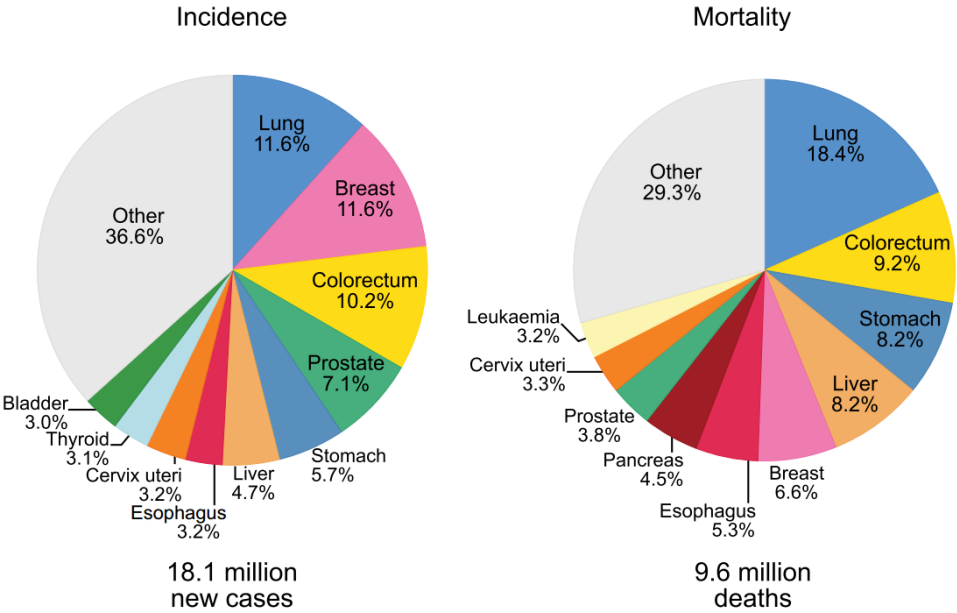
Figure 1.1 | Distribution of new cases and deaths for the 10 most common cancers in 2018 for both sexes. The area of the pie chart reflects the proportion of the total number of cases or deaths; non-melanoma skin cancers are included in the "other" category. Figure adapted from [2].

Among women, breast cancer was the number one diagnosed cancer (2,088,849 cases) and the leading cause of cancer death (626,679 deaths), followed by colorectal cancer (823,303 cases), lung cancer (725,352 cases) for incidence, and lung cancer (576,060 deaths) and colorectal cancer (396,568 deaths) for mortality; cervical cancer ranks fourth for both incidence (569,847 cases) and mortality (311,365 deaths) (**Figure 1.2A**) [2]. Among men, lung cancer was the most frequent

cancer (1,368,524 cases) and the leading cause of cancer death (1,184,847 deaths), followed by prostate cancer (1,276,106 cases) and colorectal cancer (1,026,215 cases) (for incidence) and liver cancer (548,375 deaths) and stomach cancer (513,555 deaths) (for mortality) (**Figure 1.2B**) [2].
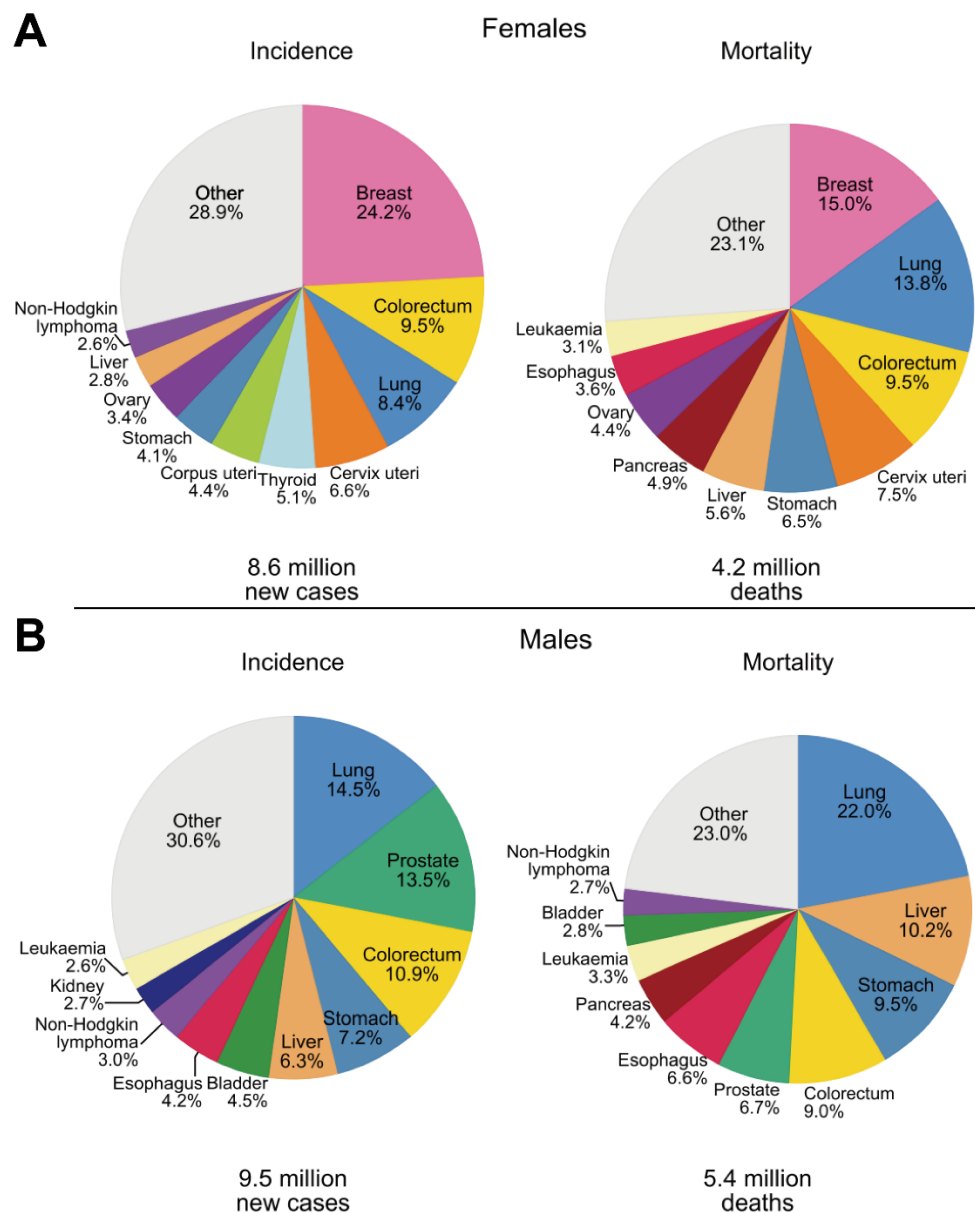
Figure 1.2 | Distribution of new cases and deaths for the 10 most common cancers in 2018 for (A) Females and (B) Males. For each sex, the area of the pie chart reflects the proportion of the total number of cases or deaths; non-melanoma skin cancers are included in the "other" category. Figure adapted and modified from [2].

1.1.2 Cancer risk factors

Cancer originates from the transformation of normal cells into tumor cells in a multi-step process that generally progresses from a pre-cancerous lesion to a malignant tumor. Accumulation of genome mutations over a period of time results in uncontrolled and rapid growth of abnormal cells leading to malignant transformation. These mutations can arise spontaneously and are

favored by external risk factors, including: 1) physical carcinogens, such as ultraviolet (UV) and ionizing radiation; 2) chemical carcinogens, such as asbestos, components of tobacco smoke, aflatoxin (a food contaminant); and 3) biological carcinogens, such as infections with certain viruses, bacteria, or parasites [3, 4]. The major human cancer risk factors therefore are tobacco use, alcohol abuse, occupational exposures, environmental contamination, and infectious agents. An estimated 15% (2,100,000 cases) of cancers diagnosed in 2012 were attributed to infections, including *Helicobacter pylori*, Human papillomavirus (HPV), Hepatitis B virus, Hepatitis C virus, and Epstein-Barr virus (**Figure 1.3**) [1].
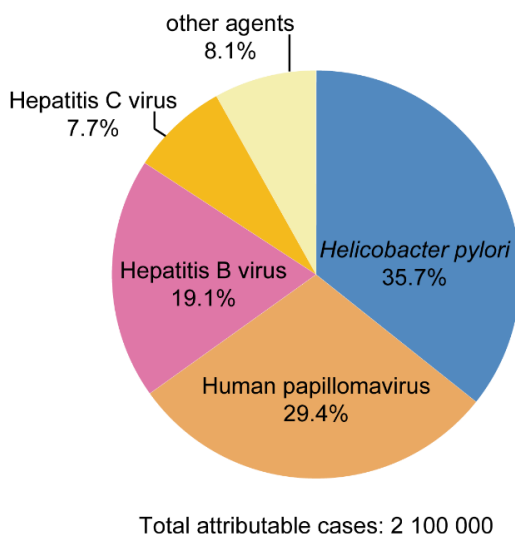
Figure 1.3 | **Cancer cases attributable to infections among both sexes worldwide in 2012.** Shown by infectious agents. Data source: [1]. Figure inspired by http://gco.iarc.fr

Approximately 70% of cancer deaths occur in low- and middle-income countries where some chronic infections have major relevance. Cancer causing infections, such as Hepatitis B/C virus and HPV, were responsible for up to 25% of cancer cases in these countries in 2012 [1].

1.1.3 Human Papillomaviruses (HPVs)

HPV infection-associated cancers were responsible for approximately 54% of cancers attributable to infections among women worldwide in 2012 (**Figure 1.4**) [1]. It has previously been reported that in 99% of cervical cancers, HPV genomes can be detected, up to 70% of which belong either to the HPV types HPV16 or HPV18 [5, 6].
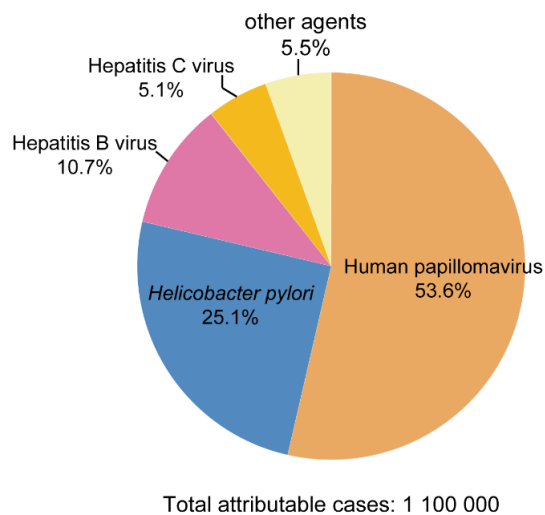
Figure 1.4 | Cancer cases attributable to infections among females worldwide in 2012. Shown by infectious agents. Data source: [1]. Figure inspired by http://gco.iarc.fr

Papillomaviruses (PVs) are a diverse group of small non-enveloped viruses with a double stranded circular DNA genome [7]. PVs infect a range of different species including reptiles, birds, marsupials, and mammals, displaying a tropism for mucosal and cutaneous epithelia [8]. Up to date more than 300 different PV types were identified including 210 human papillomaviruses (HPVs) as well as 170 animal papillomaviruses (PaVE: Papillomavirus Episteme) [9].

Based on nucleotide sequence comparison (at least 10% difference), the 210 HPV types are phylogenetically divided into five different genera, which are denominated with Greek letters: alpha-, beta-, gamma-, mu- and nu-types [10, 11]. Additionally, HPVs are often referred to as cutaneous types or mucosal types. The cutaneous HPVs exclusively infect cells of the skin, causing benign papillomas, of which most manifestations are common plantar and flat warts [12]. The mucosal HPVs infect mucosal cells, responsible for benign warts or malignancies in penis, vagina, vulva, anus, cervix and head and neck. Most cervical cancers are caused by genital HPV types of the alpha-genus [6]. According to clinical pathologies, the alpha HPV types are further classified into "low-risk" cutaneous types, "low-risk" mucosal types, and "high-risk" types. The "low-risk" cutaneous types (e.g. HPV 3, HPV 10 and HPV61 etc.) and "low-risk" mucosal types (e.g. HPV 6, HPV11 and HPV 13 etc.) cause benign warts or no apparent cellular transformation [13]. The "high-risk" types (e.g. HPV 16, HPV 18 and HPV 45) with oncogenic potential are etiologically confirmed as "human carcinogens". On the basis of epidemiological data, HPV 16, 18, 31, 33, 35, 39, 45, 51, 52, 56, 58 59, 69, 73 and 82 are responsible for 99.7% of cervical cancers and therefore are referred to as "oncogenic types" by the World Health Organization (WHO) [14].

1.1.3.1 Genomic organization of HPVs

The double stranded circular DNA genome of PVs ranges from 6953 base pairs (bp) [*Chelonia mydas* papillomavirus type 1 (CmPV1)] to 8607 bp [Canine papillomavirus type 1 (CPV1)] in

length [15]. The genomes are functionally divided into three parts: the upstream regulatory region (URR), the early region and the late region (**Figure 1.5**). Although the URR does not contain protein coding sequences, it harbors the viral origin of replication and several early promoter and enhancer motifs that contain binding sites for both viral and host transcription factors [16].
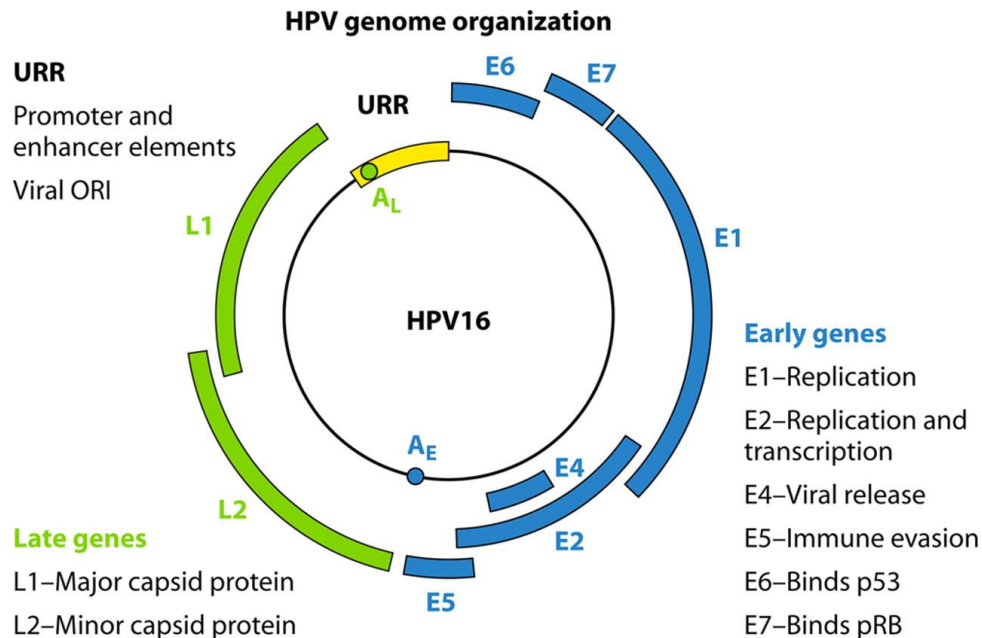
Figure 1.5 | Genomic organization of the mucosal high-risk HPV16. Viral gene expression is under the control of the upstream regulatory region (URR, yellow). The location and functions of early (blue) and late genes (green) are shown. A_L: polyadenylation (late); A_E: polyadenylation (early). ORI: origin of replication. Figure adapted from [16].

The early region contains an early promoter (p97 in HPV16 and p105 in HPV18) and encodes five to six early viral genes (*E1*, *E2*, *E4*, *E5*, *E6* and *E7*) that are transcribed as polycistronic mRNAs [17]. The cutaneous HPV types typically lack the E5 gene [18]. The proteins encoded by these early genes play a role in viral replication and transcription (E1, E2 and E4) or are essential for transformation of host cells (E5, E6 and E7). The early region also contains the late promoter (p670 in HPV16 and p765 or p811 or p829 in HPV18) within the *E7* open reading frame (ORF), which is active at final stages of the virus life cycle. It is required for the gene expression of the viral capsid proteins L1 and L2, which are encoded in the late region of all HPV genomes [17, 19].

1.1.3.2 HPV life cycle

The life cycle of HPVs is coupled to the differentiation process of the infected keratinocyte, presenting in a distinct spatial and temporal pattern [16] (**Figure 1.6**). The HPV infection initially occurs in keratinocytes in the basal layer of the epithelium via skin abrasion or micro-wounds, which can arise during scarification or sexual intercourse [20]. The entry of virus into the host cells mainly depends on the attachment of the C-terminus of the L1 protein to heparan sulfate

proteoglycans (HSPGs) and laminin on the cell surface [20, 21]. After the internalization of the virus, an uncoating process takes place in the endosome. L1 proteins are degraded during the lysosomal transport of the viral particle into the nucleus whereas the viral L2/DNA complexes enter the host cell nucleus [22, 23].

In basal layers of infected epithelia, the viral genomes are established in the nucleus as low-copy episomes (20-100 per cell). Low levels of the early genes *E1* and *E2* and the other early genes *E6* and *E7* are expressed. E1 and E2 are required for the genome replication of the virus, which takes place along with the host cell DNA replication. Since the viral DNA does not encode proteins required for DNA synthesis, it uses the host cell replication machinery [6]. The E7 protein binds to the family of retinoblastoma-associated protein (pRb) proteins leading to their dissociation from transcription factors that control the host cell cycle. This leads to the continuous synthesis of the viral as well as host DNA [24] upon which the host cell activates the tumor suppressor p53, which usually induces apoptosis. However, the E6 protein targets p53 for proteasomal degradation and hence, the HPV-infected cells do not undergo apoptosis [25, 26]. E6 also increases telomerase activity promoting immoderate cell divisions [27]. HPV E6 and E7 thus synergistically act to sustain continuous proliferation of the host cells and in turn viral DNA replication. The expression of *E6* and *E7* genes upon high-risk HPV infections is associated with the immortalization and transformation of cells, which are therefore called viral oncogenes.
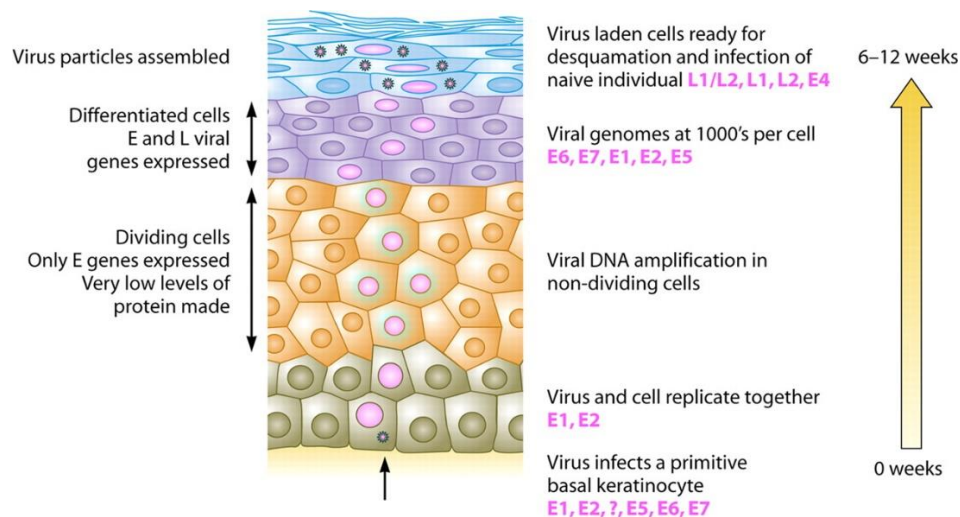
Figure 1.6 | Life cycle of HPV in infected epithelial tissue. The virus infects the basal layer of epithelia via micro-wounds. E1 and E2 proteins mediate the replication of the viral genome coinciding with the host cell division. *E6* and *E7* are expressed in the suprabasal layer, where they promote re-entry of the infected keratinocytes into the S-phase of the cell cycle and simultaneously inhibit apoptosis. Amplification of the viral genome takes place in the granular region of the epithelium resulting from the concerted action of E1, E2, E4 and E5. Finally, expression of the late genes *L1* and *L2* in the top layer results in the assembly of infectious particles which are then released from dead keratinocytes through a desquamation process. Figure adapted from [16].

A shift in the viral gene expression profile takes place with progressing differentiation of infected keratinocytes. With the concerted action of E1, E2, E4 and E5, the viral genome is dramatically amplified resulting in thousands of viral copies per cell. In the granular layer, the late viral promoter is activated. Here, the late genes L1 and L2 are expressed and the assembly of virus particles takes place. The capsid of every virus particle is usually formed by 360 L1 protein subunits that are organized into 72 pentameric capsomeres as well as a variable number of L2 protein subunits [28]. Furthermore, L2 (together with E2) is required to ensure the successful DNA packaging and capsid assembly [29]. Finally, the newly formed viral particles are passively shed from the cornified epithelia. Viral DNA can also persist in non-dividing keratinocytes of the basal epithelial layer for long periods of time, resulting in a dormant infection that can be re-activated, e.g. due to hormonal changes in the host [30].

1.1.3.3 HPV-induced carcinogenesis

HPV infections are ubiquitous in the majority of sexually active people (>80%). In general, HPV infections can be potentially cleared by the host's immune system. However, in some cases high-risk HPVs can modulate the immune response of host cells facilitating immune evasion, after which HPVs persist for longer time spans (from several months up to years) [31]. During this time, the expression of *E6* and *E7* in chronically infected cells leads to an accumulation of gene mutations due to numerous uncontrolled cell divisions, as well as chromosomal instability and inhibition of apoptosis. Continuous and repeated infection with HPVs therefore leads to the development of neoplastic lesions [6]. At the uterine cervix, these lesions are referred to as cervical intraepithelial neoplasia (CIN). Classifications have been established to stage cervical lesions based on their risk of developing into invasive carcinoma, such as the histological staging from mild to severe dysplasia classified as CIN 1 to 3. HPV-induced premalignant cervical intraepithelial lesions (CIN 1) can progress into high-grade intraepithelial lesions (CIN 2/3) and eventually into invasive cervical carcinoma (CaCx), where the viral genomes are integrated into the host genome [32] (**Figure 1.7**).
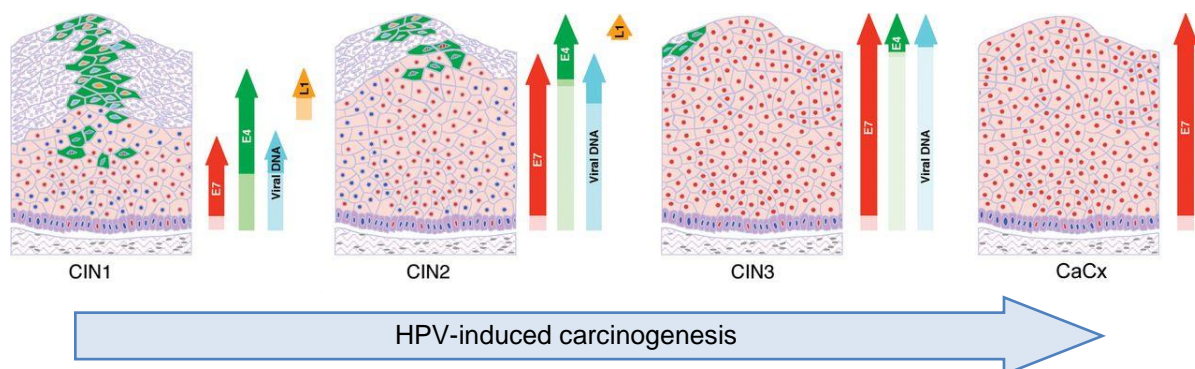
Figure 1.7 | Schematic overview of HPV-induced carcinogenesis. HPV DNA is maintained episomally and the viral life cycle is still completed in cervical intraepithelial neoplasia stages 1 and 2 (CIN 1 and 2). Upon progression into CIN 3 lesions, the early gene expression is deregulated and no progeny virus is produced. Upon further progression into cervical cancer lesions (CaCx), the viral genome is integrated into the host genome after which *E6* and *E7* are predominantly expressed. Figure adapted from [33].

In CIN 1/2 lesions, the viral genome is episomal and the HPV life cycle is still completed [34]. In the majority of cases, these lesions regress spontaneously. However, in cases where the lesions persist, the viral gene expression undergoes a deregulation and no progeny virus is produced any longer. At these stages, i.e. CIN 3, virus DNA begins to integrate into the host genome resulting in the loss of E2, which disrupts its transcriptional control over *E6* and *E7* [35]. After integration, E6 and E7 are exclusively produced throughout all layers of the infected epithelia, increasing cell division rates and the accumulation of mutations. These lesions ultimately progress to carcinomas. Notably, only a minority of high-risk HPV-infected individuals (1%) develop carcinomas during their life-time [36].

With an estimated 569,847 new cases and 311,365 deaths worldwide in 2018, cervical cancer represented the fourth most commonly diagnosed cancer and the fourth leading cause of cancer death in women worldwide (**Figure 1.2A**). Although cervical cancer incidence rates are declining in many high-income countries, incidence and mortality of this disease remain high and are predicted to further increase in low- and middle-income countries where effective screening programs are absent [2, 37-39]. Therefore, development and execution of new strategies for effective treatment and prevention are important and urgent.

1.1.4 Prevention and therapy of cervical cancer

Comprehensive cervical cancer control includes primary prevention (vaccination against HPV), secondary prevention (screening and treatment of pre-cancerous lesions), tertiary prevention (diagnosis and treatment of invasive cervical cancer) and palliative care [40].

Prophylactic vaccination

The most effective protection against diseases can be achieved by preventing their initial establishment. In the case of cervical cancer, this can be accomplished by prophylactic vaccination. There are currently three licensed vaccines protective against HPV. All of them are based on virus-like particles (VLPs) of the HPV major capsid protein L1 and lead to a strong seroconversion with antibody titers much higher than obtained by natural infection [41]. The bivalent Cervarix (GlaxoSmithKline) contains antigens of HPV16 and 18, which are known to cause at least 70% of all cervical cancers. The quadrivalent Gardasil (Merck) protects against two additional HPV types, 6 and 11, which cause roughly 90% of anogenital warts. The nonavalent Gardasil9 (Merck), the most recently developed vaccine, comprises the four HPV types (6, 11, 16 and 18) of the

quadrivalent vaccine and protects against five additional oncogenic HPV types (31, 33, 45, 52, 58), thereby covering a further 20% of HPV infection-associated cervical cancers.

All HPV vaccines are very safe and effective in preventing infections with HPV [42]. However, the vaccines cannot treat established HPV infections or HPV-associated disease. HPV vaccines work best if administered prior to exposure to HPV. Therefore, the WHO recommends that primary prevention begins with HPV vaccination of girls aged between 9 and 13 years, before they become sexually active [40]. Moreover, vaccination is directed against specific HPV types and is therefore not able to prevent 100 percent of HPV-induced cervical cancers. In many countries where HPV vaccines are introduced, screening programs often still need to be developed or strengthened.

Screening for cervical cancer

In many cases of HPV infection, the development of invasive cervical carcinomas can be prevented by screenings that detect the presence of abnormal cervical cells and pre-cancerous lesions. Screening and treatment of pre-cancer lesions in women who are sexually active is a cost-effective way to prevent cervical cancer. There are currently three different recommended types of screening tests, including HPV testing for high-risk HPV types (detection of DNA or RNA), visual inspection with Acetic Acid (VIA), and conventional (Pap smear) test and liquid-based cytology (LBC) [40]. Because pre-cancerous lesions take many years to develop, screening is recommended for women from age 30 and regularly afterwards. When pre-cancerous lesions are detected, these can easily be treated, and cancer development can be avoided. Screening can also detect cancer at an early stage and treatment has a high potential for cure. For treatment of pre-cancer lesions, the use of cryotherapy and Loop Electrosurgical Excision Procedure (LEEP) are recommended [40]. For advanced lesions, women should be referred for further investigations and adequate management.

Treatment of invasive cervical cancer

For invasive cervical cancer, the currently recommended standard treatment consists of surgery frequently combined with radiation therapy or cisplatin-based chemo- and radiation-therapy [40, 43]. Palliative care is also an essential part of cancer management to relieve unnecessary pain and suffering due to the disease.

In addition to preventive vaccines, several researches are focused on the development of therapeutic HPV vaccines. In general, these therapeutic vaccines focus on the HPV *E6* and *E7* oncogenes. Since sustained expression of the viral *E6* and *E7* is considered to be required for

maintaining the malignant phenotype of cervical cancer cells, it is hoped that immune responses against the two oncogenes might eradicate established tumors [44].

In high-income industrialized countries, programs are in place, which enable girls to be vaccinated against HPV and women to get screened regularly. However, in low-income developing countries, there is limited access to these preventive measures and cervical cancer is often not identified until it has further advanced and symptoms develop. In addition, since broad vaccination programs were started earliest in 2006 [42] and it takes decades for an initial infection to progress to cancer [33], cervical cancer will still be a major health burden for many years to come. Furthermore, the resistance of cervical cancer to currently recommended radiation- and chemo-therapy remains a problem [45, 46]. Thus, development of novel and effective therapeutic strategies has a great significance for the control of HPV-associated cancers.

1.2 Tumor hypoxia

The level of tissue oxygenation is an important biological and clinical aspect with a strong impact on the cellular phenotype [47-49]. For carcinomas of the cervix, several studies researched the relationship between intratumoral oxygen partial pressure (pO_2) and cellular behaviors and outcomes [50-52]. Low intratumoral pO_2 is reported to be an important prognostic factor of poor survival in cervical cancer patients [48, 49, 53-55].

Ambient air contains 21% oxygen (O_2), which is usually used as a standard cell culture condition for many *in vitro* studies, hereafter defined as "normoxia". However, O_2 concentrations of most normal healthy mammalian tissues are in the range between 3.5-7% ("physoxia") [47]. In the subregions of tissue with disease, such as acute and chronic vascular disease, pulmonary disease and cancer, the O_2 concentrations are even lower ("hypoxia"). Tissue hypoxia is usually defined as less than 1.5-2% O_2 and severe hypoxia or "anoxia" is defined as less than 0.02% O_2 [56, 57].

Due to the high growth rate of tumor cells and an imbalance in oxygen supply and consumption, solid tumors are heterogeneously oxygenated and often characterized by the presence of regions with O_2 concentrations significantly below the physiological level [49, 56, 58]. Tumor hypoxia is frequently categorized as chronic and acute. Inadequate supply with O_2 in tumor cells can be caused by large distances from blood vessels (more than 70 µm) that do not allow enough diffusion of O_2. This diffusion-limited and prolonged hypoxia is termed chronic hypoxia. A state of chronic hypoxia can also result from anemia or low O_2 levels in the blood (hypoxemia). Intermittent, or

acute hypoxia, is often a result of perfusion-limited O_2 delivery, e.g. due to structural and functional defects of tumor microvasculature [49, 59, 60].

Tumor hypoxia is usually associated with poor prognosis in patients and high resistance to therapy. Hypoxia contributes to malignant progression of tumors since tumor cells extensively adapt to low oxygen conditions by adjusting the signaling pathways that control proliferation, cell death, angiogenesis, local invasion, and metastatic spread. These cellular adaptations to hypoxia permit tumor cells to survive and even finally escape a hostile, growth inhibitory environment [61]. Hypoxia-induced proteomic and genomic changes promote tumor resistance. Conversely, the selection and clonal expansion of these favourably altered cells further aggravate tumor hypoxia and support a vicious circle of increasing hypoxia and malignant progression while concurrently promoting the development of a more treatment-resistant disease [61]. The alterations in gene expression are mainly regulated by hypoxia-inducible factors (HIFs, see chapter 1.2.1).

An important aspect of hypoxia-mediated resistance to therapy is the radioprotective effect of hypoxia. Ionizing radiation (IR) produces free radicals, for example in DNA that can react with oxygen to generate fixed peroxy radicals. Multiple types of DNA damage, including DNA double- and single-strand breaks (DNA DSBs/SSBs), DNA base damage and DNA-DNA and DNA-protein crosslinks caused by IR results in cancer cell death leading to the desired therapeutic effect [62, 63]. However, if oxygen is missing during radiation, the produced radicals can be reduced to their original composition. In addition to radiation therapy, hypoxic tumor cells are also more resistant to many chemotherapeutic or other anticancer drugs. This is partly caused by insufficient drug penetration through the hypoxic tumor tissue due to defects of tumor vascularization [64, 65]. Additionally, chemotherapeutics frequently target highly proliferative cells and hypoxic tumor cells commonly display lower proliferation rates than non-hypoxic tumor cells. Moreover, the before-mentioned clonal selection of malignant cells that frequently down-regulate apoptosis pathways, contributes to hypoxia-induced resistance to therapy [66].

Furthermore, hypoxia leads to immune evasion of tumor cells by activating immunosuppressive pathways and by repressing the activity of immunocompetent cells. Therefore, hypoxia is also a major obstacle for immunotherapies [67].

Consequently, in recent years there are studies developing anticancer agents that are effective under hypoxia such as hypoxia-activated prodrugs (HAPs) that are activated at hypoxic conditions or small molecule inhibitors directly targeting essential hypoxia-triggered molecular events, such as the induction of HIFs [68-70].

1.2.1 Hypoxia-inducible factors (HIFs)

A variety of biological responses are triggered in cells suffering from hypoxic conditions, including activation of signaling pathways that regulate angiogenesis, cell proliferation and cell death. Hypoxia inducible factors (HIFs), especially HIF-1, are considered master orchestrators of the cellular adaptation to hypoxia [70, 71]. HIFs are a family of heterodimeric basic helix-loop-helix (bHLH) transcription factors composed of two subunits, HIF-α and HIF-β. The beta subunit, including HIF-1β [also termed ARNT (aryl hydrocarbon receptor nuclear translocator)], is constitutively expressed. The alpha subunit of HIFs exists in three different forms (HIF-1α, HIF-2α and HIF-3α) encoded by distinct gene loci and are oxygen-labile proteins.

HIF-α can be up-regulated at the protein level via activation of the phosphatidylinositol 3-kinase (PI3K) and Erk mitogen-activated protein kinase (MAPK) pathways (**Figure 1.8**) or at the mRNA level via STAT3 and nuclear factor-κB (NF-κB) signaling [72, 73]. HIF-1α and HIF-2α share 80% of sequence homology, contain similar structural domains, and are regulated in a similar manner. However, HIF-1α is ubiquitously expressed, whereas HIF-2α occurs in specific cell types [74]. HIF-1α and HIF-2α have two oxygen-dependent degradation domains (ODD domains) located in the center of the protein that are important for the proteolytic regulation under normoxia. These domains are absent in the HIF-1β protein. HIF-3α has a different structural organization. Several variants of HIF-3α are generated by alternative splicing of mRNA or use of different transcription start sites. Studies about HIF-3α are limited, but there are indications for diverging functions of HIF-3α variants in the regulation of the activity of other HIFs [75-78].

The functionality of HIFs depends on post-translational modifications (PTMs) of the HIF-α subunits. In well-oxygenated cells (**Figure 1.8,** *Normoxia*), HIF-α subunits (for example HIF-1α) are hydroxylated on proline residues by prolyl-4-hydroxylases (PHDs), whose activity is dependent on the substrates oxygen, 2-oxoglutarate (2-OG, a Krebs cycle intermediate) and on the cofactor Fe^{2+}. Proline hydroxylations proceed in combination with acetylation by the ARD1 acyltransferase in HIF-α. These structural changes on HIF-α allow the binding to the von Hippel–Lindau protein (pVHL) which functions as an E3 ubiquitin ligase targeting HIF-α for proteasomal degradation [79, 80]. In addition, HIF-α undergoes asparaginyl hydroxylation (at the end of the C-terminus of HIF-1α and HIF-2α) by factor inhibiting HIF (FIH) under non-hypoxic conditions, which prevents binding of HIF-α to co-activators such as p300 and its paralogue CREB-binding protein (CBP) [81-83]. Under hypoxia (**Figure 1.8,** *Hypoxia*), PHD and FIH activity is substrate-limited (lacking O_2), resulting in rapid HIF-α stabilization, accumulation, nuclear translocation

and dimerization with the stably expressed HIF-1β. The HIF-1 heterodimer then binds to DNA motifs termed hypoxia-response elements (HREs) with the consensus sequence G/ACGTG within the promoter of target genes. With the help of cofactors like p300/CBP and DNA polymerase II, HIF-1 regulates the expression of its target genes under hypoxia.

Several interactions between HIF-α and its partner proteins are also required for its activation. The conformational changes induced by the chaperone protein HSP90 promote the binding of HIF-α to HIF-1β, and the further dimerization. Inhibition of HSP90 leads to ubiquitination of HIF-α and its subsequent proteasomal degradation [84, 85]. The formation of a ternary complex between HIF-1α, the mouse double minute 2 homolog (MDM2) and the tumor suppressor p53 induces the ubiquitination of HIF-1α and its destruction by the proteasome [86, 87].
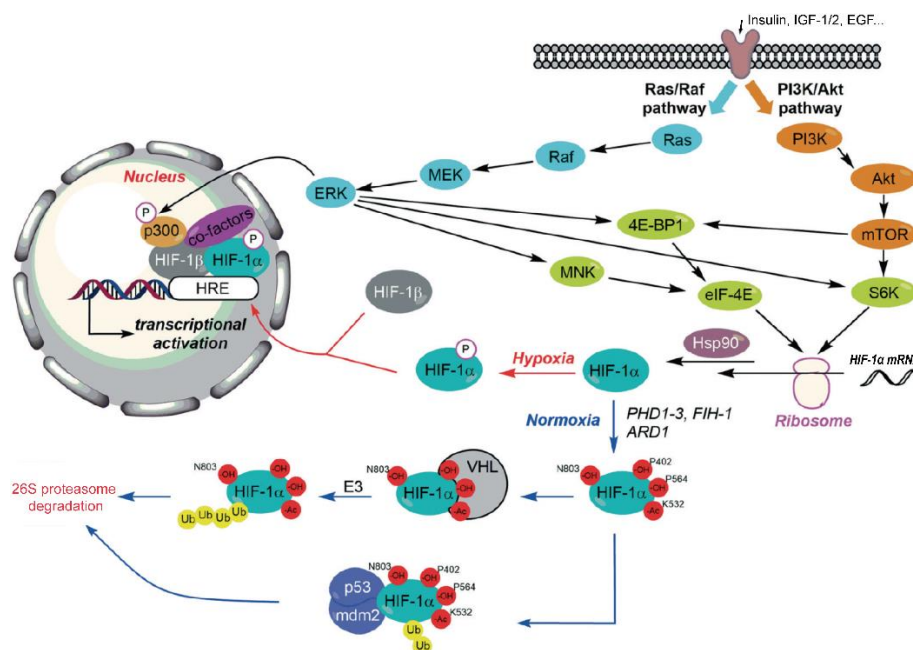
Figure 1.8 | Schematic overview of the regulation of HIF-1. HIF-α protein synthesis is regulated by two main signaling pathways: PI3K/Akt and Erk MAPK, activated by growth factors and cytokines. In non-hypoxic tissues, proline hydroxylations lead to HIF-α degradation by the proteasome or to the inhibition of recruitment of its coactivators. Under hypoxia, HIF-α is stabilized and translocalizes into the nucleus where it binds to HIF-1β and regulates gene expression. Figure adapted from [80].

In human cancers, HIF-α is overexpressed as a result of intratumoral hypoxia as well as genetic alterations, such as gain-of-function mutations in oncogenes (for example ERBB2 and SRC) and loss-of-function mutations in tumor-suppressor genes (for example p53, pVHL and PTEN) [70]. HIF-1 activates the transcription of a wide range of genes involved in angiogenesis (*VEGF*, *ANGPT2*), erythropoiesis (*EPO*), oxygen sensing (*PHD2*, *PHD3*), cell proliferation/survival (*CTGF*, *REDD1*), metabolism (*SLC2A1*, glycolytic genes and *LDHA*), autophagy (*BNIP3*, *BNIP3L*), EMT/migration/invasion (*ZEB1* and *2*, *TWIST1*, *MMP9*) and immune evasion (*CD39*, *CD47*), among others [70].

1.2.2 Metabolic alteration in cancer cells

One feature of tumor cells is an altered metabolism that is significantly different from normal cells. Normal cells use glycolysis to generate approximately 10% of the cells' ATP (adenosine triphosphate), whereas the other 90% of ATP is primarily produced from mitochondrial oxidative phosphorylation (OXPHOS). In tumor cells however, more than 50% of ATP is generated by a high rate of glycolysis followed by lactic acid fermentation and the remaining ATP is produced in mitochondria (Warburg effect) [88]. Moreover, tumor cells tend to use glycolysis for synthesising ATP even in aerobic conditions (in the presence of sufficient O_2), which is called aerobic glycolysis [89]. The Warburg effect is associated with glucose uptake and utilization [90, 91]. Aerobic glycolysis produces 2 molecules of ATP per molecule glucose substrate, whereas the OXPHOS produces 38 molecules of ATP per molecule glucose. Therefore, tumor cells require a far higher intake of glucose through glucose transporters during glycolysis to produce sufficient ATP [92, 93]. Aerobic glycolysis is less efficient than OXPHOS in terms of ATP production, but leads to the increased generation of several additional metabolites that are precursors of the synthesis of lipids, amino acids and nucleotides. All of these macromolecules are essential for highly proliferating cancer cells, since they need to double their biomass for each cell division [89].

Under hypoxic conditions, cells are even more dependent on glycolysis and inhibit mitochondrial respiration to reduce the amount of O_2 molecules that are consumed. HIFs, particularly HIF-1 [94], play an important role in glucose metabolism of tumors by stimulating glycolysis by transactivating genes encoding glucose transporters like Glut1 (also known as SLC2A1) and Glut3 used in extracellular glucose uptake [95]. HIF-1 can also induce the expression of genes responsible for glycolytic breakdown of intracellular glucose like phosphofructokinase (PFK) and aldolase [96]. Moreover, HIF-1 down-regulates OXPHOS in mitochondria by transactivating pyruvate dehydrogenase kinase (PDK) [97].

Apart from regulation of glucose metabolism, hypoxic cells carry out cellular alterations concerning glutamine metabolism, fatty acid metabolism and maintenance of adequate redox balance to cope with the demanding nature of oxygen deprivation [98].

1.2.3 Hypoxia-induced autophagy

As an energy- and nutrient-limited condition, hypoxia can affect neoplastic cells in one of two ways, either by acting as a stressor that diminishes growth (slowing of proliferation) or leads to cell death (apoptosis, or necrosis) or by serving as a selective factor that finally results in malignant

progression and increased resistance to radiation therapy and other cancer treatments [49, 58, 61, 99]. Autophagy is a self-destructive process by which eukaryotic cells degrade and recycle cellular macromolecules and organelles, and is frequently induced under hypoxic conditions [100-107]. For tumor cells, autophagy is a double-edged sword on cell fates [108, 109]: i) Cancer cells suffering limited nutrient supplies under cellular stresses can utilize autophagy to break down and recycle unnecessary or dysfunctional cellular components for survival; such improved autophagic capabilities will actually benefit the cancer cells [110-115]. ii) Cells that undergo an extreme amount of stress experience cell death either through necrosis or through apoptosis. Prolonged and excessive autophagy activation leads to a high turnover rate of proteins and organelles. A rate above the survival threshold will kill cancer cells [116, 117]. Hypoxia-induced autophagy can either promote cell survival or cell death, further linked to hypoxia tolerance in tumors [102, 118].

1.2.3.1 The autophagy signaling pathway

Autophagy is a natural mechanism of the cell that allows the orderly degradation and recycling of cellular components [119-121]. Three forms of autophagy are commonly described: chaperone-mediated autophagy (CMA), microautophagy and macroautophagy. Cellular cargo protein or materials can be sequestered into autophagosomes, which fuse with lysosomes, resulting in lysosomal degradation (macroautophagy, simply referred to as autophagy hereafter) [122, 123]. Proteins can directly be targeted to lysosomes (microautophagy) [123, 124] or bound by chaperones (such as HSC70 and HSP90) (chaperone-mediated autophagy, CMA) [125-127].

Autophagy is usually activated by conditions of nutrient deprivation but has also been associated with physiological and pathological processes such as differentiation, development, stress, infection, neurodegenerative diseases and cancer. Autophagy is a highly and finely regulated process. The kinase mTOR is a critical regulator of autophagy induction, with activated mTOR (PI3K-I/Akt and Erk MAPK signaling) suppressing autophagy, and negative regulation of mTOR (AMPK and genotoxic stress/p53 signaling) promoting it [128]. The core autophagy-related (Atg) complexes in mammals are ULK1 protein kinases, Atg9-WIPI1 and Vps34-Beclin1 class III PI3-kinase complexes, and the Atg12 and LC3 conjugation systems. Cargo protein or materials are sequestered in the form of bulk cytoplasm (in nonselective autophagy) or particular targets including intact organelles [in selective types of autophagy such as selective mitochondria degradation (mitophagy)]. Some critical components of the autophagy pathway and autophagic flux are described in the diagram below (**Figure 1.9**):
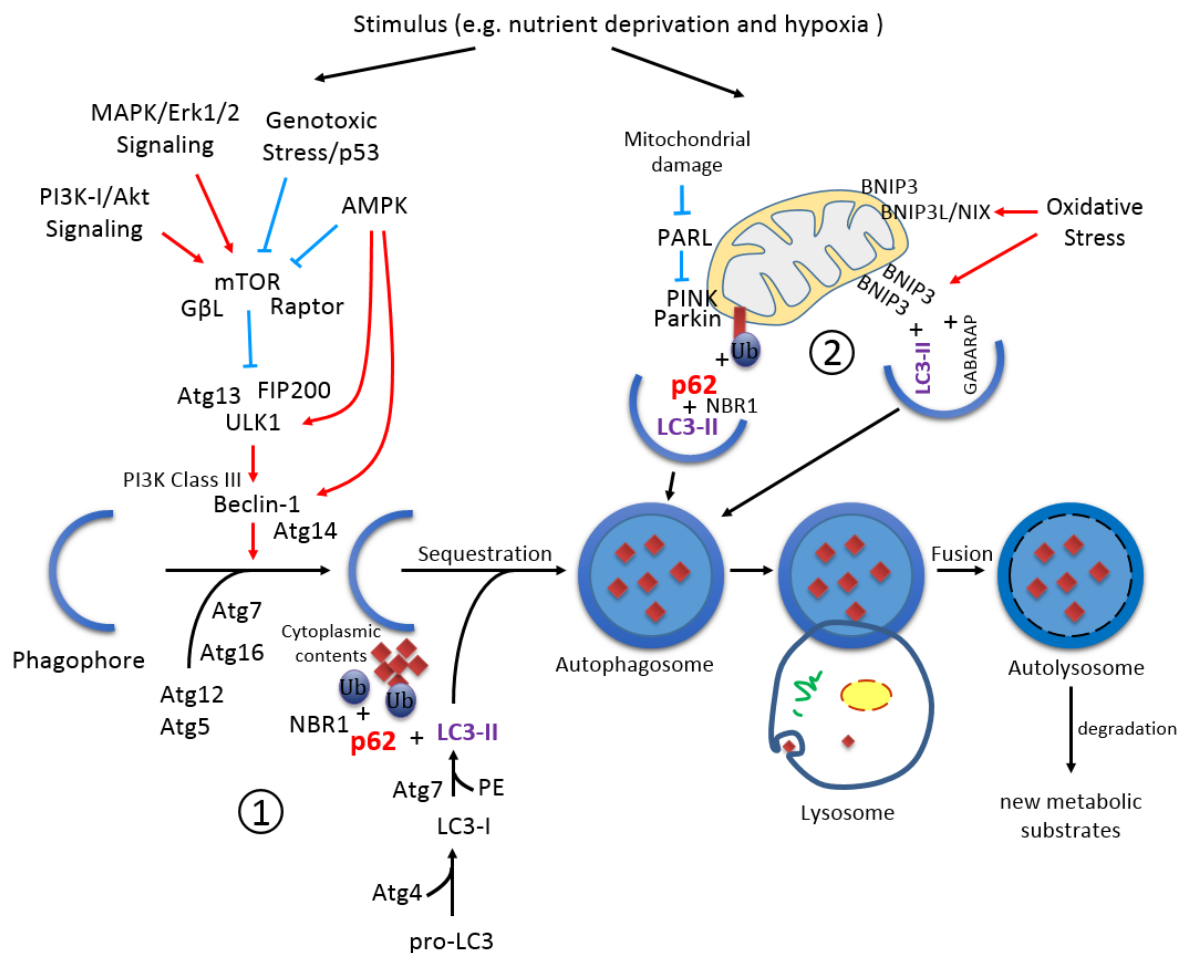
Figure 1.9 | Schematic representation of autophagy in mammalian cells. 1. The initial sequestering structure, the phagophore, expands to sequester cargo. LC3-II is recruited to the autophagosomal membrane for helping membrane elongation. The cargo is enclosed within the double-membrane bounded autophagosome through p62/SQSTM1 [129, 130]. The autophagosome fuses with an available lysosome in time, providing access to a wide range of hydrolases that break down the inner autophagosome vesicle (called an autolysosome) along with the cargo. The resulting macromolecules are released back into the cytosol for reuse. 2. Mitophagy removes damaged or unneeded mitochondria from a cell following damage or stress. Figure inspired by the diagram of autophagy signaling from Cell Signaling Technology, Inc.

The conversion of LC3-I to LC3-II via PE conjugation is critical for autophagosome formation. Atg4 cleaves pro-LC3 (MAP1-light chain 3, LC3) to form LC3-I which then is conjugated to the phosphatidylethanolamine (PE) by Atg7 for the generation of LC3-II (lipidated LC3) [131]. Adaptor protein p62/SQSTM1 binds to ubiquitinated proteins and LC3-II for mediating autophagy via localizing into autophagic compartments, transporting ubiquitinated proteins and organelles, (**Figure 1.9 ①**) and eventually is degraded in autolysosomes along with the cargo [132]. Thus, the increase of LC3-II and the decrease of p62 are two markers of autophagy.

Mitophagy is a selective autophagic process specifically designed for the removal of damaged or unneeded mitochondria from a cell [133-135] (**Figure 1.9 ②**). This process promotes turnover of mitochondria and prevents accumulation of dysfunctional mitochondria, which can lead to

oxidative stress and cellular degeneration. Upon mitochondrial damage, the protein PINK, which is continually degraded in the healthy state through the action of PARL, is stabilized and recruits the E3 ubiquitin ligase Parkin to initiate mitophagy. Polyubiquitination of mitochondrial membrane proteins by Parkin results in the recruitment of autophagy p62/SQSTM1, NBR1, and Ambra1 that bind to LC3 via their LC3-interacting region (LIR). In addition, increasing evidence indicates a critical role of BNIP3 (BCL2 interacting protein 3), which also contain LIRs, in mitophagy [104, 106, 136]. BNIP3 can promote mitophagy by triggering the translocation of Parkin to the mitochondria [137] or by directly recruiting autophagic machinery by an ubiquitin-independent mechanism to induce autophagosome formation [136] (**Figure 1.9 ②**).

Under hypoxic conditions, mitochondria are usually dysregulated and subsequently reorganized through mitochondrial fusion/fission [138]; dysfunctional or unneeded mitochondria are removed by mitophagy [106, 139, 140]. BNIP3 can induce mitophagy by disrupting the Bcl-2/Beclin-1 complex contributing to survival rather than cell death under hypoxia [106]. Increased expression of BNIP3 under hypoxia is mainly regulated by the transcription factor HIF-1α [141] and can be directly suppressed by the tumor suppressor p53 [142].

1.3 The tumor suppressor p53

p53 was first identified as a host protein of approximately 53 kilodalton (kDa) that bound to the large T-antigen of simian virus 40 (SV40) in transformed rodent cells in 1979 [143, 144]. It was initially classified as an oncogene due to the use of mutated cDNA following purification of tumor cell mRNA [145]. In 1989, scientists recognized that wild-type p53 (wt p53), encoded by *TP53*, suppresses growth and oncogenic transformation in cell culture [146]. That p53 is a tumor suppressor was confirmed in 1990 by the finding that patients with Li–Fraumeni syndrome, which predisposes to diverse tumor types, had inherited *TP53* mutations [147], and further confirmed in 1992 by experiments showing that *Trp53* (encoding mouse p53) knockout mice are prone to develop tumors [148]. Subsequent studies have demonstrated that the *TP53* gene is the most frequently mutated gene in human cancers [149, 150], indicating that p53 plays a crucial role in preventing cancer formation.

p53 has been described as a "cellular gatekeeper" [151] or "guardian of the genome" [152] because of its central role in cell cycle arrest and DNA repair. p53 prevents genome mutation and maintains genomic integrity by serving as a stress sensor, responding to DNA damage [induced by either UV, ionizing radiation (IR), or chemical agents such as hydrogen peroxide (H_2O_2)]. Upon DNA damage, p53 is activated and induces cell cycle arrest at the restriction point at the end of

the G1 phase [153]. This cell cycle arrest at this point allows the cell to fix the damage prior to the next cell division. If DNA damage proves to be irreparable, p53 may also initiate programmed cell death (apoptosis).

1.3.1 The structure of p53

In humans, p53 is encoded by the gene *TP53* located on the short arm of chromosome 17 (17p13.1) [154, 155]. The *TP53* gene contains 11 exons and 10 introns [155, 156]. In addition to the full-length protein (p53α), the human *TP53* gene encodes at least 15 protein isoforms, ranging in size from 3.5 to 43.7 kDa [157]. The full-length p53 protein consists of 393 amino acids (aa). Based on the sum of masses of the amino acid residues, the actual mass of p53 is only 43.7 kDa. The name p53 is however describing its apparent molecular mass (approximately 53 kDa) in SDS-PAGE analysis. Due to the high number of proline residues in the p53 protein, its migration is slowed down on SDS-PAGE, thus making it appear bigger than it actually is [158].

The 393 amino acids of p53 protein are divided into several structural and functional domains (**Figure 1.10**). The N-terminus of p53 contains two tandem transcriptional activation domains (TADs), TAD1 (residues 1-40) and TAD2 (residues 40-60). C-terminal to the TADs lies the proline-rich domain (PRD) that encompasses residues 61-94. Residues 102-292 represent the central core of p53, comprising the DNA-binding domain (DBD) that is responsible for sequence-specific binding of this protein to p53 response elements (p53REs) in DNA. The consensus sequence of p53REs is classically defined as two DNA half sites of PuPuPuC(A/T)-(T/A)GPyPyPy (Pu represents A or G and Py represents C or T) with a spacer of 0-13 bp between half sites. p53 binds cooperatively to p53REs as a tetramer (dimer of dimers), the formation of which depends on the oligomerization domain (OD) comprising residues 324-355 in the C-terminal region (residues 301 -393). p53 tetramerization is also essential for its C-terminal acetylation [159]. The C-terminal region also contains a nuclear localization signal (NLS) and a nuclear export signal (NES) that facilitate the nuclear-cytoplasmic shuttling of p53. Finally, the extreme C-terminus (residues 363-393) holds a basic lysine-rich carboxy-terminal domain (CTD). This basic region furthermore comprises the main acetylation sites including Lys370, Lys372, Lys373, Lys381 and Lys382 [160]. These sites also undergo ubiquitination, modulating p53 stabilization and sequence-specific DNA binding [161, 162].
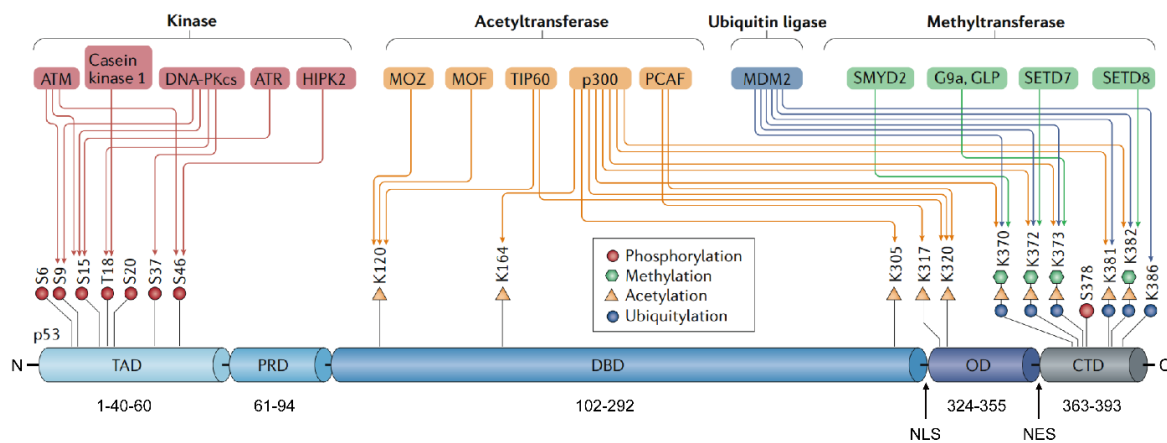
Figure 1.10 | Schematic overview of the structure of the p53 protein and its post-translational modifications. The N-terminus of p53 contains two tandem transcriptional activation domains (TADs), TAD1 (residues 1-40) and TAD2 (residues 40-60), followed by a proline-rich region (PRD). The central core domain contains the DNA-binding domain (DBD). The C-terminal region contains the nuclear localization signal (NLS) followed by the oligomerization domain (OD), the nuclear export signal (NES) and a basic carboxy-terminal domain (CTD). The main post-translational modifications (PTMs) by the indicated enzymes known to affect p53 function are shown. Phosphorylation sites are prevalent in the TADs, whereas acetylation sites occur in the DBD, OD and CTD. Methylation sites are enriched in the CTD. The PRD contains few well-studied PTMs. Figure adapted and modified from [163].

1.3.2 The regulation of p53 abundance and activity

The regulation of p53 responding to stress signals is achieved by the control of i) protein stability, ii) protein activity and iii) cellular localization. These are tightly regulated by extensive post-translational modifications (PTMs) of p53 by different enzymes (**Figure 1.10**). Approximately fifty amino acid residues of p53 are subjected to PTMs. A single residue can be modified by multiple enzymes in a mutually exclusive manner, resulting in an antagonism between different modifications. The PTMs of p53 include phosphorylation, ubiquitination, acetylation, methylation, sumoylation, hydroxylation, glycosylation, neddylation and polyribosylation [164].

PTMs either influence the conformation of p53, modulating protein oligomerization or its interaction with partners, or the functionality of p53 directly. Moreover, the interplay between the diverse PTMs is essential for the p53-mediated response (such as proper gene expression) and cell fate.

Regulation of p53 abundance

p53 is presented at low levels in unstressed cells. These low levels are due to a continuous degradation of p53 after protein synthesis [165]. Depending on the cellular context, several E3 ubiquitin ligases are thought to be the rate-liming factors in the regulation of p53 protein expression. MDM2 (also called HDM2 in humans) is regarded as the master regulator of p53 protein levels in a variety of cellular systems [166] (**Figure 1.10**). MDM2 binds to the TAD of p53

and covalently attaches ubiquitin to p53 thus marking it for degradation by the proteasome. This binding also inhibits p53 transactivation function by blocking the recruitment of essential transcriptional machinery components [167, 168]. Additionally, MDM2 can regulate p53 localization by transporting it from the nucleus to the cytosol. MDM2 itself is transcriptionally induced by the p53 protein [169, 170]. Thus, p53 and MDM2 set up a feedback loop that ensures that cellular p53 levels are kept low in the absence of stress. In response to stress signals, p53 is stabilized by inhibition of MDM2, through any of several mechanisms: stress-induced PTMs of both MDM2 and p53, which disrupt MDM2-binding; oncogene-induced sequestration of MDM2 by the tumor suppressor ARF (alternate reading frame); and nucleolar-stress-triggered ribosomal protein binding and inhibition of MDM2-mediated ubiquitination of p53.

Other E3 ubiquitin ligases, like Pirh2, COP1 and ARF-BP1, also negatively regulate p53 protein levels and antagonize p53 function [171]. Certain pathogens can also influence the p53 protein. One such example, are cells infected with high-risk HPV (described in chapter 1.1.3.2), such as HPV16 and HPV18, in which the viral E6 protein promotes the binding of p53 to the E3 ubiquitin ligase E6-AP (encoded by *UBE3A*), which ubiquitinates p53 efficiently and causes the proteasomal degradation of p53. Of note, ubiquitination levels of p53 are not exclusively regulated by the forward reaction of the ligases. The ubiquitination of p53 is reversible. A family of proteases, the deubiquitinases (DUBs), three of which, USP7 (or HAUSP), USP10 and USP42, can cleave ubiquitin off p53, thereby protecting it from ubiquitin-proteasome-dependent degradation [172-175].

Activation of p53

The critical event leading to the activation of p53 protein is the phosphorylation of its N-terminal domain. The N-terminal TAD of p53 contains many phosphorylation sites and can be considered as the primary target for protein kinases transducing stress signals (**Figure 1.10**). The protein kinases that are known to target the TAD of p53 can be roughly divided into two groups. A first group of protein kinases belongs to the MAPK family (JNK1-3, Erk1-2 and p38 MAPK), which is known to respond to several types of stress, such as membrane damage, oxidative stress, osmotic shock, heat shock, etc. A second group of protein kinases (ATR, ATM, CAK, CHK1-2, DNA-PK and TP53RK) is implicated in the genome integrity checkpoint, a molecular cascade that detects and responds to DNA damage caused by genotoxic stress.

Phosphorylation of the N-terminal region of p53 by the protein kinases, for example DNA damage-induced phosphorylation at ser15 and ser20, disrupts MDM2-p53 interaction [176]. Other

proteins, such as Pin1, are then recruited to p53 and induce a conformational change in p53, which further prevents MDM2-p53 interaction, promoting both the accumulation and activation of p53. Phosphorylation also allows for the binding of transcriptional coactivators, such as acetyltransferases p300 and PCAF (p300/CBP-associated factor), which then acetylate the carboxy-terminal end of p53 (**Figure 1.10**), exposing the DBD of p53, allowing it to activate or repress specific genes [177, 178]. Deacetylase enzymes, such as Sirt1 and Sirt7, can deacetylate p53, leading to an inhibition of apoptosis [179]. MDM2 can recruit histone deacetylase 1 (HDAC1) to p53 and facilitate HDAC1-mediated deacetylation of p53 [180]. Some activated oncogenes can stimulate the transcription of proteins that bind to MDM2 and inhibit its activity. p19ARF, the alternate reading frame product of the p16/INK4A locus, interacts with MDM2 upon oncogenic stress and sequesters it in the nucleolus and thus away from p53 [181, 182]. The above-mentioned protein kinases like ATM and ATR can promote the degradation of MDM2 to activate p53 [183]. Other PTMs, like methylation, sumoylation and neddylation, can also influence the activation of p53. p53 is, for instance, methylated at lys370 by SMYD2, at lys372 by SETD 7/9, and at lys382 by SETD8 (**Figure 1.10**). Methylation of these sites either impairs acetylation of p53 or its DNA binding and transcriptional activity.

The activity of p53 depends on its localization and both nuclear import and export of p53 are tightly regulated [184]. The nuclear-cytoplasmic shuttling of p53 is regulated by the nuclear localization signal (NLS) and the nuclear export signal (NES). p53 is synthesized in the cytoplasm and needs to be transported into the nucleus to exert its transcriptional activity responding to several types of cellular stress. Upon cellular stress, like DNA damage, p53 is imported into the nucleus through the NLS and activates its target genes [185]. p53 tetramerization masks the NES and thereby blocks its nuclear export [186]. Several proteins can modulate p53 localization. One of the most important of these modulations is MDM2-mediated nuclear export of p53.

1.3.3 p53-induced transcriptional programs involved in different responses

In addition to the aforementioned functions in cell cycle arrest, DNA repair and apoptosis upon DNA damage, p53 elicits several other cellular responses including senescence, autophagy and cell metabolism, responding to a broad range of cellular stresses. p53 can be modulated by oncogenic stress, ribosome dysfunction, spindle damage, telomere attrition, ribonucleotide depletion, nutrient deprivation, hypoxia, oxidative stress, osmotic shock and heat/cold shock [187, 188] (**Figure 1.11**). In response to these myriad of cellular stress signals, p53 regulates the diverse biological processes primarily through transactivation of its target genes (**Figure 2.11**).
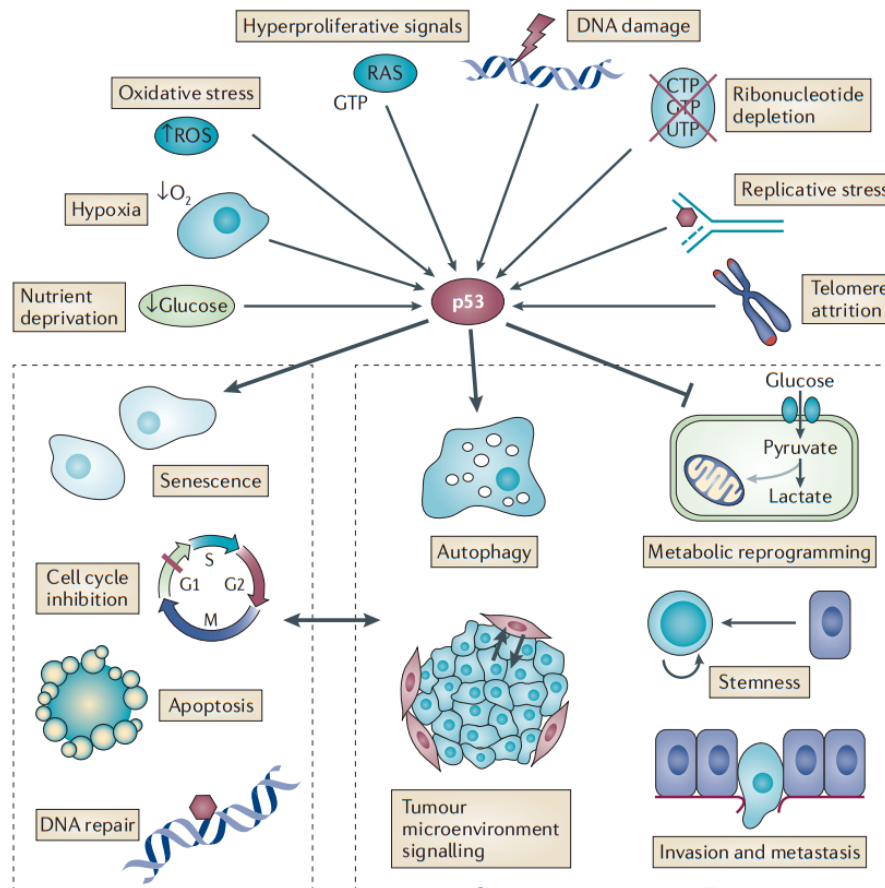
Figure 1.11 | Schematic overview of p53-activating signals and p53-triggered cellular responses. A host of different stress signals can activate p53, including nutrient deprivation, hypoxia, oxidative stress, hyperproliferative signals, DNA damage, ribonucleotide depletion, replicative stress and telomere attrition. p53 activation by these signals can consequently promote cellular responses of cell cycle arrest, DNA repair, senescence and apoptosis. Beyond triggering these classical responses, p53 that is activated by various stressors can modulate several additional biological processes including autophagy, metabolism control, stem cell biology, tumor microenvironment crosstalk and invasion and metastasis. Regulation of these processes by p53 may impinge on the canonical functions, such as apoptosis or senescence. Similarly, classical responses may affect novel functions. Figure adapted from [188].

Activated p53 binds to sequence-specific DNA as a tetramer. The sites of p53REs are frequently found in either the promoters or the first introns of its target genes. Once p53 tetramers are bound to DNA, they can activate the transcription of numerous protein-coding and non-protein-coding genes (e.g. microRNAs or lncRNAs), which is a function of fundamental importance for p53-mediated cellular responses.

The cell fates specified by activated p53 depend on cell type and the nature and extent of the stresses. Under conditions of lower levels of stress causing damage, p53 activates its target genes, such as *CDKN1A* (p21) and *GADD45A*, to engage a temporary program of cell cycle arrest and DNA repair to allow cells to pause and repair the damage incurred, thereby preventing inappropriate proliferation of cells carrying damaged DNA. p53 can also maintain genomic stability at the chromosomal level, by limiting the accumulation of cells with aberrant

chromosomal numbers [189-191]. Therefore, p53 is also considered to be "a guardian of ploidy" [192]. Another protective, pro-survival mechanism is the ability of p53 to activate antioxidant genes, such as *TIGAR*, *GPX1* and *SESN1-2* (sestrins 1 and 2), which inhibit the accumulation of reactive oxygen species (ROS), thereby maintaining genomic integrity [193, 194].

In response to severe or sustained stress signals, p53 drives irreversible cell fates, such as cell death (apoptosis) and permanent cell cycle arrest (senescence). p53-induced apoptosis involves the transcriptional activation of components of both the intrinsic and extrinsic death pathways, including *BAX*, *FAS*, *APAF1* and *PUMA*, amongst others, which collaboratively promote cell death [195, 196]. In the cases responding to potent stress, p53 induces cellular senescence through transcriptional induction of target genes such as *CDKN1A*, *PML* (promyelocytic leukemia protein) and *PAI1* (plasminogen activator inhibitor) [195, 197].

p53 can promote oxidative phosphorylation (through *SCO2*) [198] and inhibit glycolysis (through *TIGAR*, *GLUT1* and *4*) [199, 200], opposing oncogenic metabolic reprogramming (known as the Warburg effect, see chapter 1.2.2) [201]. p53 can also induce autophagy to provoke cell death by activating genes such as *DRAM1*, *AMPK*, *SESN1* and *SESN2*. As described in chapter 1.2.3, autophagy is a double-edged sword on cell fates. The role of autophagy depends on the cell type and the nature of the stress.

In addition to activating transcription, p53 can inhibit the expression of genes such as *CDC2*, *CDC25C* and *TERT* [202, 203].

1.3.4 Transcription-independent activities of p53 in apoptosis and autophagy

Besides its role as a transcription factor, p53 has additional functions, such as exonuclease activity [204] and its cytoplasmic roles in apoptosis and autophagy [205, 206]. In response to apoptosis-inducing stress signals, p53 can participate directly in the intrinsic apoptosis pathway by shuttling to mitochondria where it interacts with the members of the Bcl-2 family, leading to robust mitochondrial outer membrane permeabilization (MOMP), unleashing the enzymatic apoptotic machinery of caspases and of chromatin degradation [207, 208].

p53 has a dual role in regulating autophagy. As mentioned above, activated nuclear p53 upregulates the expression of pro-autophagy target genes [201]. Cytoplasmic p53 is able to repress autophagy via transcription-independent effects on the AMPK/mTOR-dependent pathway [206]. p53 can also post-transcriptionally down-regulate LC3 mRNA to reduce autophagy [209]. In addition, negative regulation of autophagy by p53 involves its functions as a transrepressor. p53

can directly suppress *BNIP3* expression to inhibit hypoxia-induced autophagy [142] (see chapter 1.2.3.1).

1.3.5 Hypoxia and p53 in HPV-positive cervical cancer cells

Hypoxia is one of the stresses that have been shown to affect p53 signaling. Hypoxia very differently influences p53 protein levels and its consequences for cellular functions seem to be dependent on the cell line, the severity and the duration of oxygen deprivation [210-212].
Cervical cancers often display strongly reduced O_2 content, with a median O_2 concentration of 1.18%. Therefore, hypoxia is frequently detected in cervical cancer patients and has a negative impact on patient prognosis [48, 49]. Nevertheless, functional studies of HPV-positive cancer cells under hypoxic conditions are rare. In these few studies, the regulation of p53 in hypoxic HPV-positive cells is controversial. In primary cervical epithelial cells infected with the HPV16 *E6* and *E7* genes, low-oxygen conditions stimulate apoptosis as well as the induction of p53 protein. Cell lines derived from HPV16-associated human cervical squamous cell carcinomas display resistance to hypoxia-induced apoptosis although p53 protein level increased under hypoxia [51]. Recently, it has been reported that despite efficient *E6/E7* repression, p53 protein levels did not increase in HPV16-positive cancer cell lines under hypoxia, but even decreased further [50]. In sharp contrast to their senescent phenotype when *E6/E7* is deficient and p53 is reconstituted under normoxia, hypoxic HPV-positive cancer cells enter a dormant state, characterized by an evasion of cellular senescence and a reversible growth arrest [50].

1.4 Aims of study

Although studies have investigated the divergent regulation of the p53 tumor suppressor by hypoxia, the dynamics of p53 during different periods of hypoxic conditions in cervical cancer cells is still not well explored. The role of p53 for this cellular adaptation under hypoxic conditions was not well studied. The effect of p53 regulation on downstream responses during hypoxia remains elusive. In addition, the mechanisms controlling the regulation of p53 by hypoxia in HPV-positive cervical cancer cells are diverse [213, 214]. Which downstream pathway of p53 signaling contributes to the fate of hypoxic cells is not fully understood, yet. The aims of this present study therefore are:

i)   To determine time-dependent changes in p53 in hypoxic HPV16-positive cervical cancer cells

ii) To analyze how this mechanism is mediated

iii) To reveal the role of p53 regulation in cellular adaptation to hypoxia

iv) To explore the effect of p53 regulation on downstream pathway responses in hypoxic cells

v)   To identify which downstream pathway contributes to the behavior of hypoxic cells

The elucidation of the underlying mechanism and pathway will provide important new insights into cellular adaptation to hypoxia and should be relevant for prospective therapeutic methods, which aim to prevent cancer recurrence in poorly oxygenated regions of HPV-positive tumors.

2. Results

2.1 Regulation of p53 by hypoxia in HPV16-positive cervical cancer cells

2.1.1 p53 protein levels under hypoxia (24 h) in HPV16-positive cervical cancer cells

In order to investigate the effect of hypoxia on the tumor suppressor p53 in HPV16-positive cervical cancer cells, the SiHa and CaSki cell lines were incubated under normoxic conditions (N, 21% O_2) or hypoxic conditions (H, 1% O_2) for 24 hours (h).

qPCR analyses revealed a strong down-regulation of HPV16 *E6/E7* oncogene expression under hypoxia in both SiHa and CaSki cells (**Figure 2.1A**). These results are consistent with the previous findings reported by Hoppe-Seyler *et al.* [50]. The transcript of vascular endothelial growth factor (*VEGF*) that is known to be transcriptionally up-regulated under hypoxia [215] was used as a hypoxia control gene. The strong up-regulation of *VEGF* under hypoxia (1% O_2) (**Figure 2.1A**) indicates that the hypoxic treatment was efficient. Despite efficient *E6/E7* repression, p53 protein levels did not reconstitute in HPV16-positive cancer cells under hypoxia, but were actually completely depleted (**Figure 2.1B**). The down-regulation of p53 protein coincides with the accumulation of hypoxia-inducible factor-1α (HIF-1α) (**Figure 2.1B**). The hypoxic stabilization of HIF-1α protein is considered a major event in the cellular response to hypoxia and was previously described [216]. The strong up-regulation of HIF-1α under hypoxia (1% O_2) also indicates that the hypoxic incubation was effective under the chosen conditions.
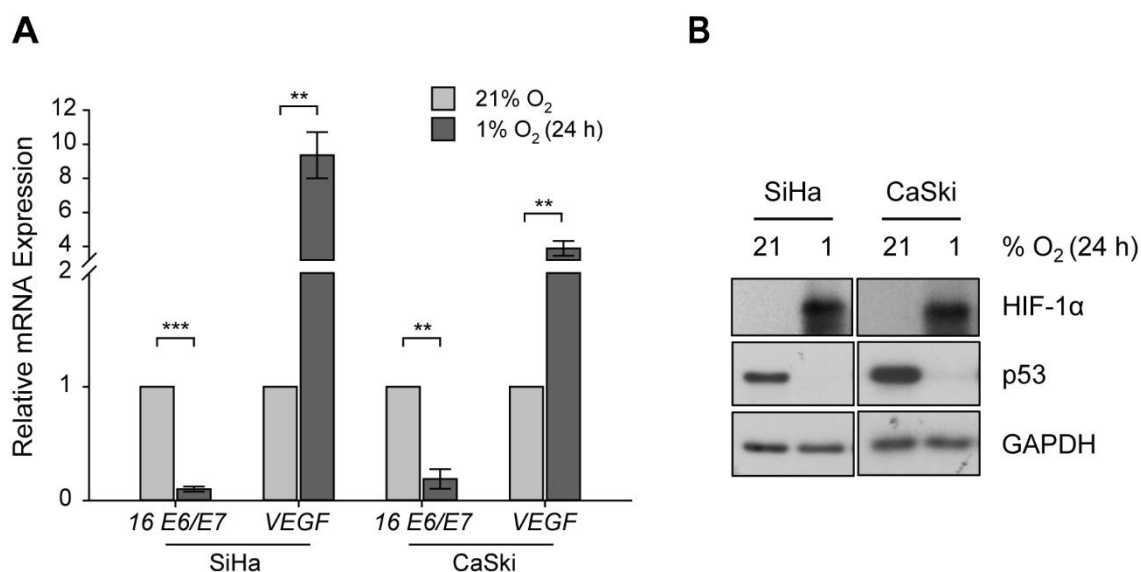
Figure 2.1 | Levels of *E6/E7* oncogene transcripts and p53 protein in HPV16-positive cervical cancer cells under normoxia and hypoxia. HPV16-positive SiHa and CaSki cells were cultured for 24 h at the indicated O_2 concentrations (normoxia: 21% O_2 and hypoxia: 1% O_2). Total RNA and total protein were extracted. (A) qPCR analyses of HPV16 *E6/E7* transcripts. Transcript levels of *VEGF* were monitored as marker for

hypoxia. *18S* rRNA served as internal control for normalization. Error bars indicate the SD of three independent experiments. Respective transcript levels under normoxia were arbitrarily set to 1 and set as control for the calculation of significant differences (Two-tailed Student's *t* test was employed, **p < 0.01, ***p < 0.001). (B) Western Blot analyses using antibody against p53. HIF-1α was used as marker for hypoxia, and GAPDH served as a loading control.

To conclude, the above results indicate that hypoxia (1% O_2 for 24 h) strongly affects p53 protein levels in HPV16-positive cervical cancer cells. To further analyze this finding, the effect of different periods of hypoxia on p53 protein levels was determined.

2.1.2 Time-dependent changes of p53 protein levels in hypoxic HPV16-positive cancer cells

In order to determine time-dependent changes of p53 under hypoxia in HPV16-positive cervical cancer cells, time course experiments were performed. SiHa and CaSki cells were therefore incubated under hypoxia for different periods of time.

As depicted in **Figure 2.2**, the expression of the HPV16 oncogenes *E6/E7* was continuously down-regulated under hypoxic conditions (0, 6, 24, 48, and 72 h). Interestingly, different from the stable or slightly increased p53 protein levels under normoxic conditions, p53 protein showed a biphasic regulation in hypoxic HPV16-positive cancer cells. Here, p53 levels rapidly and strongly decreased to complete depletion under hypoxia (6-24 h), then recovered to baseline (p53 protein levels under normoxia) after 48 h. Prolonged hypoxia (72, 96, and 120 h) markedly increased p53 protein levels in HPV16-positive cancer cells compared to the normoxic controls (**Figures 2.2C** and **2.2D**).
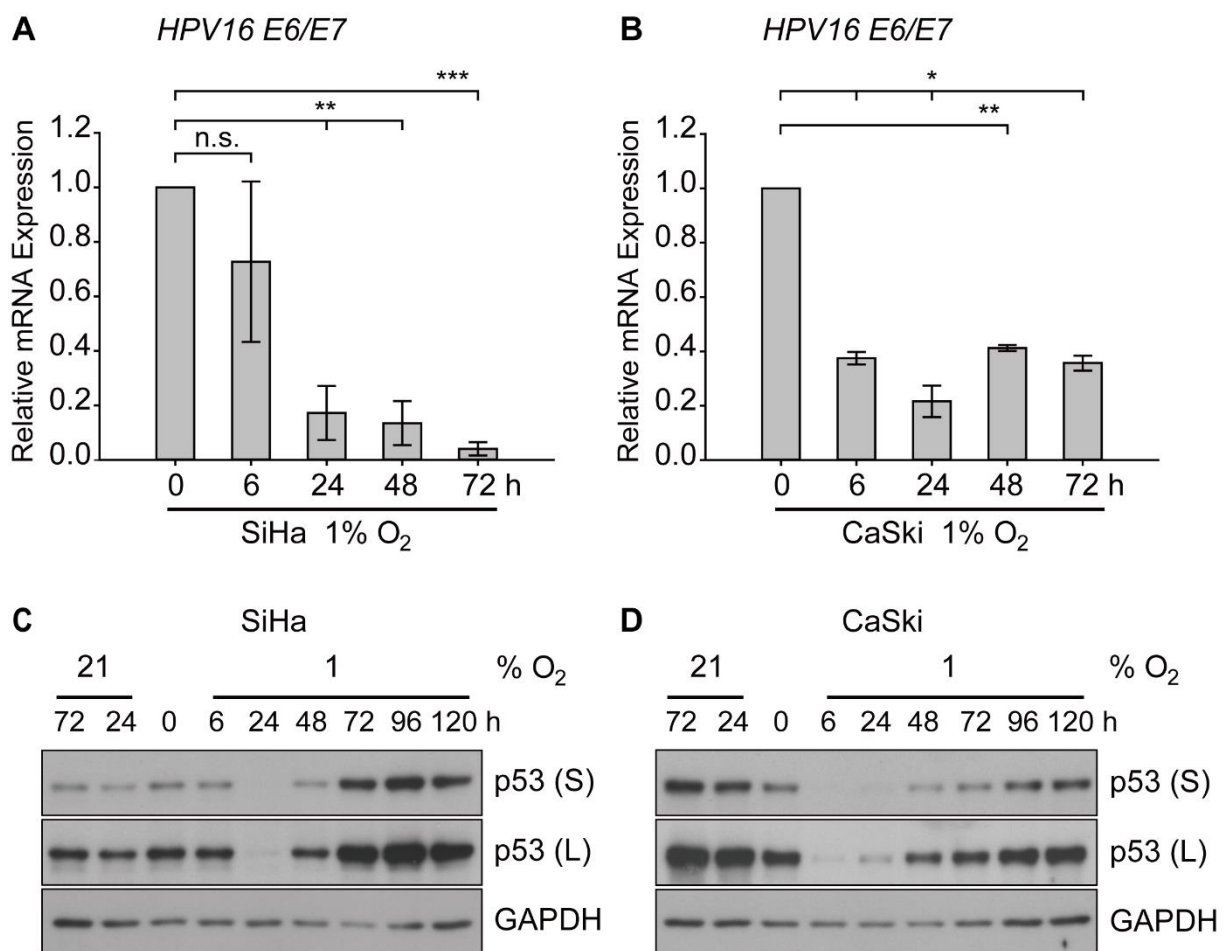
Figure 2.2 | Levels of *E6/E7* oncogene transcripts and p53 protein in hypoxic HPV16-positive cancer cells. HPV16-positive SiHa and CaSki cells were cultured for the indicated time periods at 21% O_2 or at 1% O_2. Total RNA and total protein were extracted after respective time intervals. (A) and (B) qPCR analyses of HPV16 *E6/E7* transcripts in SiHa (A) and CaSki cells (B). *18S* rRNA served as internal control for normalization. Error bars indicate the SD of three independent experiments. The 0 h value of *E6/E7* expression was set as a control for the calculation of significant differences (Two-tailed Student's *t* test was employed, *p < 0.05, **p < 0.01, ***p < 0.001 and n.s., statistically not significant). (C) and (D) Western Blot analyses using antibody against p53. GAPDH served as a loading control. (S, short exposure; L, long exposure)

These results show a new regulation pattern of p53 protein by hypoxia in HPV16-positive cancer cells. During different periods of hypoxia, p53 protein was not unidirectionally regulated in SiHa and Caski cells, but showed a "biphasic" change.

2.2 Mechanism of biphasic regulation of p53 protein in hypoxic HPV16-positive cervical cancer cells

2.2.1 Transcript levels of p53 in hypoxic HPV16-positive cervical cancer cells

To decipher the mechanism underlying the biphasic regulation of p53 in hypoxic HPV16-positive cervical cancer cells, first the transcript levels of the p53 gene (*TP53*) were analyzed. Neither during short-term nor under prolonged hypoxia, any fluctuation was found at *TP53* mRNA levels in SiHa or CaSki cells (**Figure 2.3**). Hypoxia had no significant effects on *TP53* mRNA levels at 6 h in either SiHa or CaSki cells. Hypoxia reduced the *TP53* mRNA levels by half in SiHa cells after 24 h, after which p53 transcript levels remained relatively stable at this decreased amount under hypoxia in SiHa cells (**Figure 2.3A**). In hypoxic CaSki cells, *TP53* mRNA levels showed a significant decrease only after 48 h of hypoxia (**Figure 2.3B**).
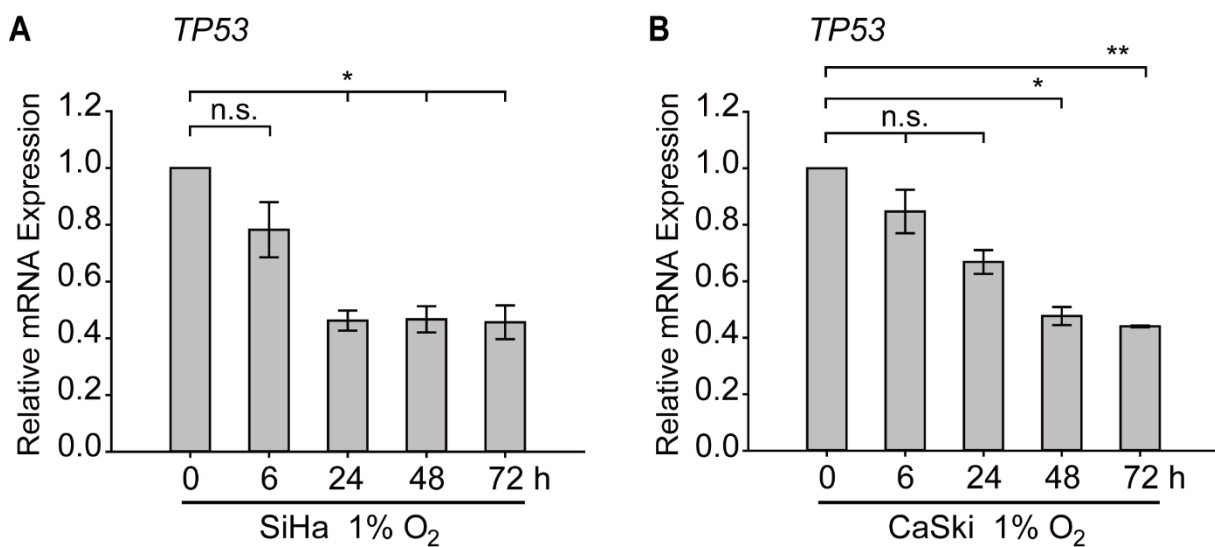
Figure 2.3 | Transcript levels of p53 in hypoxic HPV16-positive cancer cells. SiHa (A) and CaSki cells (B) were cultured for the indicated time periods at 1% O_2. Total RNA was extracted after respective time intervals. (A) and (B) qPCR analyses of p53 transcripts. *18S* rRNA served as internal control for normalization. Error bars indicate the SD of three independent experiments. The 0 h value of *TP53* expression was set as a control for the calculation of significant differences (Two-tailed Student's *t* test was employed, *$p < 0.05$, **$p < 0.01$ and n.s., statistically not significant).

These findings show that the *TP53* transcript levels are not consistent with the time-dependent changes observed for p53 protein in hypoxic HPV16-positive cancer cells, indicating that the biphasic regulation of p53 protein levels is not (exclusively) due to the hypoxic regulation of p53 mRNA levels.

2.2.2 Hypoxia affects p53 protein stability in HPV16-positive cancer cells

To determine whether the reduction of p53 protein levels under hypoxia was attributable to a post-translational modulation, SiHa and CaSki cells were incubated with cycloheximide (CHX), an inhibitor of protein synthesis [217]. Pre-incubation under hypoxia reduced p53 protein half-life assayed by a CHX-chase experiment (**Figure 2.4**). Calculation of the half-life of p53 protein was described in chapter 5.4. Here, the half-life of p53 protein decreased from 8.41 minutes (min) under normoxia to 4.64 min under hypoxia in SiHa cells, and from 9.04 min under normoxia to 6.03 min under hypoxia in CaSki cells.
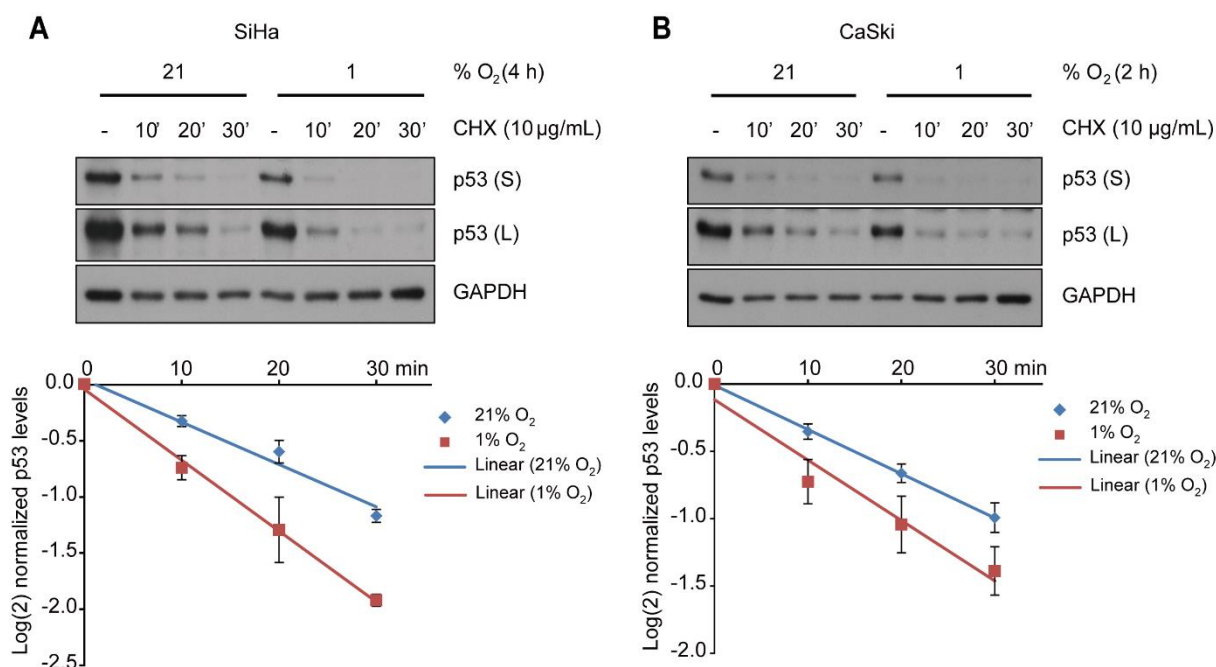
Figure 2.4 | p53 protein stability in HPV16-positive cancer cells under normoxia and hypoxia. SiHa (A) and CaSki cells (B) were incubated at 21% O_2 or at 1% O_2, respectively, for indicated time and treated afterward with/without cycloheximide (CHX, 10 mg/mL) for up to 30 min. Total protein was extracted after respective time intervals. (A and B, *top*) Western Blot analyses using antibody against p53. GAPDH served as a loading control. (S, short exposure; L, long exposure) (A and B, *bottom*) The grayscale of p53 from (A) and (B) was quantified using the ImageJ software. The relative grayscale values of p53 normalized to the respective (21% O_2 or 1% O_2) 0-time point were plotted on an xy diagram with log(2)-transformed x-axis to visualize the protein half-life. Error bars are SD, and n = 2 independent experiments.

These results suggest that hypoxia affects p53 protein levels by post-translationally targeting it for degradation in HPV16-positive cancer cells.

2.2.3 Proteasomal degradation is not solely responsible for the reduction of p53 levels in hypoxic HPV16-positive cancer cells

Since hypoxia affects p53 protein stability in HPV16-positive cancer cells, which cellular pathway for protein degradation is involved in the initial hypoxic reduction of p53 was determined next. MG132, an inhibitor of the 26S proteasome [218], was used to block the proteasomal degradation pathway, which plays an important role in p53 degradation both in the presence and absence of HPV oncoproteins (see chapter 1.1.3.2 and 1.3.2). As demonstrated in **Figure 2.5**, the p53 protein levels in hypoxic SiHa and CaSki cells could not be fully rescued to the comparable levels detected under normoxic conditions when incubated with MG132, indicating that in HPV16-positive cancer cells the reduction of p53 levels by hypoxia was not (solely) mediated via proteasomal degradation.
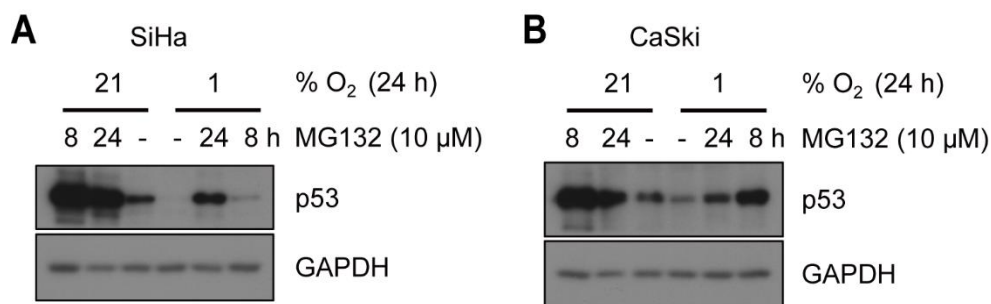
Figure 2.5 | Effect of MG132 on the hypoxic decrease of p53 in HPV16-positive cancer cells. SiHa (A) and CaSki cells (B) were incubated at 21% O_2 or at 1% O_2 for 0 h or 16 h prior to the treatment with 10 µM MG132. Total protein was extracted after 24 h. (A) and (B) Western Blot analyses using antibody against p53. GAPDH served as a loading control.

2.2.4 Lysosomal degradation is required for the down-regulation of p53 in hypoxic HPV16-positive cancer cells

Besides the ubiquitin/proteasome system, the autophagy-lysosome-dependent pathway is another important cellular system for protein degradation [119-121, 219, 220] (see chapter 1.2.3.1). Cellular cargo protein or cellular debris can be surrounded with a crescent-shaped isolation membrane (phagophore), which forms a closed double-membrane autophagosome. The autophagosome fuses with a lysosome to become an autolysosome, where its sequestered content is degraded (macroautophagy, simply referred to as autophagy hereafter) [122, 123]. Proteins can directly be targeted to lysosomes (microautophagy) [123, 124] or bound by chaperones (such as

HSC70 and HSP90) (chaperone-mediated autophagy, CMA) [125-127]. Of note, afore-used MG132 is not a selective inhibitor for proteasomes. It can also inhibit the function of lysosomes [218, 221, 222]. The autophagy-lysosome-dependent pathway was therefore suspected to be involved in the initial hypoxic reduction of p53.

The lysosomal inhibitors chloroquine (CQ) and Bafilomycin A1 (Baf A1) were next used to assess the putative role of autophagy-lysosome-dependent degradation on the hypoxic reduction of p53 protein. The adaptor protein p62/SQSTM1, a marker of autophagy, is a representative cargo protein sequestered in autophagosomes and degraded in the autolysosome [132] (**Figure 1.9**). In this experiment, both CQ and Baf A1 prevented the decrease of p62 in hypoxic HPV16-positive cancer cells (**Figure 2.6**), indicating that the degradation by autolysosomes was blocked efficiently under these conditions. As further shown in **Figure 2.6**, the autolysosome inhibitor CQ [223, 224] prevented the p53 degradation triggered by hypoxia. Bafilomycin A1, which inhibits the fusion of autophagosomes and lysosomes [225-227], however, only prevented the degradation of p62 but not p53, suggesting that, unlike p62, p53 was not sequestered by autophagosomes, but degraded via the lysosomal pathway.
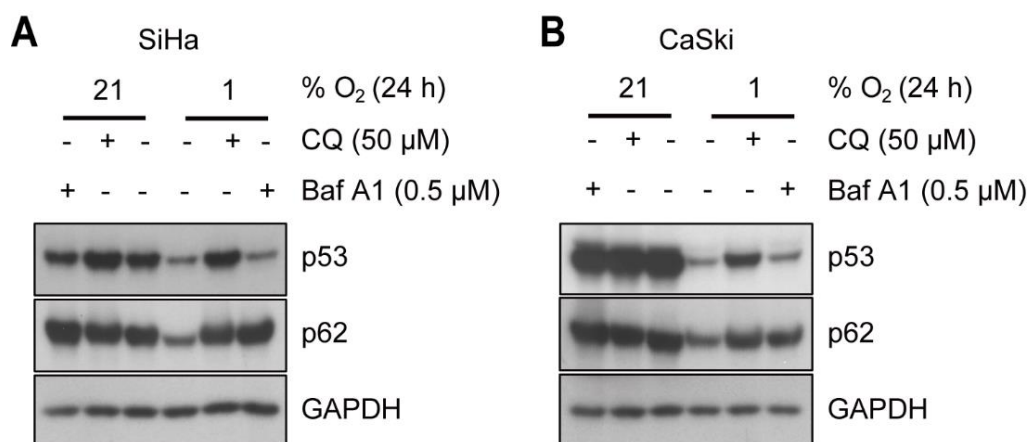
Figure 2.6 | Effect of lysosomal inhibitors on hypoxic reduction of p53 and p62 in HPV16-positive cancer cells. SiHa (A) and CaSki cells (B) were cultivated for 24 h under normoxia (21% O_2) or hypoxia (1% O_2), in either the absence (–) or the presence (+) of 50 µM chloroquine (CQ) or 0.5 µM Bafilomycin A1 (Baf A1). Total protein was extracted and Western Blot analyses using antibodies against p53 and p62 were performed. GAPDH served as a loading control.

Furthermore, p53 levels increased in a dose-dependent fashion in hypoxic cells incubated with CQ but were unchanged in cells incubated with Baf A1 (**Figure 2.7**).
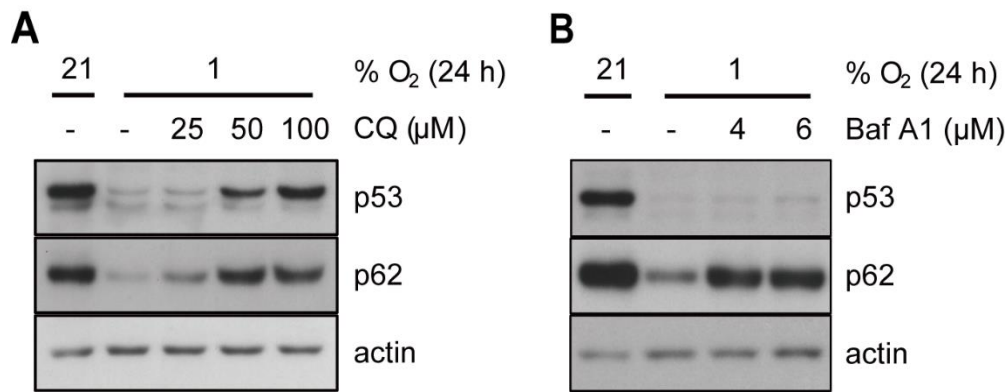
Figure 2.7 | Dose-dependent effect of lysosomal inhibitors on p53 and p62 protein in hypoxic HPV16-positive cancer cells. SiHa cells were cultivated for 24 h under normoxia (21% O_2) or hypoxia (1% O_2), in either the absence (-) or the presence of chloroquine (CQ, 25, 50, 100 µM) (A) or Bafilomycin A1 (Baf A1, 4, 6 µM) (B). Total protein was extracted and Western Blot analyses using antibodies against p53 and p62 were performed. Actin served as a loading control.

qPCR analyses showed that hypoxia reduced the *TP53* mRNA levels by about 50% in SiHa cells after 24 h. With the treatment of CQ, the *TP53* mRNA level showed a minor increase but was not statistically significant in hypoxic SiHa cells (**Figure 2.8**). Baf A1 had no effect on the *TP53* mRNA levels in SiHa cells. These findings revealed that the restoration of p53 protein levels by CQ was not due to an increase of mRNA levels.

Unexpectedly, treatment with CQ reduced the transcript levels of HPV16 *E6/E7* under normoxia in SiHa cells (**Figure 2.8**).
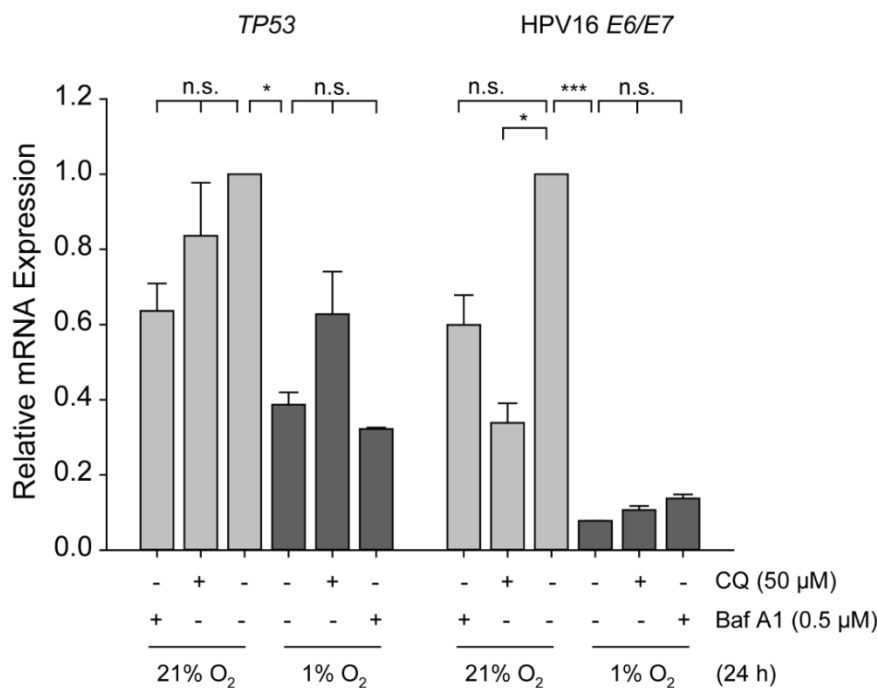
Figure 2.8 | Effect of lysosomal inhibitors on *TP53* and HPV16 *E6/E7* transcript levels in HPV16-positive cancer cells under normoxia and hypoxia. SiHa cells were cultivated for 24 h under normoxia (21% O_2) or hypoxia (1% O_2), in either the absence (–) or the presence (+) of 50 µM chloroquine (CQ) or 0.5 µM

Bafilomycin A1 (Baf A1). Total RNA was extracted. qPCR analyses of *TP53* and HPV16 *E6/E7* levels. *18S* rRNA served as internal control for normalization. Respective transcript levels of normoxic control samples were arbitrarily set to 1. Error bars indicate the SD of three independent experiments. (For calculation of significant differences, vs. respective normoxic control or hypoxic control, two-tailed Student's *t* test was employed, *p < 0.05, ***p < 0.001 and n.s., statistically not significant).

2.2.5 Autophagy is not responsible for the depletion of p53 in hypoxic HPV16-positive cancer cells

In order to determine the effect of autophagy (macroautophagy) on the depletion of p53 in hypoxic HPV16-positive cancer cells, specific small interfering RNA (siRNA) was used to silence the autophagy-related genes *ATG12* and *p62/SQSTM1* [228-232]. Autophagy requires the covalent attachment of the protein Atg12 to Atg5 through an ubiquitin-like conjugation system involving also Atg7 as an E1-like activating enzyme and Atg10 as an E2-like conjugating enzyme. The Atg12-Atg5 conjugate then promotes the conjugation of LC3-I to the phosphatidylethanolamine for the generation of LC3-II, which is recruited to the autophagosomal membrane for helping membrane elongation. p62/SQSTM1 is a multifunctional ubiquitin-binding protein. It acts as a cargo protein that targets other proteins that bind to it for autophagy-lysosome-dependent degradation. p62/SQSTM1 also functions as a scaffolding/adaptor protein in concert with TNF receptor-associated factor 6 to mediate activation of NF-κB in response to upstream signals.

Western Blot analyses showed that the expression of Atg12 and p62 were efficiently knocked down by specific siRNAs (**Figure 2.9**). The reduction of p62 after silencing of *ATG12* may be attributable to a compensatory increase of lysosomal degradation that is independent of the autophagosome. With the silencing of *ATG12* or *p62/SQSTM1*, p53 protein levels were not rescued under hypoxia (**Figure 2.9**). These results suggest the formation of autophagosomes is not required for the hypoxic reduction of p53. Furthermore, p53 is not targeted by p62 for degradation.

	21			1		% O_2 (24 h)
-	-	+	+	-	-	si-scramble
-	+	-	-	+	-	si-Atg12
+	-	-	-	-	+	si-p62

p53 (S)

p53 (L)

p62

Atg12

GAPDH
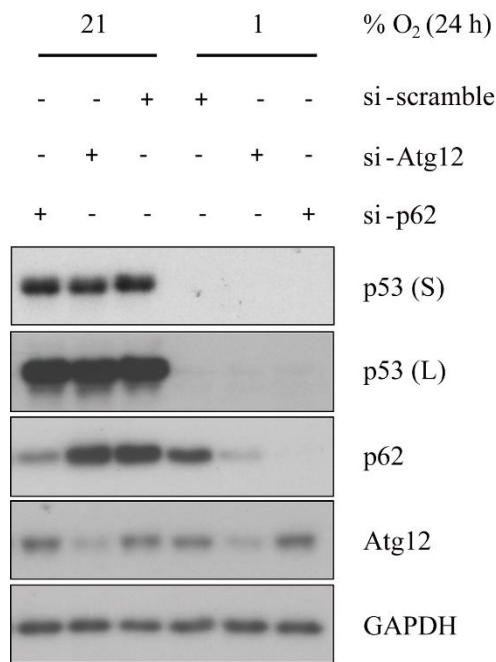
Figure 2.9 | Effect of silencing of Atg12 or p62 on p53 in HPV16-positive cancer cells. CaSki cells were transfected with scrambled control, Atg12- or p62-specific siRNA. 48 h post transfection, the cells were cultured for 24 h at 21% O_2 or at 1% O_2. Total protein was extracted after this time. Western Blot analyses were performed using antibodies against p53, Atg12 and p62. GAPDH served as a loading control. (S, short exposure; L, long exposure)

Collectively, these results indicate that autophagy is not responsible for the depletion of p53, whereas lysosomal degradation is required for the down-regulation of p53 in hypoxic HPV16-positive cancer cells.

In summary, in spite of continuous down-regulation of HPV16 *E6/E7* oncogenes under hypoxia, p53 protein does not immediately reconstitute, but instead shows a biphasic regulation [rapidly and strongly depleted under hypoxia (24 h), then recovered after prolonged hypoxia]. The initial reduction of p53 protein is mediated via a lysosome-dependent mechanism in hypoxic HPV16-positive cervical cancer cells.

2.3 Role of the biphasic regulation of p53 protein in the evasion of senescence by hypoxic HPV16-positive cancer cells

2.3.1 Hypoxic HPV16-positive cancer cells do not enter senescence

Repression of *E6/E7* oncogenes in HPV-positive cells results in the rapid induction of cellular senescence, a central tumor-suppressive, irreversible pathway [233, 234]. Mechanistically, inhibition of *E6/E7* expression activates p53 signaling, which in turn is required for senescence [235, 236]. RNA interference (RNAi)-mediated *E6/E7* repression under normoxia leads to the emergence of HPV-positive cells staining strongly positive for SA-β-Gal (Senescence-Associated β-Galactosidase, a marker of cellular senescence [237]) [50].

Since HPV16 *E6/E7* continuously decreased under hypoxia (**Figures 2.2A** and **2.2B**) and p53 protein displayed a biphasic regulation and markedly increased after prolonged hypoxia (**Figures 2.2C** and **2.2D**), the question whether hypoxic HPV16-positive cancer cells go into senescence was next investigated.

The SA-β-Gal staining assay showed that *E6/E7*-repressed hypoxic cells did not show strong SA-β-Gal staining (**Figure 2.10A**), indicating no induction of senescence. Under normoxic conditions, among SiHa cells, SA-β-Gal-positive cells increased from 7.99 ± 1.71% at 24 h to 10.42 ± 0.48% at 72 h; among normoxic CaSki cells, SA-β-Gal-positive cells increased from 1.74 ± 0.21% at 24 h to 6.11 ± 0.98% at 72 h. Compared to the normoxic cells, hypoxic HPV16-positive cancer cells possessed a decreased percentage of SA-β-Gal-positive cells (3.32 ± 1.35 at 24 h and 5.19 ± 1.73 at 72 h in SiHa cells; 1.84 ± 0.04 at 24 h and 3.06 ± 0.73 at 72 h in CaSki cells) (**Figure 2.10B**).

Compared to the cells at 24 h of hypoxia, the percentage of SA-β-Gal-positive cells at 72 h showed a minor increase but not statistically significant in hypoxic HPV16-positive cancer cells. These results indicate senescence was not induced despite efficient *E6/E7* repression and p53 reconstitution after prolonged hypoxia.

Figure 2.10 | Hypoxia modulates senescence in *E6/E7*-repressed HPV16-positive cancer cells. (A) SiHa and CaSki cells were cultured under normoxia (21% O$_2$) or hypoxia (1% O$_2$). After 24 h or 72 h, cells were stained for the expression of the senescence marker SA-β-Gal. Scale bar: 300 μm. Scheme *lower left*: Treatment protocol. (B) The percentages of SA-β-Gal-positive cells were quantified using the ImageJ Analyze Particles program. Error bars indicate the SD of three independent experiments. (Two-tailed Student's *t* test was employed, *p < 0.05, **p < 0.01 and n.s., statistically not significant)

2.3.2 Regulation of p53 responsive genes in hypoxic HPV16-positive cancer cells

p53 is a key regulator of the cellular senescence response [235, 236, 238-240]. Preliminary experiments of cell fractionation analysis with SiHa cells indicate that in normoxic cells, p53 protein was uniformly distributed in both cytoplasm and nucleus. At 24 h of hypoxia, there was no detectable p53 protein in either cytoplasm or nucleus in SiHa cells. After prolonged hypoxia (72 h), however, the restored p53 protein was predominantly localized in the nucleus (**Figure 3.7**). In light of the obtained data, demonstrating that hypoxic HPV16-positive cancer cells evade senescence despite reconstituted p53 protein levels, the biphasic regulation of p53 under hypoxia was hypothesized to have different effects on downstream pathways in the p53 network. To

understand how downstream genes of p53 signaling respond, p53 responsive genes involved in different functional pathways and cellular outcomes were selected [195] (**Figure 2.11**).
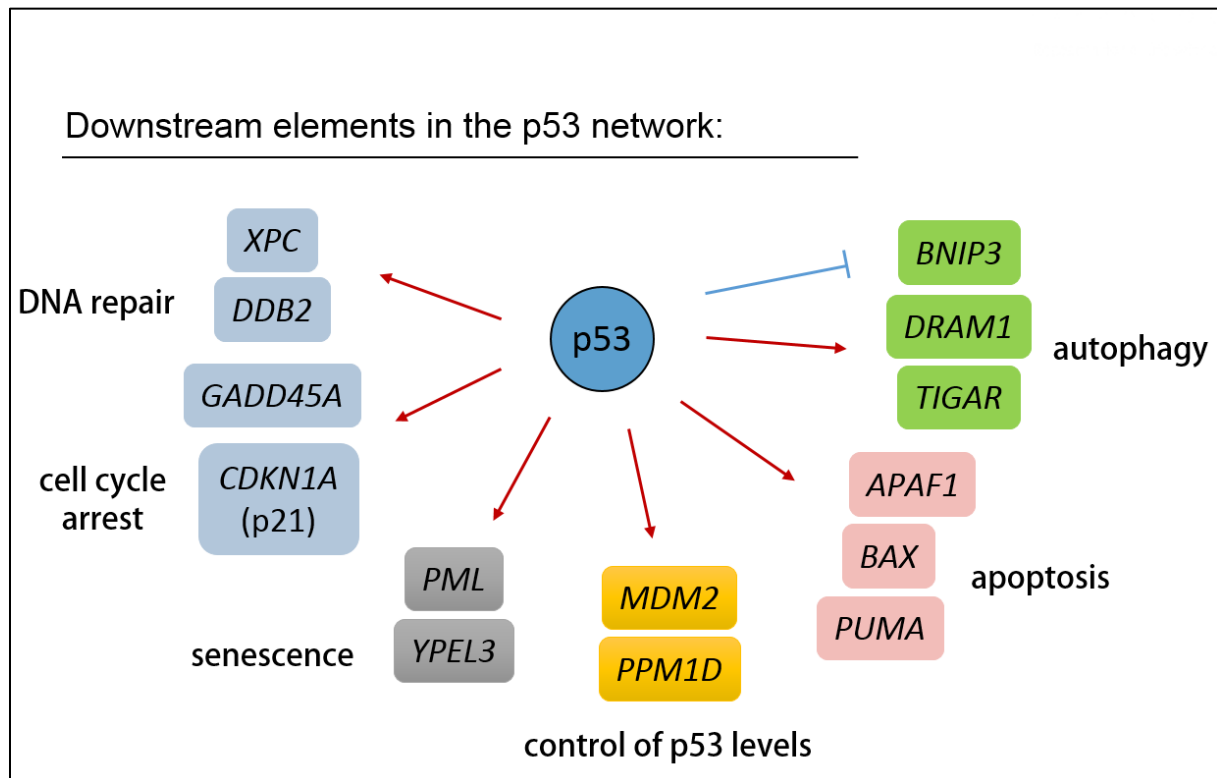
Figure 2.11 | Schematic overview of p53 responsive genes involved in different functional pathways and cellular outcomes. Induction of p53 triggers multiple cellular programs ranging from transient responses, such as DNA repair, autophagy and cell cycle arrest, to terminal fates such as cell death (apoptosis) and permanent cell cycle arrest (senescence). Shown are representative p53-responsive genes involved in the respective responses. Red arrows: transactivation; blue line: transrepression.

Meanwhile, to know the extent to which hypoxia modulates p53 responsive genes, siRNA was used to knock down HPV16 *E6/E7* under normoxia. Western Blot analysis (preliminary result) showed that when *E6/E7* is inhibited under normoxia by RNAi, p53 protein was strongly reconstituted (**Figure 2.12**). In *E6/E7*-repressed hypoxic HPV16-postive cancer cells, p53 protein showed a biphasic regulation (**Figures 2.2** and **2.12**)
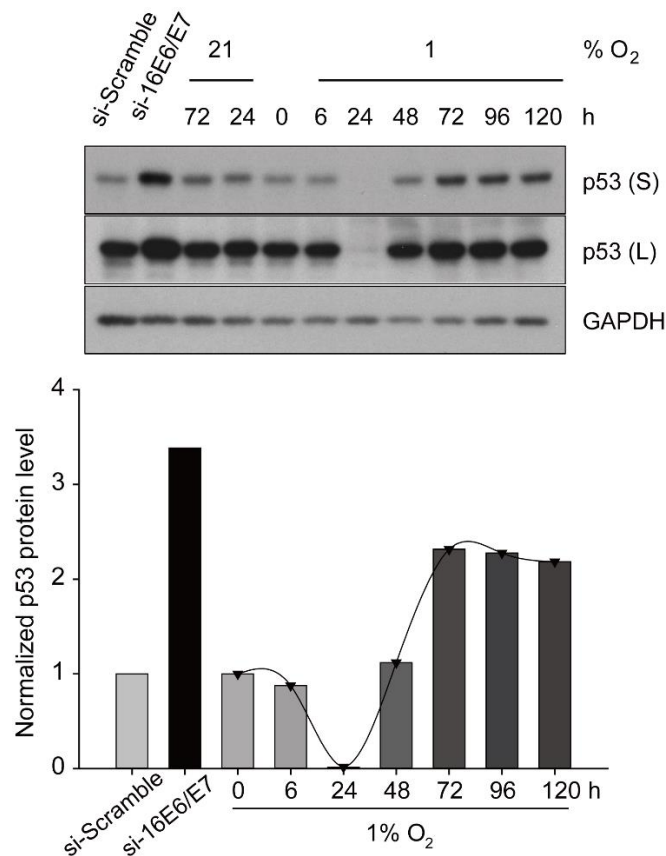
Figure 2.12 | Effect of HPV16 *E6/E7* silencing and hypoxia on the protein levels of p53 in HPV16-positive cancer cells. The *E6/E7* expression was silenced by RNAi under normoxia in SiHa cells (si-16E6E7) and total protein was extracted 48 h after transfection. In parallel, cells were cultured for the indicated time periods under normoxia (21% O_2) or hypoxia (1% O_2) and total protein was extracted after respective time intervals. (*top*) Western Blot analysis using antibody against p53. GAPDH served as a loading control. (S, short exposure; L, long exposure) (*bottom*) The grayscale of p53 from indicated samples was quantified using the ImageJ software. The relative grayscale values of p53 were normalized to the si-scramble group or 0 h value, respectively.

2.3.2.1 Genes whose products control p53 levels (*MDM2* and *PPM1D*)

The protein encoded by *MDM2* is a nuclear-localized E3 ubiquitin ligase, which targets p53 for nuclear export and proteasomal degradation. As described in chapter 1.3.2, *MDM2* is itself transcriptionally regulated by p53.

qPCR analyses showed that RNAi-mediated HPV16 *E6/E7* repression under normoxia resulted in increases in *MDM2* mRNA levels. Under hypoxic conditions, *MDM2* showed responses that mirrored p53 protein dynamics (decreased first, then recovered, **Figure 2.13**), indicating a transcriptional activity of p53 after prolonged hypoxia.
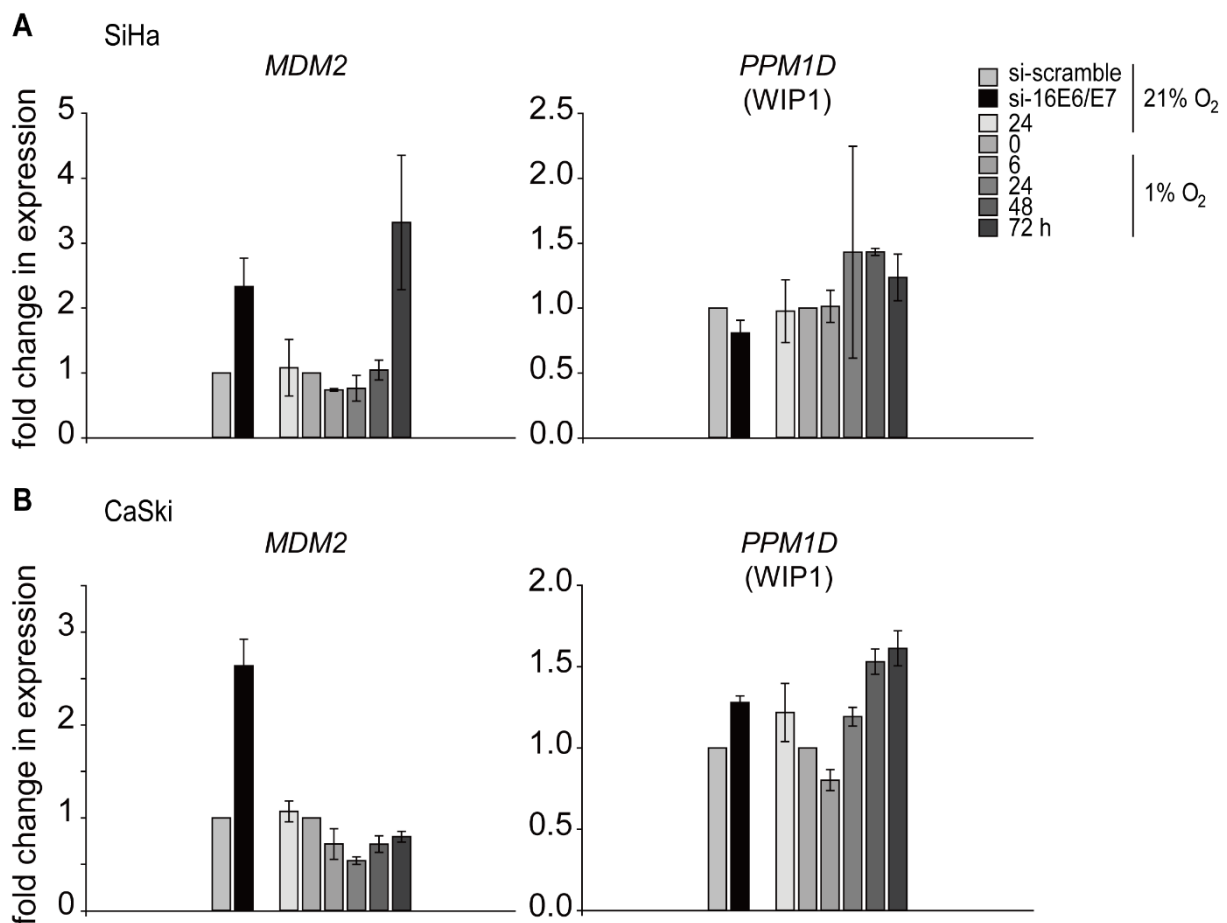
Figure 2.13 | Transcript levels of *MDM2* and *PPM1D* in HPV16-positive cancer cells. The *E6/E7* expression was silenced by RNAi under normoxia in SiHa and CaSki cells (si-16E6E7) and total RNA was extracted 48 h after transfection. In parallel, cells were cultured for the indicated time periods under normoxia (21% O_2) or hypoxia (1% O_2) and total RNA was extracted after respective time intervals. (A) and (B) qPCR analyses of *MDM2* and *PPM1D* transcripts. *18S* rRNA served as internal control for normalization. Error bars indicate the SD of three independent experiments. The si-scramble group or 0 h value of gene expression was set as a control (set to 1.0).

Protein phosphatase magnesium-dependent 1 delta (ppm1d)/wild-type p53 induced phosphatase 1 (WIP1) encoded by *PPM1D* is a member of the PP2C family of serine/threonine protein phosphatases, negative regulators of cell stress response pathways. The expression of *PPM1D* is induced in a p53-dependent manner in response to various environmental stresses. WIP1 negatively regulates the activity of p38 MAPK through which it reduces the phosphorylation of p53, and in turn suppresses p53-mediated transcription and apoptosis. WIP1 thus mediates a feedback regulation of p38-p53 signaling that contributes to growth inhibition and the suppression of stress induced apoptosis. The results of qPCR analyses showed that *PPM1D* (WIP1) remained relatively stable in hypoxic HPV16-positive cancer cells (**Figure 2.13**).

2.3.2.2 Transcripts encoding apoptotic proteins (*APAF1*, *BAX* and *PUMA*)

APAF1 (apoptotic peptidase activating factor 1) encodes a cytoplasmic protein (Apaf1) that initiates apoptosis. Upon binding dATP and cytochrome *c*, Apaf1 forms an oligomeric apoptosome. The apoptosome binds and cleaves caspase 9 preproprotein to release its mature, activated form. Activated caspase 9 stimulates the subsequent caspase cascade committing the cell to apoptosis. Apaf1 could also be a pro-survival molecule [241].

The results of qPCR analyses showed that *APAF1* was not strongly impaired (slightly decreased then marginally increased) in hypoxic CaSki cells, whereas in hypoxic SiHa cells, *APAF1* was transiently increased (~2 fold) at 6 h of hypoxia then showed a response that mirrored p53 protein dynamics (**Figure 2.14**).

Figure 2.14 | Transcript levels of *APAF1*, *BAX* and *PUMA* in HPV16-positive cancer cells. The *E6/E7* expression was silenced by RNAi under normoxia in SiHa (A) and CaSki cells (B), and total RNA was extracted 48 h after transfection. In parallel, cells were cultured for the indicated time periods under normoxia (21% O_2) or hypoxia (1% O_2) and total RNA was extracted after respective time intervals. (A) and (B) qPCR analyses of *APAF1*, *BAX* and *PUMA* transcripts. *18S* rRNA served as internal control for normalization. Error bars indicate the SD of three independent experiments. The si-scramble group or 0 h value of gene expression was set as a control (set to 1.0).

The genes *BAX* and *PUMA* encode members of the BCL-2 family of proteins. Bax (Bcl-2-associated X protein) forms a heterodimer with BCL2, and functions as an apoptotic activator. Bax can also interact with, and increase the opening of, the mitochondrial voltage-dependent anion channel (VDAC), which leads to a loss in membrane potential and the release of cytochrome *c*.

Puma (p53 upregulated modulator of apoptosis) belongs to the BH3-only pro-apoptotic subclass. Puma cooperates with direct activator proteins to induce mitochondrial outer membrane permeabilization (MOMP) and apoptosis. It can bind to anti-apoptotic Bcl-2 family members to induce caspase activation.

As depicted in **Figure 2.14**, the transcripts encoding apoptotic proteins Bax and Puma showed a tendency that is clearly consistent with the biphasic regulation observed in p53 protein levels. Transcripts of *BAX* and *PUMA* were repressed by hypoxia (0-24 h) but induced after prolonged hypoxia. The recovered mRNA levels of *BAX* and *PUMA* under prolonged hypoxia were comparable to the levels under RNAi-mediated *E6/E7* repression under normoxia (**Figure 2.14**).

Preliminary observations showed that under hypoxia (24 h), cleavage of Poly (ADP-ribose) polymerase (PARP) (MW: 89 kD), which is a marker of apoptosis [242, 243], was not induced (**Figure 3.9**). Cleaved-PARP was slightly induced after prolonged hypoxia (72 h, **Figure 3.9**). These data suggest that apoptosis was not induced under short-term hypoxia.

2.3.2.3 Genes involved in cell cycle arrest and DNA repair (*GADD45A* and *XPC*)

GADD45A (growth arrest and DNA damage inducible alpha) is a member of a group of genes whose transcript levels are increased following stressful growth arrest conditions and treatment with DNA-damaging agents. GADD45 proteins play important roles in regulation of cell cycle arrest and are also involved in DNA nucleotide excision repair and maintenance of genome stability.

The results of qPCR analyses showed that *GADD45A* showed a slight increase in SiHa cells and a two-fold increase in CaSki cells at 24 h of hypoxia (**Figure 2.15**). After prolonged hypoxia, *GADD45A* was strongly increased in SiHa cells (20 fold at 48 h, 10 fold at 72 h of hypoxia, **Figure 2.15A**), whereas it was decreased again in CaSki cells (decreased by half at 72 h of hypoxia, **Figure 2.15B**).

The protein encoded by *XPC* is a key component of the XPC complex, which plays an important role in the early steps of global genome nucleotide excision repair (NER). XPC is important for damage sensing and DNA binding, and shows a preference for single-stranded DNA.

qPCR analyses showed that the mRNA levels of *XPC* displayed a tendency that well mirrored p53 protein dynamics (decreased first, then recovered, **Figure 2.15**). *XPC* mRNA levels showed a

dramatic reduction of almost 80% at 24 h of hypoxia in SiHa cells and a decrease of almost 50% at 6 h of hypoxia in CaSki cells (**Figure 2.15**). After prolonged hypoxia, the transcript levels of *XPC* recovered to near normal levels (**Figure 2.15**).
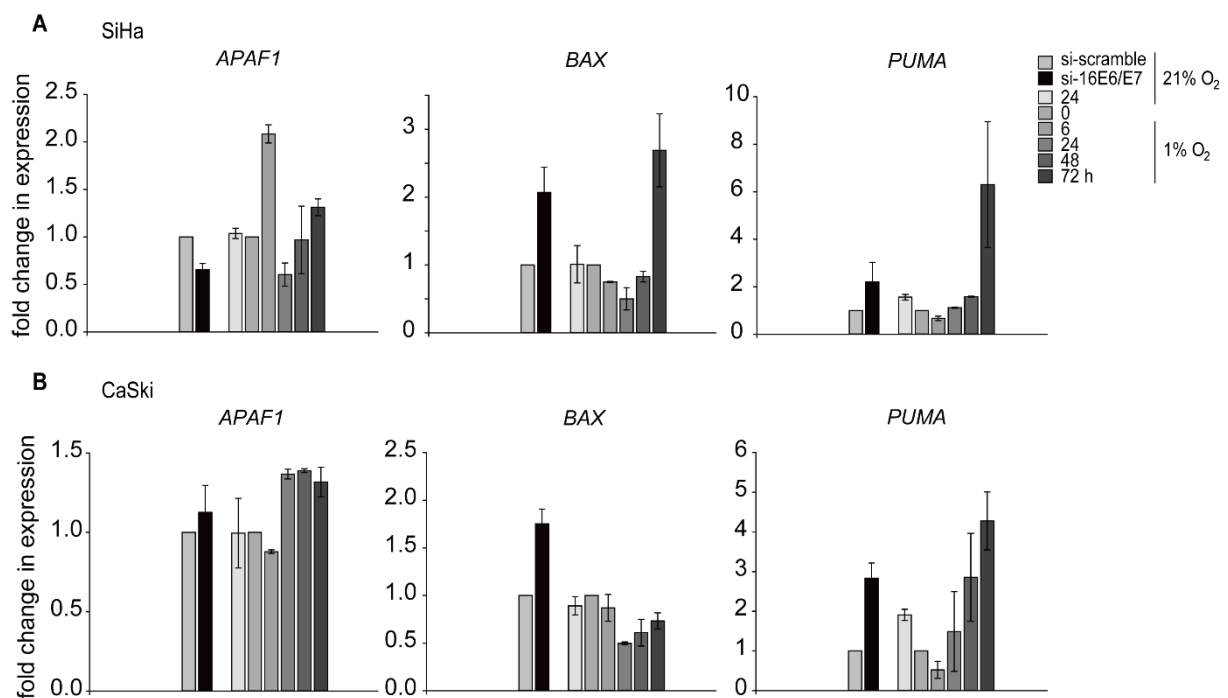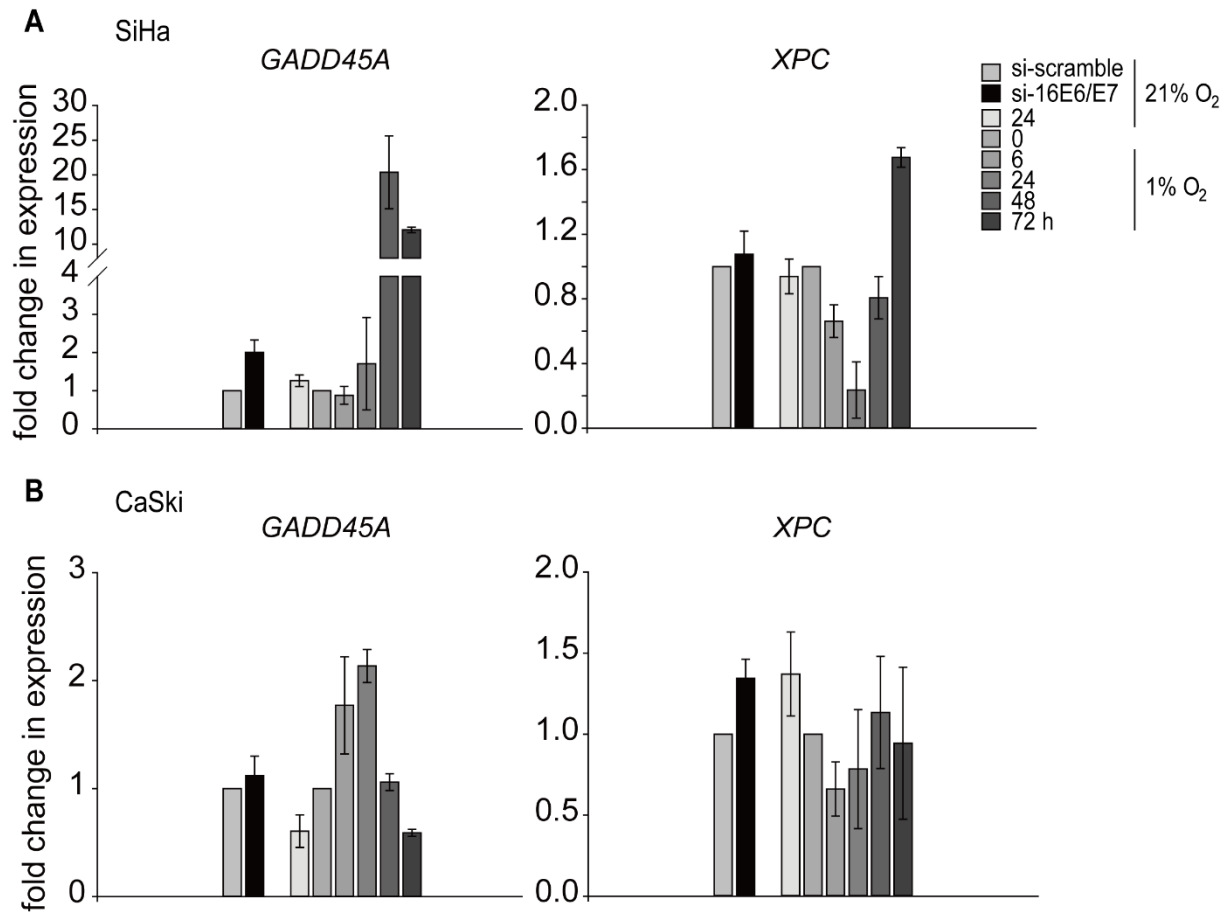

Figure 2.15 | Transcript levels of *GADD45A* and *XPC* in HPV16-positive cancer cells. The *E6/E7* expression was silenced by RNAi under normoxia in SiHa (A) and CaSki cells (B), and total RNA was extracted 48 h after transfection. In parallel, cells were cultured for the indicated time periods under normoxia (21% O_2) or hypoxia (1% O_2) and total RNA was extracted after respective time intervals. (A) and (B) qPCR analyses of *GADD45A* and *XPC* transcripts. *18S* rRNA served as internal control for normalization. Error bars indicate the SD of three independent experiments. The si-scramble group or 0 h value of gene expression was set as a control (set to 1.0).

2.3.2.4 Genes associated with p53-dependent senescence (*PML* and *YPEL3*)

Activation of the p53 signaling pathway is a classical cellular response leading to senescence when exposure to stresses occurs. Senescent cells are characterized by increased expression of certain p53 targets, such as p21, PML, PAI-1, and Yippee-like-3 (YPEL3) [239], all of which are recognized as senescence markers, and in turn are able to induce senescence themselves [244-249].

PML localizes to nuclear bodies where it functions as a transcription factor and tumor suppressor. PML nuclear bodies (PML-NBs) accumulate in senescent cells. PML is induced by several factors, including oncogenic stress and p53 activation [238, 248]. In turn, PML regulates the p53 response to oncogenic signals [248]. PML recruits p53, p16, and the pRb/E2F complex to PML-NBs and hence regulates the transcription of downstream target genes of these factors, resulting in cellular senescence [248, 250].

YPEL3, a member of the putative zinc finger motif coding gene family, is a p53-regulated gene. YPEL3 expression induced by stress leads to the recruitment of p53 to a *cis*-acting DNA response element located near the YPEL3 promoter. Induction of YPEL3 leads to a significant decrease in cell viability and triggers premature senescence [239].

The results of qPCR analyses showed that in SiHa cells, the transcript levels of *PML* and *YPEL3* were decreased under hypoxia and showed only a marginal recovery after prolonged hypoxia (**Figure 2.16A**). In hypoxic CaSki cells, *PML* mRNA levels were continuously decreased, whereas the transcript level of *YPEL3* showed a response that mirrored p53 protein dynamics (**Figure 2.16B**). The mRNA levels of *PML* and *YPEL3* showed minor increases under RNAi-mediated *E6/E7* repression under normoxia in both SiHa and CaSki cells (**Figure 2.16**).
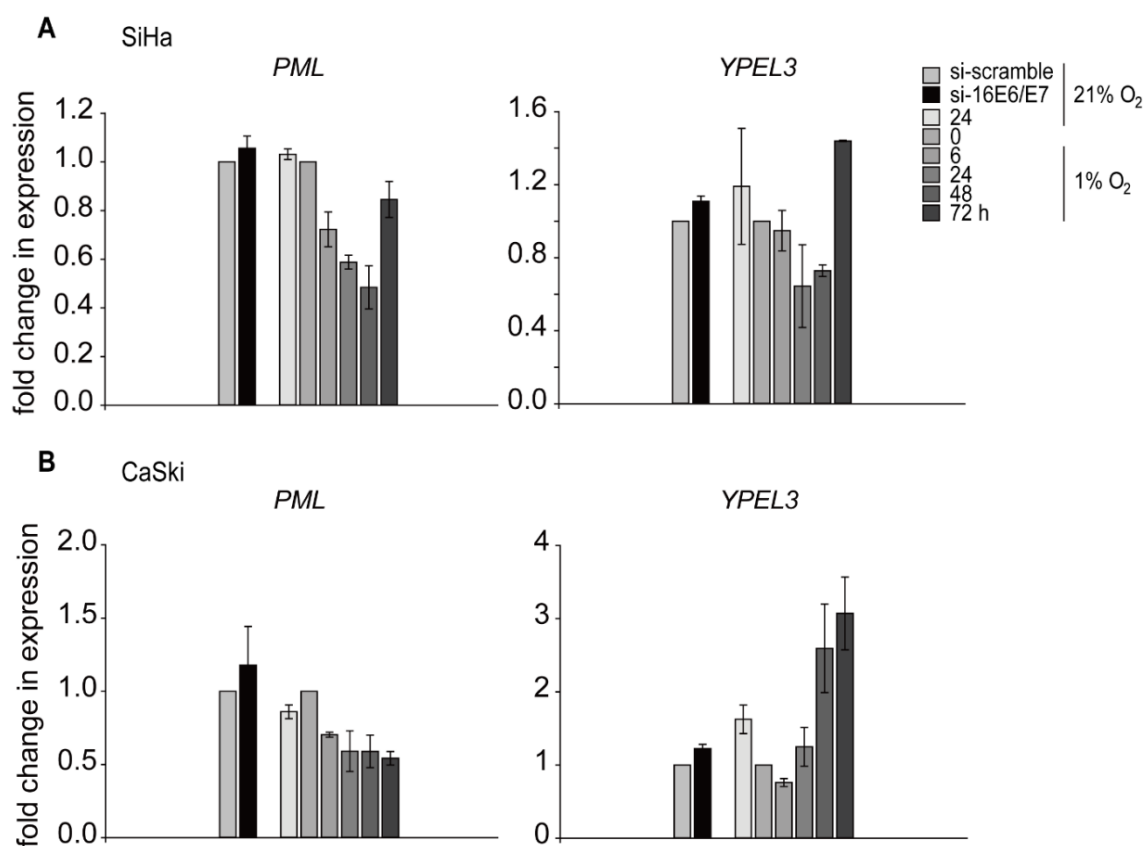
Figure 2.16 | Transcript levels of *PML* and *YPEL3* in HPV16-positive cancer cells. The *E6/E7* expression was silenced by RNAi under normoxia in SiHa (A) and CaSki cells (B), and total RNA was extracted 48 h after transfection. In parallel, cells were cultured for the indicated time periods under normoxia (21% O_2) or

hypoxia (1% O_2) and total RNA was extracted after respective time intervals. (A) and (B) qPCR analyses of *PML* and *YPEL3* transcripts. *18S* rRNA served as internal control for normalization. Error bars indicate the SD of three independent experiments. The si-scramble group or 0 h value of gene expression was set as a control (set to 1.0).

These results indicate that down-regulation of p53 by hypoxia (24 h) allows inactivation of genes associated with cell death (apoptosis) and cellular senescence.

2.3.2.5 *CDKN1A* (p21) involved in both cell cycle arrest and senescence

CDKN1A (cyclin dependent kinase inhibitor 1A) encodes p21 (also named Waf1/Cip1), a potent cyclin-dependent kinase (Cdk) inhibitor. The expression of *CDKN1A* is tightly controlled by p53, through which p21 mediates the p53-dependent cell cycle G1 phase arrest in response to a variety of stress stimuli. Besides its role for cell cycle arrest, p21 is also required for p53-dependent cellular senescence [251, 252].

CDKN1A mRNA levels showed fluctuations (increased 6 fold at 24 h, then decreased to normal level at 48 h, but increased 4 fold again at 72 h of hypoxia) in hypoxic SiHa cells (**Figure 2.17A**). In hypoxic CaSki cells, *CDKN1A* mRNA levels showed minor increases (**Figure 2.17B**). RNAi-mediated HPV16 *E6/E7* repression under normoxia resulted in increased *CDKN1A* mRNA levels (approximately 3 fold) in both SiHa and CaSki cells (**Figures 2.17A** and **2.17B**).

Figure 2.17 | Transcript levels of *CDKN1A* (p21) in HPV16-positive cancer cells. The *E6/E7* expression was silenced by RNAi under normoxia in SiHa (A) and CaSki cells (B), and total RNA was extracted 48 h after transfection. In parallel, cells were cultured for the indicated time periods under normoxia (21% O_2) or hypoxia (1% O_2) and total RNA was extracted after respective time intervals. (A) and (B) qPCR analyses of *CDKN1A* transcripts. *18S* rRNA served as internal control for normalization. Error bars indicate the SD of three independent experiments. The si-scramble group or 0 h value of *CDKN1A* expression was set as a control (set to 1.0).

2.3.2.6 Genes involved in autophagy (*DRAM1*, *BNIP3* and *TIGAR*)

DRAM1 (DNA damage-regulated autophagy modulator 1) is regulated as part of the p53 tumor suppressor pathway. It encodes a lysosomal membrane protein DRAM that is required for the induction of autophagy by the p53 signaling pathway mediating autophagic cell death [253].

The results of qPCR analyses showed that in SiHa cells the transcript levels of *DRAM1* were not strongly induced at the early stage of hypoxia (0-24 h) but increased after prolonged hypoxia (~4 fold at 48 and 72 h) (**Figure 2.18A**). In hypoxic CaSki cells, the *DRAM1* mRNA levels (**Figure 2.18B**) showed a response that mirrored p53 protein dynamics (**Figure 2.2D**), but its recovery after prolonged hypoxia was not as strong as the levels detected in hypoxic SiHa cells. The mRNA levels of *DRAM1* showed minor increases under RNAi-mediated *E6/E7* repression under normoxia in both SiHa and CaSki cells (**Figures 2.18A** and **2.18B**).

BNIP3 (BCL2 interacting protein 3) encodes a mitochondrial protein that contains a Bcl-2 homology 3 (BH3) domain and a carboxyl-terminal transmembrane (TM) domain. BNIP3 is regarded as a pro-apoptotic factor, interacting with anti-apoptotic proteins, such as Bcl2 and Bcl-xL [254-256]. Although linked to cell death, the normal function of BNIP3 appears to be in mitochondrial autophagy (mitophagy) [104, 257]. Accumulating evidence suggests that BNIP3 can protect against cell death by inducing mitophagy [106, 136, 137, 258] (see chapter 1.2.3.1). Increased expression of BNIP3 under hypoxia is mainly regulated by the transcription factor HIF-1α and can be directly suppressed by p53.

As depicted in **Figure 2.18**, the transcript levels of *BNIP3* were strongly induced under hypoxia. The *BNIP3* transcripts increased about tenfold already after 6 h of hypoxic incubation in SiHa cells. The induction of *BNIP3* reached the peak (~20 fold) at 24 h of hypoxia in SiHa cells (**Figure 2.18A**). In hypoxic CaSki cells, the transcript levels of *BNIP3* increased roughly five fold after 6 h of hypoxic incubation. It increased ~20 fold and ~28 fold at 24 h and 48 h of hypoxia, respectively in CaSki cells (**Figure 2.18B**). *BNIP3* was repressed under RNAi-mediated *E6/E7* inhibition under normoxia in SiHa cells (**Figure 2.18A**).
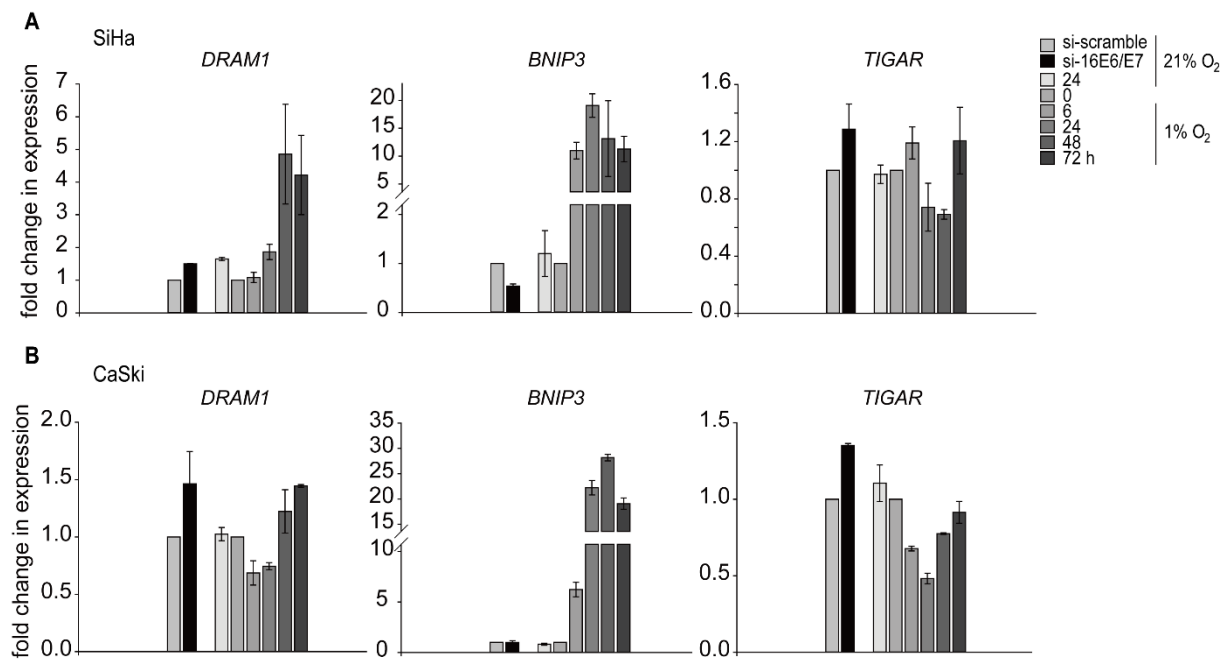
Figure 2.18 | Expression of genes involved in autophagy in HPV16-positive cancer cells. The *E6/E7* expression was silenced by RNAi under normoxia in SiHa (A) and CaSki cells (B), and total RNA was extracted 48 h after transfection. In parallel, cells were cultured fo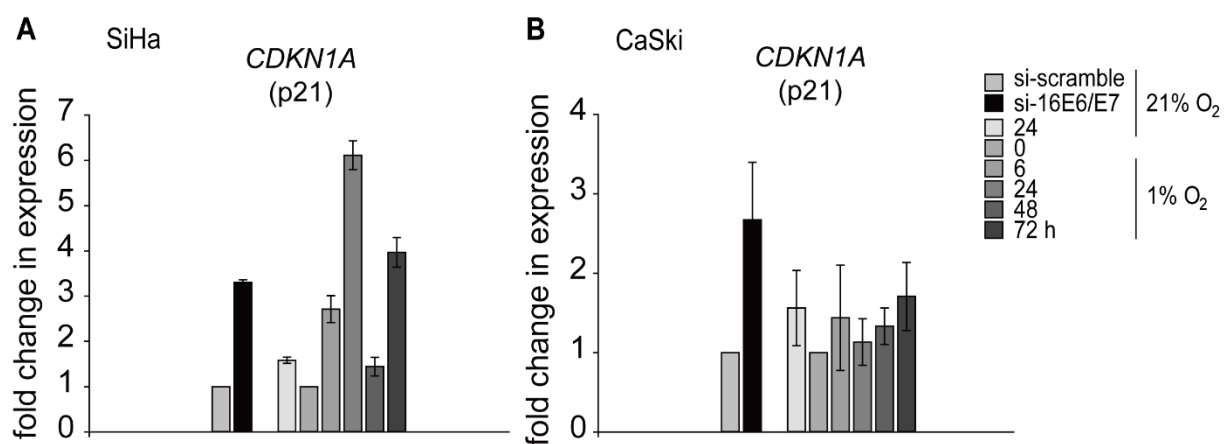r the indicated time periods under normoxia (21% O_2) or hypoxia (1% O_2) and total RNA was extracted after respective time intervals. (A) and (B) qPCR analyses of *DRAM1*, *BNIP3* and *TIGAR* transcripts. *18S* rRNA served as internal control for normalization. Error bars indicate the SD of three independent experiments. The si-scramble group or 0 h value of gene expression was set as a control (set to 1.0).

TIGAR (TP53 induced glycolysis regulatory phosphatase), also known as *C12orf5*, is regulated as part of the p53 tumor suppressor pathway [259], thereby controlling apoptosis, autophagy and metabolism [199, 260]. Containing a bisphosphate domain similar to the glycolytic enzyme fructose-2,6-bisphosphatase (FBPase-2), TIGAR converts fructose-2,6-bisphosphate to fructose-6-bisphosphate. Fructose-2,6-bisphosphate functions as a potent allosteric activator of 6-phosphofructo-1-kinase (PFK), a rate-limiting enzyme of glycolysis [261]. Hence, TIGAR blocks glycolysis, thereby redirecting cellular glucose metabolism into the pentose phosphate shunt. TIGAR also protects cells from oxidative stress as it reduces the production of reactive oxygen species (ROS) in cells [199, 262]. Loss of TIGAR induces autophagy and apoptosis [263, 264], and its expression protects cells from DNA damaging ROS-related cell death [265].

Under hypoxic conditions, the transcript levels of *TIGAR* showed responses that mirrored p53 protein dynamics (decreased first, then recovered, **Figure 2.18**). The mRNA levels of *TIGAR* showed minor increases under RNAi-mediated *E6/E7* repression under normoxia in both SiHa and CaSki cells (**Figure 2.18**).

These results suggest the possibility that autophagy is induced by hypoxia in HPV16-positive cancer cells.

In summary, hypoxic HPV16-positive cancer cells do not enter senescence despite efficient E6/E7 repression and p53 reconstitution. Hypoxia activates cellular programs involved in transient responses, such as cell cycle arrest and DNA repair. p53 downstream genes associated with terminal fates such as cell death (apoptosis) and permanent cell cycle arrest (senescence) are inactivated by hypoxia (24 h). Genes involved in promoting autophagy are strongly induced in hypoxic HPV16-positive cancer cells. The balance in downstream gene profiles of reconstituted p53 after prolonged hypoxia may contribute to cellular homeostasis and select cells resistant to apoptosis.

2.4 The evasion of hypoxic HPV16-positive cancer cells from senescence is attributable to the induction of autophagy

Autophagy (macroautophagy) is a self-destructive process by which eukaryotic cells degrade and recycle cellular macromolecules and organelles to provide nutrients for cell metabolism, particularly under conditions of nutrient deprivation [100, 101]. Cancer cells suffering limited nutrient supplies under cellular stresses may utilize autophagy for survival; such improved autophagic capabilities will benefit the cancer cells [110-115] (see chapter 1.2.3). Autophagy is essential to suppress cellular stress and has previously been shown to induce a dormant state, and prevent senescence [266-269]. Hypoxia-induced autophagy is further linked to hypoxia tolerance and tumor cell survival [102]. Genes involved in promoting autophagy were strongly induced, whereas a gene related to repression of autophagy (*TIGAR*) was not induced by hypoxia (**Figure 2.18**). It was therefore tested whether autophagy is involved in the evasion of hypoxic HPV16-positive cancer cells from senescence.

2.4.1 Hypoxia induces autophagy in HPV16-positive cervical cancer cells

The increase of LC3-II and the decrease of p62 are two markers of autophagy (described in chapter 1.2.3.1). As demonstrated in **Figure 2.19**, hypoxia induced autophagy in HPV16-positive cancer cells, as indicated by the increase of LC3-II and the quantitative reduction of p62. Preliminary observations showed that the mRNA levels of *LC3A*, *LC3B* and *p62* remained stable under hypoxia, indicating LC3 and p62 were post-translationally regulated by hypoxia (**Figure 3.10**).
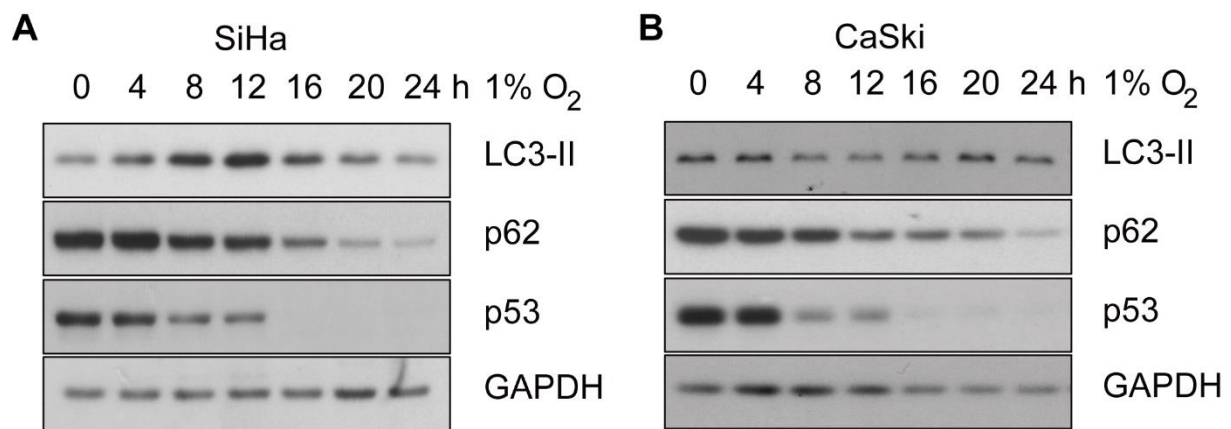
Figure 2.19 | Protein levels of LC3-II, p62 and p53 in hypoxic HPV16-positive cancer cells. HPV16-positive SiHa (A) and CaSki cells (B) were cultured for the indicated time periods at 1% O_2. Total protein was extracted after the respective time intervals. (A) and (B) Western Blot analyses using antibodies against LC3-II, p62 and p53. GAPDH served as a loading control.

2.4.2 p53 overexpression inhibits hypoxia-induced autophagy

As shown in **Figure 2.19**, LC3-II and p62 decreased after the reduction of p53. Tasdemir *et al.* showed that depletion of p53 facilitates autophagy in several cell lines, in response to several distinct stimuli [206].

In order to investigate whether the induction of autophagy observed in hypoxic HPV16-positive cancer cells is triggered by p53 depletion, p53 was overexpressed prior to hypoxic incubation. Compared to cells transfected with empty vector, overexpression of p53 diminished hypoxia-induced autophagy, as shown by the increased amounts of p62 at 1% O_2 (**Figures 2.20** and **3.13**). These results suggest that restoration of p53 protein prevents autophagy under these conditions.
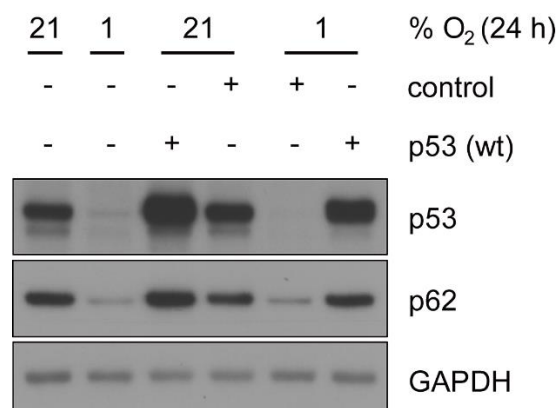
Figure 2.20 | Effect of overexpression of p53 protein on p62. SiHa cells were transfected with/without an empty vector control (control) or wild-type (wt) p53. 48 h post transfection, the cells were cultured for 24 h at 21% O_2 or at 1% O_2. Total protein was extracted. Western Blot analyses using antibodies against p53 and p62. GAPDH served as a loading control.

2.4.3 Inhibition of autophagy induces senescence in hypoxic HPV16-positive cancer cells

The above evidence raises the possibility that hypoxia-associated initial reduction of p53 facilitates the induction of autophagy to allow HPV16-positive cervical cancer cells to evade senescence.

In order to investigate whether inhibition of autophagy induces senescence, SiHa and CaSki cells were incubated with the autophagy inhibitor chloroquine (CQ). Although the hypoxic cells treated with CQ did not stain strongly positive for SA-β-Gal, these cells showed the characteristic morphological signs of senescence (for example cell enlargement, flattening) and an apparent inability to grow when switched back to normoxic culture conditions (**Figures 2.21** and **3.14**). These findings indicate that autophagy is critical for the evasion of senescence during hypoxia.
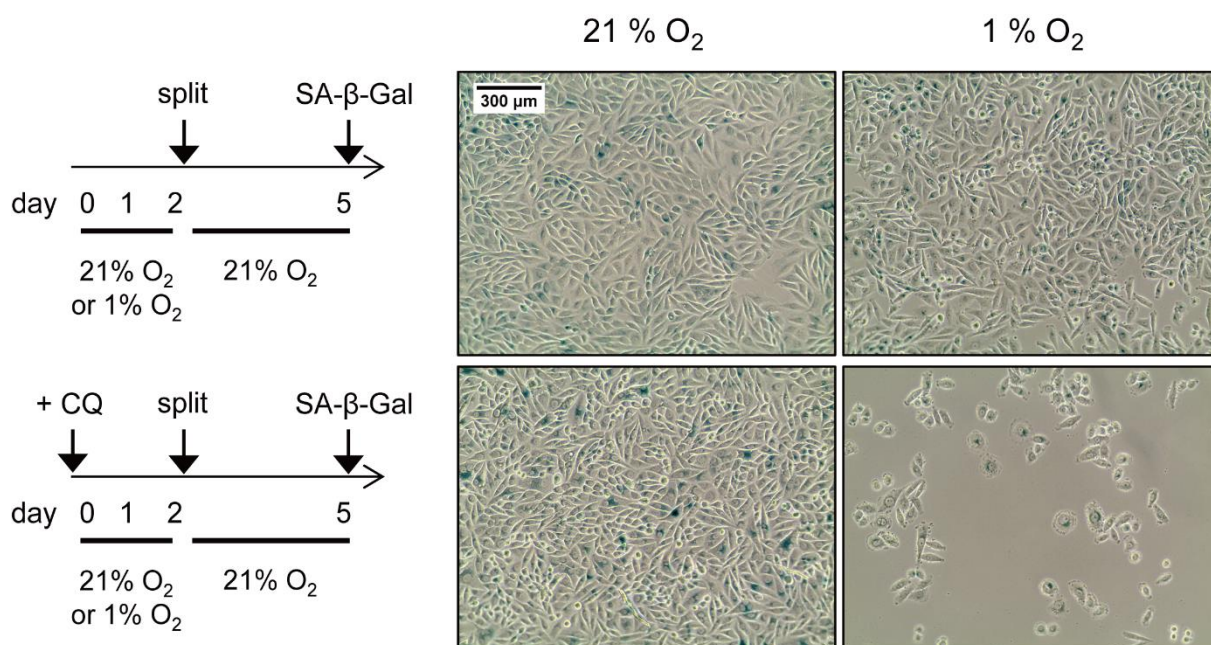
Figure 2.21 | Analyses of cellular senescence upon treatment with autophagy inhibitor CQ in HPV16-positive cancer cells. SiHa cells were cultivated for 48 h under normoxia (21% O$_2$) or hypoxia (1% O$_2$), in either the absence (*top*) or the presence (*bottom*) of 50 μM chloroquine (CQ). Cells for senescence assays (SA-β-Gal staining) subsequently cultured under normoxia. Scale bar: 300 μm. Scheme *left*: Treatment protocol.

In summary, hypoxia-associated initial reduction of p53 facilitates the induction of autophagy. The evasion of hypoxic cells from senescence appears to be attributable to the induction of autophagy.

Taken together, these findings revealed a new regulation pattern of p53 during hypoxia and provide new insights into the effect of p53 regulation on downstream pathway responses and

cellular adaptation. In spite of continuous down-regulation of HPV16 *E6/E7* oncogenes under hypoxia, p53 protein does not immediately reconstitute, but shows a biphasic regulation [rapidly and strongly depleted under hypoxia (24 h), then recovered after prolonged hypoxia]. p53 is predominantly degraded via a lysosome-dependent mechanism in hypoxic cells. Down-regulation of p53 by hypoxia (24 h) helps to avoid the boost of downstream genes associated with terminal fates such as cell death (apoptosis) and permanent cell cycle arrest (senescence). The balance in downstream gene profiles of reconstituted p53 after prolonged hypoxia may contribute to cellular homeostasis and select cells resistant to apoptosis. Hypoxic activation of cellular programs involved in transient responses, such as DNA repair and autophagy protect cells from committing to an irreversible fate. Hypoxia-associated initial reduction of p53 facilitates the induction of autophagy to allow HPV16-positive cervical cancer cells to evade senescence. Inhibition of autophagy can induce senescence in hypoxic HPV16-positive cancer cells.

3. Discussion

The tumor suppressor p53, a pivotal regulator of cellular responses, functions as a stress-activated transcription factor. p53 regulates numerous cellular responses including cell cycle arrest, DNA repair, apoptosis, senescence, autophagy and metabolism. Oxygen deprivation (hypoxia) is one of the stresses that have been shown to affect p53 signaling.

Cervical cancers often display strongly reduced O_2 content, with a median O_2 concentration of 1.18%. Therefore, hypoxia is frequently detected in cervical cancer patients and has a negative impact on patient prognosis [48, 49]. Nevertheless, functional studies of HPV-positive cancer cells under hypoxic conditions are rare. In these few studies, the regulation of p53 by hypoxia in HPV-positive cells appears to be controversial and the role of p53 in the cellular adaptation to hypoxia remains elusive [50, 51, 213, 214, 270]. This PhD thesis describes for the first time a biphasic regulation of p53 under hypoxic conditions in HPV16-positive cervical cancer cells and reveals the mechanism controlling this regulation of p53 by hypoxia. This study provides also new insights into the effect of p53 regulation on p53 downstream pathway responses and cellular adaptation under hypoxia. The biphasic regulation of p53 and its role in cellular adaptation to hypoxia will be discussed in this section.

3.1 Using standard O_2 concentration and serial duration of hypoxia for systematic study

Although different studies have been performed to investigate the regulation of p53 under hypoxia in the context of HPV, the methods used in these studies to obtain hypoxic conditions are widely divergent. The O_2 concentration used ranges from 0.02% to 1% [50, 51, 213, 214]. In all tested cell lines, the duration of hypoxic incubation was only up to 24 h. Under the different experimental conditions in these studies using completely different O_2 concentrations, p53 protein showed multiple trends under hypoxia in the investigated HPV-positive cell lines.

As mentioned above, cervical cancers display reduced O_2 content with a median O_2 concentration of 1.18%. Moreover, cancer cells are differentially exposed to hypoxia for minutes to hours or even days [271-275]. Therefore, this PhD thesis conducted experiments using a standard O_2 concentration (1% O_2) for hypoxic conditions to systematically investigate the dynamics of p53 during different periods of hypoxia in HPV-positive cervical cancer cells.

3.2 Regulation of HPV16 *E6/E7* oncogenes and p53 protein under hypoxia (1% O$_2$)

Under normoxic conditions, the HPV oncoproteins E6 and E7 target the tumor suppressors p53 and pRb for degradation and inactivation, respectively. Sustained expression of the viral *E6* and *E7* genes is considered to be required for maintaining the malignant phenotype of HPV-positive cervical cancer cells

3.2.1 Repression of HPV16 *E6/E7* oncogenes under hypoxia

In this study, HPV16 oncogenes *E6* and *E7* were found repressed under hypoxic conditions (**Figures 2.1** and **2.2**). The HPV oncogenes normally induce cell proliferation. This process consumes cellular energy in the form of ATP and needs a sufficient nutrient supply. Preliminary observations found that under hypoxia, the supply of energy (cellular ATP levels) was limited in SiHa cells (**Figure 3.1A**) and cell numbers reached a plateau after 24 h (**Figure 3.1B**), suggesting hypoxia inhibits the proliferation of SiHa cells. The decrease in relative ATP levels after 24 h of normoxia in SiHa cells may be due to a reduced cell metabolic activity resulting from overgrowth of cells under normoxic culture conditions.

Hypoxic down-regulation of HPV *E6/E7* oncogenes might serve as a survival strategy of the infected cells under stress. In other words, the cells down-regulate HPV oncogenes and instead of undergoing extensive proliferation they maintain their survival under hypoxia.
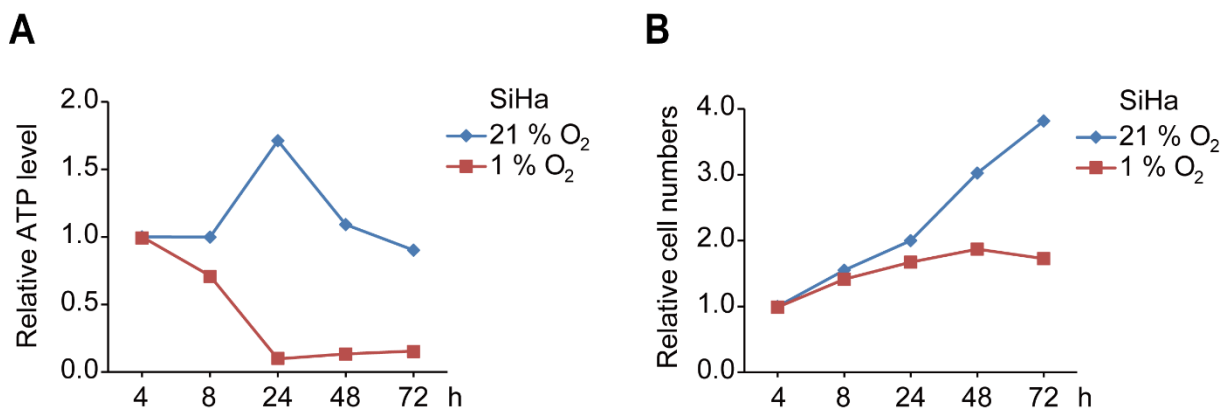
Figure 3.1 | Relative ATP Levels and cell numbers in HPV16-positive SiHa cells under normoxia and hypoxia. SiHa cells were cultured for the indicated times at 21% O$_2$ or at 1% O$_2$. Relative ATP levels (A) and cell numbers (B) were determined after respective time intervals. For each assay, initial values (time point 4 h) were set to 1.0.

CaSki cells possess more than 500 viral genome copies, of which however only few are expressed, whereas the SiHa cell line was reported to contain only 1-2 copies of HPV16 [276, 277]. Furthermore, both E6 and E7 have very short half-lives of less than 60 min [278]. Thus, transcript

levels of HPV16 *E6/E7* oncogenes were used to investigate hypoxic regulation of HPV *E6/E7* oncogenes in cervical cancer cells (**Figures 2.1** and **2.2**).

3.2.2 Biphasic regulation of p53 protein in hypoxic HPV16-positive cancer cells

The down-regulation of HPV oncogenes upon hypoxia was hypothesized to reconstitute p53 protein and reactivate pRb. Hoppe-Seyler *et al.* reported that phosphorylated pRb levels decreased and pRb protein remained stable when *E6/E7* oncogenes were repressed under hypoxia (24 h) [50]. These results coincided with the fact that under hypoxia the pace of cervical cancer cell growth was slowed down, with cell numbers reaching a plateau after 24 h (**Figure 3.1B**). After prolonged hypoxia, phosphorylated pRb levels might continue to be down-regulated, as indicated by the cessation of cell growth.

In spite of the strong down-regulation of HPV16 *E6/E7* oncogenes under hypoxia, p53 protein did not immediately reconstitute, but rather showed a biphasic regulation (rapidly and strongly depleted first, then markedly recovered after prolonged hypoxia) (**Figure 2.2**).

Expression and activation of the tumor suppressor p53 can be influenced by diverse cellular stresses. The abundance and activity of p53 depend on cell type and the nature and extent of the stresses. Among the studies investigating the regulation of p53 under hypoxia in the context of HPV, severe hypoxic conditions (0.02% O_2 or < 0.2% O_2) are prone to induce p53 [51, 213] and a standard hypoxic condition (1% O_2) represses p53 at 24 h [50, 214]. In this study, p53 protein was decreased at 24 h of hypoxia (1% O_2). Prolonged hypoxia (> 48 h) induced p53 in these cells (**Figure 2.2**). The divergent regulation patterns of p53 under hypoxia can be explained by the use of different severity and duration of oxygen deprivation [51, 210-212]. The difference in the course of biphasic regulation and the extent of recovery of p53 under hypoxia could be due to the different cell types.

3.3 Different glucose levels and cell types

Different glucose levels

As described in chapter 1.2.2, one feature of tumor cells is an altered glucose metabolism that is significantly different from normal cells. Tumor cells tend to use glycolysis for obtaining ATP (Warburg effect). It is well known that hypoxia activates glycolysis and inhibits mitochondrial respiration. The Warburg effect is associated with glucose uptake and utilization [90, 91]. Altered

glucose metabolism is therefore suspected to influence the regulation of p53 under hypoxic conditions.

Preliminary observations found that higher levels of glucose delayed the course of the biphasic regulation of p53 protein in hypoxic HPV16-positive cancer cells (**Figure 3.2B**). When CaSki cells were cultured in medium containing higher glucose levels (2 g/L), the reduction and the recovery of p53 appeared later (at 12 h and 72 h of hypoxia, respectively, **Figure 3.2B**) than those observed in cells cultured in medium containing physiological serum glucose levels (1 g/L) (at 6 h and 48 h of hypoxia, respectively, **Figures 2.2 D** and **3.2A**).
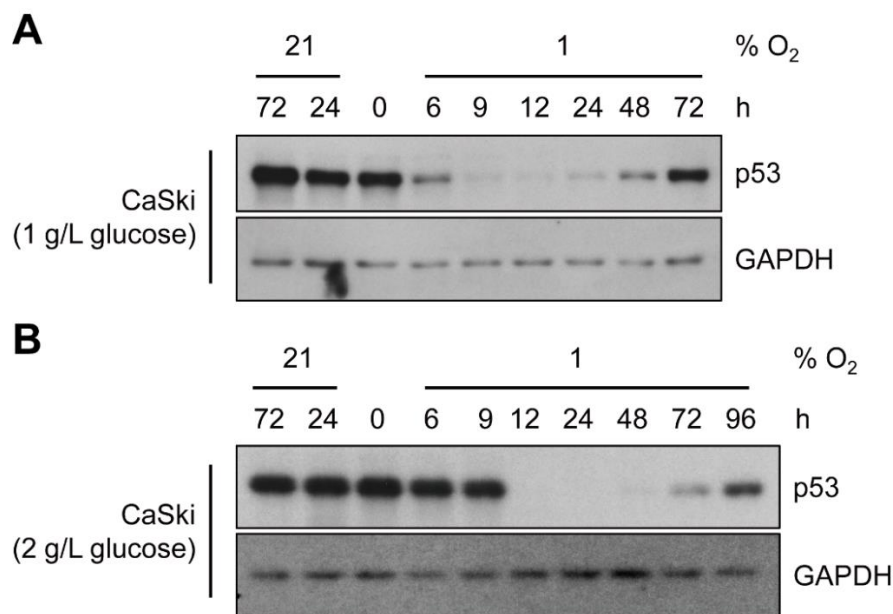
Figure 3.2 | Effect of different levels of glucose on the course of the biphasic regulation of p53 protein in hypoxic HPV16-positive CaSki cells. CaSki cells were cultured in the medium containing different levels of glucose (A, 1 g/L and B, 2 g/L) for the indicated time periods under normoxia (21% O_2) or hypoxia (1% O_2). Total protein was extracted after respective time intervals. Western Blot analyses were performed using antibody against p53. GAPDH served as a loading control.

When SiHa cells were cultured in medium devoid of glucose or serum (0 g/L), the hypoxic depletion of p53 protein was advanced by the glucose deprivation (already appeared at 4 h of hypoxia, **Figure 3.3A**), but not by serum deprivation (**Figure 3.3B**). These preliminary data suggest that glucose metabolism plays an important role in the regulation of p53 under hypoxia.

A

B
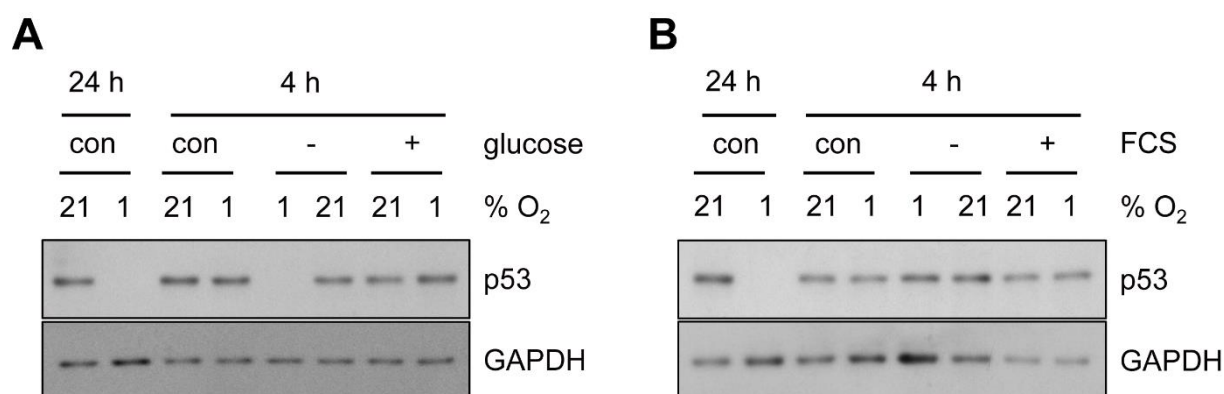
Figure 3.3 | **Effect of glucose deprivation or serum deprivation on depletion of p53 in hypoxic SiHa cells.** SiHa cells were grown in medium containing 1 g/L glucose and 10% FCS (control group, con). The absence (–) or presence (+) of glucose (A) or FCS (B) in the medium is indicated. Cells were cultured for 4 h or 24 h under normoxia (21% O_2) or hypoxia (1% O_2). Total protein was extracted after respective time intervals. Western Blot analyses were performed using antibody against p53. GAPDH served as a loading control.

Different cell types

In addition to the severity as well as the duration of oxygen deprivation, previous studies suggest that the regulation of p53 by hypoxia also depends on the cell line. Preliminary experiments using the HPV-negative hepatocellular carcinoma cell line HepG2 (wild-type p53) showed that during different periods of hypoxia, the tendency of a biphasic regulation of p53 protein could also be observed in hypoxic HepG2 cells (**Figure 3.4**). This implied that the biphasic regulation of p53 under hypoxia seems to occur independently of HPV oncogenes.
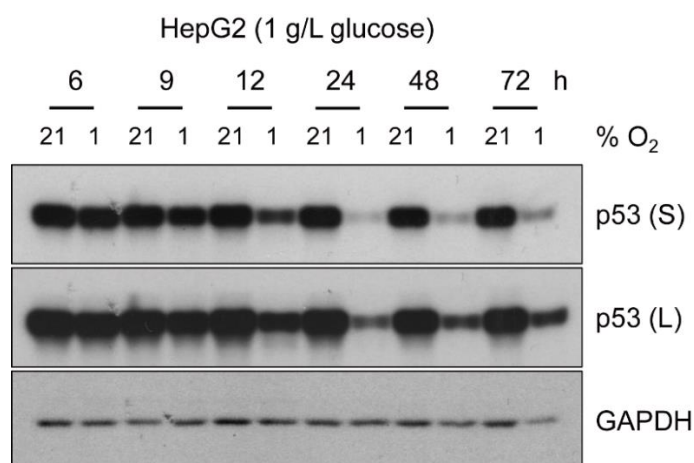
Figure 3.4 | **p53 protein levels in HPV16-negative HepG2 cancer cells under normoxia and hypoxia.** HepG2 cells were cultured in medium containing low levels of glucose (1 g/L) for the indicated time periods under normoxia (21% O_2) or hypoxia (1% O_2). Total protein was extracted after respective time intervals. Western Blot analysis was performed using antibody against p53. GAPDH served as a loading control. (S, short exposure; L, long exposure)

Discussion

When HepG2 cells were cultured in medium containing higher glucose levels (4.5 g/L), p53 protein levels gradually decreased in HepG2 cells (**Figure 3.5**). This suggests that glucose levels should be considered when the effect of hypoxia on p53 is investigated.
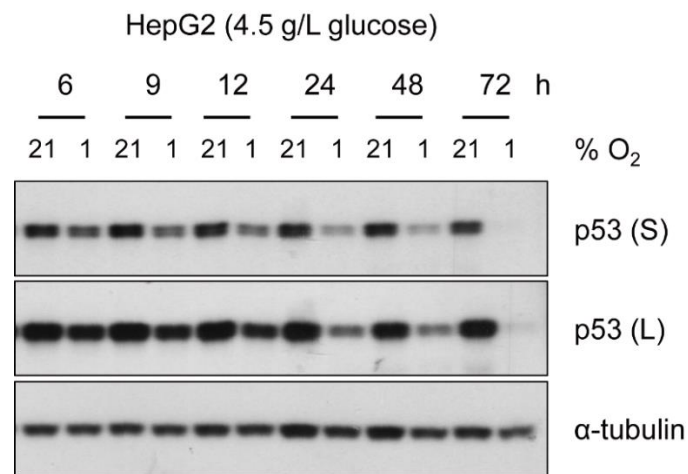
Figure 3.5 | p53 protein levels in HPV16-negative HepG2 cancer cells under normoxia and hypoxia. HepG2 cells were cultured in medium containing high levels of glucose (4.5 g/L) for the indicated time periods under normoxia (21% O_2) or hypoxia (1% O_2). Total protein was extracted after respective time intervals. Western Blot analysis was performed using antibody against p53. α-tubulin served as a loading control. (S, short exposure; L, long exposure)

It has been shown that the loss of p53 function contributes to the metabolic switch of glucose metabolism from oxidative mitochondrial respiration to glycolysis [279]. As described in chapter 1.3.3, p53 modulates the balance between the utilization of the respiratory and glycolytic pathways but in an opposite way to hypoxia, by promoting oxidative phosphorylation and dampening glycolysis [201]. As shown in **Figure 2.18**, TIGAR which lowers fructose-2,6-bisphosphate levels to inhibit glycolysis was decreased in hypoxic HPV16-positive cancer cells. Thus, hypoxic initial down-regulation of p53 may facilitate the metabolic switch to glycolysis in HPV16-positive cancer cells.

3.4 Mechanisms underlying the regulation of p53 in hypoxic HPV16-positive cancer cells

3.4.1 p53 transcript levels and protein stability

In this study, the tendency of p53 transcript levels (**Figure 2.3**) are not accompanied by time-dependent changes of p53 protein (**Figure 2.2**). Acute hypoxia (6 h) had no significant effects on *TP53* mRNA levels (**Figure 2.3**). The decrease in *TP53* mRNA levels under hypoxia (after 24 h in SiHa cells and after 48 h in CaSki cells, **Figure 2.3**) could be due to an overall down-regulation of

gene expression, which might be impaired by limited energy and cellular material under hypoxic stress, in HPV16-positive cancer cells.

Among reports that describe the regulation of p53 by hypoxia, most argue for p53 stabilization under hypoxia. However, Wang *et al.* showed that increased p53 protein levels by hypoxia were due to an increase in p53 mRNA levels [280]. Galban *et al.* showed an increased p53 mRNA translation under hypoxia without any change in mRNA levels [281]. pVHL (Von Hippel Lindau protein), which is a transcriptional target of HIF-1 and therefore induced under hypoxia, could enhance p53 translation in a way involving the RNA-binding protein HuR [281]. A transcriptional repression of the human p53 gene was shown when HIF-1a was accumulated by $CoCl_2$ [282]. Fu *et al.* reported that accumulation of HIF-1α by $CoCl_2$ inhibited the expression of p53 in HPV18-positive HeLa cells [270].

Hypoxia reduced the *TP53* mRNA levels by half in SiHa cells at 24 h (**Figure 2.3A**). One therefore cannot exclude that the depletion of p53 protein at 24 h under hypoxia was partially due to decreased transcription in SiHa cells (**Figures 2.2C** and **2.3A**). However, treating HPV16-positive cancer cells with CHX, an inhibitor of eukaryotic protein synthesis [217], pre-treating with hypoxia was found to decrease p53 protein half-life (**Figure 2.4**). This suggested that down-regulation of p53 protein under hypoxia (0-24 h) was attributable to decreased p53 protein stability in HPV16-positive cancer cells.

For further studies, it would be interesting to perform a CHX-chase experiment after prolonged hypoxia (48 or 72 h) to detect whether p53 stability was increased under prolonged hypoxia in HPV16-positive cancer cells. Despite a decrease in p53 mRNA levels, p53 protein was recovered after prolonged hypoxia (**Figures 2.2** and **2.3**). As mentioned before, hypoxia-induced pVHL could enhance p53 translation [281]. Hence, one could hypothesize that prolonged hypoxia may increase p53 translation and protein stability.

3.4.2 Proteasomal degradation and lysosomal degradation

As described in chapter 1.3.2, localization and stability of p53 protein are tightly regulated by a variety of post-translational modifications (PTMs). Protein stability, as well as localization, are regulated by mono-ubiquitination and poly-ubiquitination mediated by ubiquitin ligases. MDM2 is regarded as the master regulator not only of p53 protein levels but also of p53 localization in a variety of cellular systems (see chapter 1.3.2). Additionally, in cells infected with HPV, such as

Discussion

HPV16 and HPV18, the viral E6 protein promotes the binding of p53 to the E3 ubiquitin ligase E6-AP, which ubiquitinates p53 efficiently and causes the proteasomal degradation of p53. Hengstermann *et al.* described a complete switch from MDM2 to HPV E6-mediated degradation of p53 in cervical cancer cells [283]. Thus, proteasomal degradation plays a key role in the regulation of p53 protein levels.

However, in this study, the p53 protein levels in hypoxic HPV16-positive cancer cells could not be fully increased to comparable levels detected under normoxic conditions when incubated with MG132 (**Figure 2.5**). As mentioned in chapter 2.2.4, MG132 is not a selective inhibitor for proteasomes. It can also inhibit the function of lysosomes [218, 221, 222]. One can therefore conclude that in HPV16-positive cancer cells the reduction of p53 levels by hypoxia was not (solely) mediated via proteasomal degradation.

Besides the ubiquitin/proteasome system, the autophagy-lysosome-dependent pathway is another important cellular system for protein degradation (see chapter 1.2.3.1 and 2.2.4).

Hoppe-Seyler *et al.* showed that hypoxic HPV-positive cells do not appear to switch from E6-dependent to MDM2-dependent p53 degradation, given that treatment with Nutlin-3, a potent inhibitor of the MDM2/p53 interaction [284], did not appreciably increase p53 levels in HPV-positive cancer cells [50]. Vakifahmetoglu-Norberg *et al.* reported that suppression of macroautophagy promotes the degradation of mutant p53 through chaperone-mediated autophagy (CMA) in a lysosome-dependent fashion [285]. Hence, lysosome-mediated degradation was suspected to play a role in the regulation of p53 protein in hypoxic HPV16-positive cancer cells.

Here, the autolysosome inhibitor CQ [223, 224] could prevent the p53 degradation triggered by hypoxia in HPV16-positive cancer cells. Bafilomycin A1, which inhibits the fusion of autophagosomes and lysosomes [225-227], however, only prevented the degradation of p62 but not p53, suggesting that, unlike p62, p53 was not sequestered by autophagosomes, but degraded via the lysosomal pathway (**Figure 2.6**).

In normoxic HPV-positive cancer cells, the p53 levels are predominantly dependent on E6/E6-AP-mediated proteolytic p53 degradation [25, 286, 287]. In this study, under hypoxia, the E6/E6-AP-dependent ubiquitination system was impaired, as indicated by the repression of *E6* oncogene and the diminishment of E6-AP (**Figures 2.2** and **3.6**). Moreover, hypoxic HPV-positive cells did not switch from E6-dependent to MDM2-dependent p53 degradation [50]. These clues suggest that the ubiquitination of p53 may be severely impaired in hypoxic HPV-positive cancer cells.

Vakifahmetoglu-Norberg *et al.* reported that susceptibility to ubiquitination determines the degradation pathways of wild-type (wt) and mutant p53 proteins [285]. The wt p53 protein, which was susceptible to ubiquitination, was subjected to proteasomal degradation. The mutant p53, which was degraded through chaperone-mediated autophagy (CMA) in a lysosome-dependent manner, was not ubiquitinated [285]. Furthermore, interestingly, Gogna *et al.* described that the conformation of wt p53 is oxygen-dependent and exists in mutant conformation in hypoxic tumors [288]. Hypoxia is known to induce the disappearance of homeodomain-interacting protein kinase 2 (HIPK2), resulting in an increased p53 "mutant-like" conformation [289]. Moreover, chaperones (such as CHIP [290], HSP90, and HSP70 [291]) interact with p53 under stress conditions. These considerations raise the possibility that p53 was subjected to chaperone-mediated lysosomal degradation in hypoxic HPV-positive cancer cells.

The exact mechanism by which the lysosome-dependent pathway induces the down-regulation of p53 in hypoxic HPV16-positive cervical cancer cells is not determined yet. It would be interesting to investigate whether the ubiquitination of p53 is impaired under hypoxia and whether a lower ubiquitination rate of p53 contributes to lysosomal degradation. In addition, the cofactors contributing to p53 degradation in hypoxic HPV-positive cancer cells could be determined by immunoprecipitation followed by mass spectrometry analysis (IP-MS).

3.4.3 Autophagy (macroautophagy) is not required for p53 degradation

Tasdemir *et al.* showed that many different inducers of autophagy (for example starvation and rapamycin) stimulated proteasome-dependent degradation of p53 through a pathway relying on the E3 ubiquitin ligase MDM2 [206]. Inhibition of p53 degradation prevented the activation of autophagy (macroautophagy) in several cell lines, in response to several distinct stimuli [206]. The group found that autophagy is not required for depletion of p53. Rather, depletion of p53 seems to be necessary for the induction of autophagy [206].

Here, inhibition of autophagy (macroautophagy) by silencing *ATG12* or *p62/SQSTM1* did not rescue p53 levels under hypoxia (**Figure 2.9**). Overexpression of p53 prevented hypoxia-induced autophagy in HPV16-positive cancer cells (**Figures 2.20** and **3.13**).

Moreover, Hoppe-Seyler *et al.* showed that p53 levels were not restored in hypoxic HPV-positive cancer cells upon activation of mTOR signaling, which represses autophagy [292], and did not decrease upon inactivation of mTOR signaling in normoxic cells [50].

Discussion

These results are consistent with the conclusion by Tasdemir *et al.* [206], suggesting autophagy is not responsible for the depletion of p53, whereas depletion of p53 is required for induction of autophagy. However, hypoxic HPV16-positive cancer cells utilized a lysosome-dependent pathway, but did not rely on MDM2-proteasome-dependent degradation to remove p53, "the brake of autophagy".

3.4.4 Restoration of p53 after prolonged hypoxia

The regulation of p53 protein by hypoxia depends on the duration of oxygen deficiency. Here, p53 protein markedly increased after prolonged hypoxia (**Figures 2.2C** and **2.2D**). The biphasic regulation of p53 under hypoxia may be caused by different PTMs of p53 protein during different stages of hypoxia, such as phosphorylation on different sites of p53. The dynamically changing PTMs of p53 under hypoxia may cause nuclear-cytoplasmic shuttling of p53 and nuclear/cytoplasmic redistribution of p53, which is critical for p53 degradation [293] and has a major role in the regulation of autophagy [206].

MDM2 acts not only as an E3 ligase modulating p53 protein levels but also as a regulator controlling p53 localization [166]. HPV E6-mediated degradation of p53 required the nuclear export function of MDM2 [294]. It was proposed that hypoxic suppression of MDM2-mediated nuclear export of p53 plays a key role in p53 stabilization under hypoxia [295]. Decrease of MDM2 levels by hypoxia has indeed been observed in several studies [213, 296, 297].

Although *MDM2* transcript levels were induced after prolonged hypoxia in SiHa cells (**Figure 2.13A**), preliminary experiments that investigated the changes of E3 ligases of p53 protein showed that E6-AP and MDM2 were diminished after prolonged hypoxia in SiHa cells (**Figures 3.6** and **3.7**).
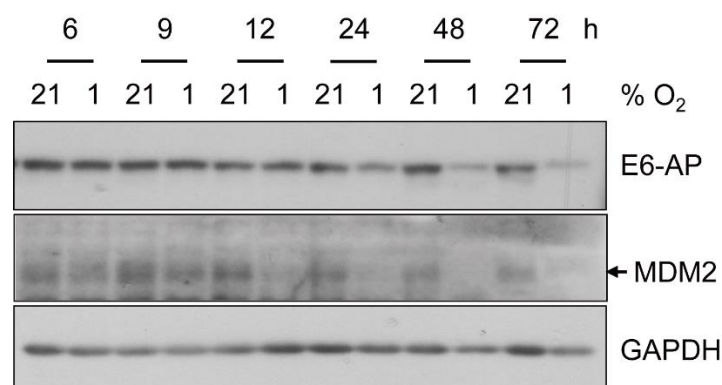
Figure 3.6 | Protein levels of E6-AP and MDM2, E3 ligases of p53, in SiHa cells under normoxia and hypoxia. SiHa cells were cultured for the indicated time periods at the indicated O_2 concentrations (normoxia: 21% O_2 and hypoxia: 1% O_2). Total protein was extracted after respective time intervals. Western Blot analysis was performed using antibodies against E6-AP and MDM2. GAPDH served as a loading control.

As already mentioned in chapter 2.3.2, preliminary experiments of cell fractionation analysis with SiHa cells indicate that after prolonged hypoxia, the restored p53 was predominantly localized in the nucleus (72 h, **Figure 3.7**). These preliminary results suggest that prolonged hypoxia could repress MDM2 protein to promote p53 nuclear localization contributing to p53 stabilization.
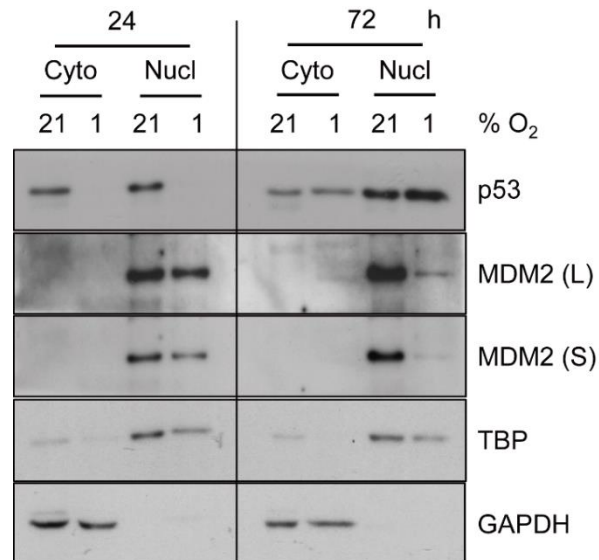
Figure 3.7 | Cellular localization of p53 and MDM2 in SiHa cells under normoxia and hypoxia. SiHa cells were cultivated for 24 h or 72 h under normoxia or hypoxia. Nuclei were extracted. Shown are immunoblots of p53 and MDM2 protein levels. TBP and GAPDH served as loading controls for cytoplasmic (Cyto) and nuclear (Nucl) proteins, respectively. (L, long exposure; S, short exposure)

Stabilization via phosphorylation of p53 on serine 15 is also frequently observed under hypoxia and could be a result of the activation of ataxia-telangiectasia mutated (ATM) or ataxia-telangiectasia mutated and Rad3-related kinases (ATR) by hypoxia [298, 299]. Serine 15 phosphorylation of p53 has also been reported to prevent its interaction with MDM2 [176]. One could hypothesize that prolonged hypoxia may increase PTMs of p53 that promote p53 stability and lead to the nuclear localization of p53 in HPV16-positive cancer cells. It would be interesting to explore the dynamics of PTMs of p53 protein during different periods of hypoxic conditions in HPV16-positive cancer cells (phosphorylation, ubiquitination, acetylation, and hydroxylation).

According to all that has been observed by us, the following model can be hypothesized (**Figure 3.8**). During different periods of hypoxia, p53 protein shows a biphasic regulation [rapid and strong depletion under hypoxia (0-24 h), then recovery after prolonged hypoxia] in HPV16-positive cancer cells. Under hypoxic conditions (0-24 h), since the E6/E6-AP-dependent ubiquitination system is impaired, p53 protein is predominantly degraded via a lysosome-dependent mechanism in HPV16-positive cancer cells. After prolonged hypoxia, with the

elimination of inhibitory factors (E6/E6-AP and MDM2), p53 protein is stably synthesized and transported into the nucleus in HPV16-positive cancer cells.
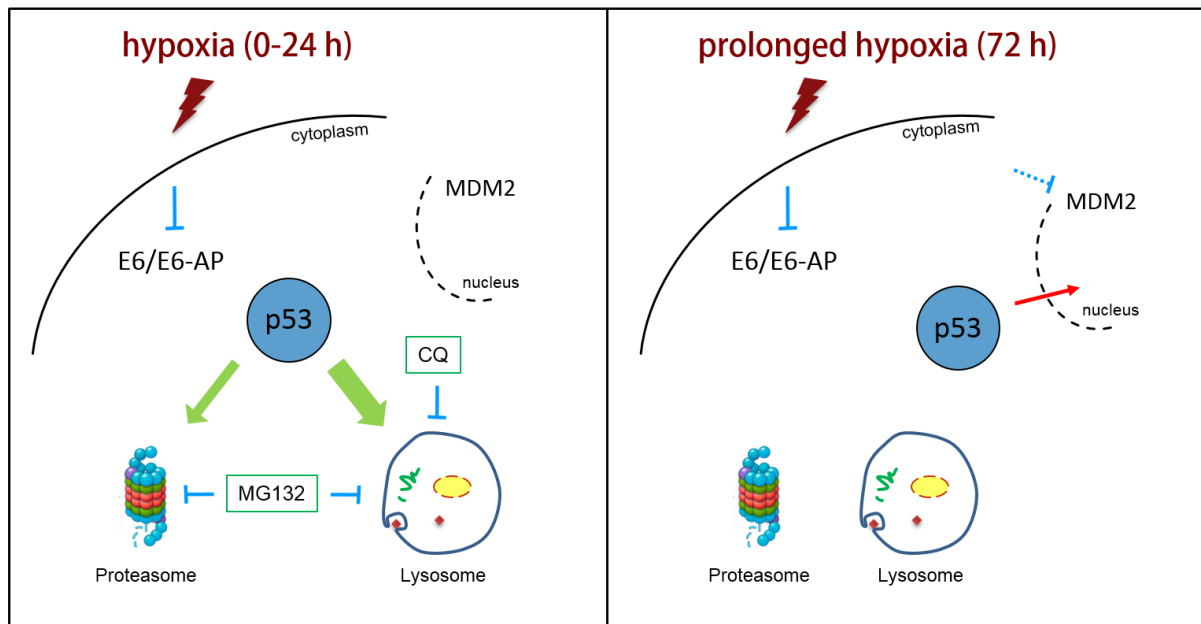
Figure 3.8 | Schematic overview of the biphasic regulation of p53 protein in HPV16-positive cancer cells. (*Left*) Under hypoxic conditions (0-24 h), MDM2 promotes nuclear export of p53. p53 protein is predominantly degraded via a lysosome-dependent mechanism in HPV16-positive cancer cells. (*Right*) After prolonged hypoxia, p53 protein is stably synthesized and transported into the nucleus in HPV16-positive cancer cells.

3.5 Downstream effects of the hypoxia-induced biphasic regulation of p53 protein in HPV16-positive cancer cells

The effect of hypoxia on p53 has been studied for decades. The regulation of p53 by hypoxia has usually been linked to induction of apoptosis [51, 211] or selection of cells resistant to cell death [51, 142].

Although the best-studied functions of p53 relate to its control of cell cycle arrest and cell death, accumulating evidence suggests that this protein represents a pleiotropic regulator in the stress-induced cellular response networks. Diverse activities of p53 are important not only in DNA repair, induction of cell cycle arrest and apoptosis but also in senescence, autophagy and metabolism. The effect of p53 regulation on these cellular responses in hypoxic cervical cancer cells remains elusive. Moreover, the dynamics of p53 during different periods of hypoxic conditions in cervical cancer cells are still not well explored. The effect of p53 dynamics on downstream responses (target gene expression and cellular outcomes) in hypoxic HPV16-positive cervical cancer cells will be discussed in this chapter.

In this study, target genes of p53 displayed different expression dynamics in response to the biphasic regulation of p53 in hypoxic HPV16-positive cervical cancer cells. Some of them showed responses that mirrored p53 protein dynamics (decreased first, then recovered), including *MDM2*, *BAX*, *PUMA*, *XPC*, *YPEL3* and *TIGAR* in both SiHa and CaSki cells (**Figures 2.13**, **2.14**, **2.15**, **2.16** and **2.18**). Other p53 target genes, like *PPM1D* (WIP1), *APAF1* and *DRAM1*, showed a relatively stable tendency or minor increases. The different expression dynamics of these p53 target genes may be determined by their distinct mRNA half-lives. Porter *et al.* reported that patterns of p53 target gene expression responding to stress cluster into groups with stereotyped temporal behaviors, including pulsing and rising dynamics. These behaviors correlate statistically with the mRNA decay rates of target genes: short mRNA half-lives produce pulses of gene expression [300]. Melanson *et al.* also reported that the expression of most p53-induced transcripts was rapidly reversible, consistent with active mRNA decay. Short-lived p53 targets were induced faster, reaching maximum transcript levels earlier than the stable p53 targets [301].

The different fold change in expression of p53 target genes, such as *MDM2*, *BAX*, and *DRAM1* (**Figures 2.13**, **2.14** and **2.18**), when p53 protein recovered in SiHa and CaSki cells may be due to the different amounts of recovered p53 protein in these cells (**Figure 2.2**). Furthermore, the transactivation activity of hypoxia-induced p53 was impaired under hypoxia [296, 302-305]. The transactivation activity of p53 under prolonged hypoxia in SiHa and CaSki cells may be different, thereby resulting in different transcript levels of p53 target genes.

The role of target gene expression dynamics for downstream responses and cellular outcomes/ fates will be discussed in the following parts.

3.5.1 Control of p53 levels

Despite increases in *MDM2* mRNA levels, p53 protein was strongly reconstituted upon repression of HPV16 *E6/E7* mediated by RNAi in normoxic SiHa cells (**Figures 2.12** and **2.13**). The reconstitution of p53 protein may be due to PTMs (such as serine 15 phosphorylation) on p53, which prevent its interaction with MDM2, even though *MDM2* was induced in *E6/E7*-specific siRNA-transfected SiHa cells.

Under hypoxic conditions, the remaining MDM2 at 24 h of hypoxia (**Figure 3.7**) may cause nuclear export of p53 in hypoxic HPV16-positive cancer cells. As discussed in chapter 3.4.4, although *MDM2* transcript levels were induced after prolonged hypoxia in SiHa cells (**Figure**

2.12A), preliminary experiments showed that MDM2 protein levels were diminished after prolonged hypoxia in SiHa cells (**Figures 3.6** and **3.7**). The decrease in MDM2 protein levels might be caused by its auto-ubiquitination, which allows for its degradation by the proteasome [306].

WIP1 (*PPM1D*), a phosphatase, negatively regulates the activity of p38 MAP kinase, MAPK/p38, through which it reduces the phosphorylation of p53, and in turn suppresses p53-mediated transcription and apoptosis. This phosphatase thus mediates a feedback regulation of p38-p53 signaling contributing to inhibition of growth and the suppression of stress-induced apoptosis. Here, *PPM1D* remained relatively stable in hypoxic HPV16-positive cancer cells (**Figure 2.12**). It has already been reported that hypoxia had no effect on *PPM1D* [307]. This phosphatase might help to dephosphorylate p53 protein leading to its interaction with MDM2 and nuclear export under hypoxia (0–24 h).

3.5.2 Cell death (apoptosis)

As for the analyses of p53 target genes associated with apoptosis in hypoxic SiHa cells, *APAF1* was transiently increased (~2 fold) at 6 h of hypoxia (**Figure 2.13**). This can be explained by a possible transient transcriptional activation of Apaf1 by p53 at 6 h of hypoxia in SiHa cells. It was proposed that Apaf1 has a pro-survival effect. Ferraro *et al.* found that Apaf1-depleted cells exhibit low Bcl-2 and Bcl-XL expression, under an apoptotic stimulus, rapidly releasing cytochrome *c* [241]. Loss of Apaf1 impairs cell homeostasis and leads to an enhanced responsiveness to stressful conditions. Compared with wild-type cells, Apaf1-depleted cells are more fragile and have a lower threshold to stress [241].

In addition, cytochrome *c*-initiated activation of Apaf1 is a crucial step in the mitochondrial signaling pathway for the activation of death-executing caspases in apoptosis. Decreased oxygen levels cause dysfunction and reorganization of mitochondria, major places of oxygen consumption [97] and induce mitochondrial autophagy (mitophagy) [106, 139, 140]. These effects may influence the release of cytochrome *c* and then impair the formation of the apoptosome by Apaf1 in hypoxic HPV16-positive cancer cells.

Repression of *BAX* and *PUMA* under hypoxia (0-24 h, **Figure 2.14**) might help to avoid MOMP and the release of cytochrome *c* and inhibit apoptosis when *E6/E7* is repressed in hypoxic HPV16-positive cancer cells. As discussed in chapter 1.3.4, p53 itself can translocate to mitochondria to

trigger MOMP and cytochrome *c* release. Furthermore, Sansome *et al.* reported that hypoxia induces p53 translocation toward mitochondria [308]. Thus, rapid and strong degradation of p53 by hypoxia (0-24 h) might serve as a protective strategy of the hypoxic HPV16-positive cancer cells to avoid the pro-apoptotic functions of p53 and to prevent mitochondrial functions of p53 (induction of mitochondrial membrane permeabilization and cytochrome *c* release).

Under conditions of sustained hypoxia, the up-regulation of *BAX* and *PUMA* by hypoxia-induced p53 may promote apoptosis, thus contributing to the selection of HPV16-positive cervical cancer cells resistant to apoptosis.

It has previously been reported that hypoxic conditions contribute to the selection of cells with reduced apoptotic potential [51, 309]. Hoppe-Seyler *et al.* reported that hypoxia induced HPV-positive cancer cells enter a dormant state [50]. Upon reoxygenation, the growth arrest of the HPV-positive cancer cells was overcome and cells resumed proliferation [50], suggesting that the hypoxic HPV-positive cancer cells were viable.

Previous lab results (a FACS analysis using propidium iodide (PI) dye) obtained by Dr. Khalkar found that no G1 arrest of the HPV-positive cells was observed under hypoxia (24 h), indicating an inhibition of apoptosis. As mentioned in chapter 2.3.2.2, in this study, preliminary observations showed that under hypoxia (24 h), cleavage of PARP was not induced in HPV16-positive cancer cells (**Figure 3.9**). Cleaved-PARP was slightly induced after prolonged hypoxia (72 h, **Figure 3.9**).
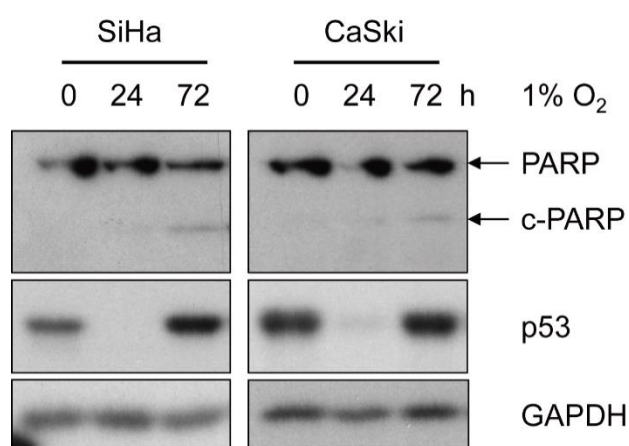
Figure 3.9 | **Cleavage of PARP in hypoxic HPV16-positive cancer cells.** SiHa and CaSki cells were cultured for the indicated time periods at 1% O_2. Total protein was extracted after respective time intervals. Western Blot analyses using antibodies against PARP, cleaved PARP (c-PARP) and p53 are shown. GAPDH served as a loading control.

These data suggest that apoptosis was not induced in hypoxic HPV16-positive cancer cells. The resistance to apoptosis of cervical cancer cells SiHa and CaSki under hypoxia might be due to pre-accumulation of several mutations that favour cell proliferation/survival and inhibit apoptosis under stress conditions [51]. After prolonged hypoxia, some cancer cells facing a severe hypoxic condition with limited energy and nutrient supplies may however go into apoptosis. The selected

hypoxic HPV16-positive cervical cancer cells resistant to stress conditions may serve as reservoirs for cancer recurrence upon reoxygenation.

3.5.3 Cell cycle arrest and DNA repair

Hypoxia is known to induce cell cycle arrest, drive genomic instability, and alter DNA damage repair pathways [210, 310-312]. The inhibition of growth is a cellular response to hypoxia induced via the induction of the cyclin-dependent kinase inhibitors p21 and p27 as well as via the de/hypo-phosphorylation of pRb [311]. Hypoxia-induced replication stress was shown to induce activation of ATM and ATR, the DNA damage response (DDR) apical kinases, and phosphorylation of downstream targets such as Chk1, Chk2, and p53, albeit in the absence of detectable DNA damage [298, 299, 313]. As described in chapter 3.2.1, the pace of cervical cancer cell growth was slowed down under hypoxia, with cell numbers reaching a plateau after 24 h (**Figure 3.1**) suggesting hypoxia caused a proliferative halt in HPV-positive cancer cells.

In the analyses of expression of genes involved in cell cycle arrest and DNA repair, despite the depletion of p53 under hypoxia (24 h, **Figure 2.2**), *GADD45A* increased at 24 h of hypoxia (**Figure 2.15**). After prolonged hypoxia, *GADD45A* was more increased in SiHa cells (**Figure 2.15A**), whereas it was decreased again in CaSki cells (**Figure 2.15B**).
CDKN1A (p21) mRNA levels showed fluctuations in hypoxic SiHa cells (**Figure 2.17A**). In hypoxic CaSki cells, *CDKN1A* mRNA levels showed minor increases (**Figure 2.17B**). RNAi-mediated HPV16 *E6/E7* repression under normoxia resulted in increased *CDKN1A* mRNA levels (approximately 3 fold) in both SiHa and CaSki cells (**Figure 2.17**).
It is important to note that the transcriptions of *GADD45A* and *CDKN1A* are mediated by both p53-dependent and -independent mechanisms, a fact that can explain the divergent changes of *GADD45A* and *CDKN1A* mRNA levels in hypoxic HPV16-positive cancer cells. *GADD45A* is also transcriptionally regulated by ATF4 (activating transcription factor-4) [314]. ATF4 is a transcription factor translationally regulated by severe hypoxic stress [315, 316]. p21 has also been described to be induced by hypoxia in a p53-independent manner. Hypoxia causes a HIF-1α-dependent increase in the expression of the cyclin-dependent kinase inhibitor p21 [317]. Moreover, several studies reported that cell cycle arrest under hypoxia occurred independently of p53 [210, 311]. Therefore, hypoxia and p53 may act synergistically to induce cell cycle arrest via regulation of GADD45 α and p21 during different time periods in HPV16-positive cancer cells.

As discussed in chapter 3.2.1, due to the limited energy and nutrient supplies under hypoxic conditions, induction of cell cycle arrest instead of proliferation might serve as a survival strategy of HPV16-positive cancer cells.

It has been reported that exposure to hypoxia results in a rapid stop of DNA synthesis in the absence of DNA damage [318]. Sustained exposure to hypoxia induces DNA damage [319]. Acute or short-term hypoxia (0-24 h), however, may not cause DNA damage in HPV16-positive cancer cells. DNA damage and DNA repair may rather occur after prolonged hypoxia (72 h). As a DNA damage sensor, the regulation of XPC might occur dependent on the severity and the duration of hypoxia.

Besides the induction of the DNA damage response (DDR) under hypoxic conditions, hypoxic cells can acquire a "mutator" phenotype (decreased DNA repair, an increased mutation rate and increased chromosomal instability) [310]. As observed in **Figure 2.15**, after prolonged hypoxia, the recovered *XPC* mRNA levels were no more than two fold as high compared to the 0 h values in HPV16-positive cancer cells. A decrease in DNA repair might contribute to the accumulation of mutations that favour cell survival under hypoxic stress conditions in HPV16-positive cancer cells.

3.5.4 Senescence

In this study, HPV16 *E6/E7* continuously decreased under hypoxia (**Figures 2.2A** and **2.2B**) and p53 protein displayed a biphasic regulation and markedly increased after prolonged hypoxia (**Figures 2.2C** and **2.2D**). Hypoxic HPV16-positive cancer cells did not stain positive for the senescence marker SA-β-Gal despite efficient *E6/E7* repression and p53 reconstitution. Neither at 24 h of hypoxia nor after prolonged hypoxia (72 h) was senescence induced (**Figure 2.10**).

Activation of the p53 signaling pathway is a classical cellular response leading to cellular senescence when exposure to stresses occurs. Senescent cells are characterized by increased expression of certain p53 targets, such as p21, PML, PAI-1, and YPEL3, all of which are recognized as senescence markers, and in turn are able to induce senescence themselves [244-249]. Here, unlike the increases in transcript levels under RNAi-mediated *E6/E7* repression under normoxia, the downstream target genes of p53 (*PML*, *YPEL3*, and *CDKN1A*) associated with p53-dependent senescence were not stably expressed during hypoxia (decreased or fluctuated, **Figures 2.16** and **2.17**).

De Stanchina *et al.* showed that loss of PML reduces the propensity of cells to undergo apoptosis or senescence in response to the activation of p53 signaling, in spite of the induction of several downstream target genes of p53 [238]. Moreover, Purvis *et al.* proposed that in addition to the amplitude of p53 signaling, PTMs of p53 and cofactors binding to p53, the dynamics of p53 protein can be a critical part of p53 signaling, directly affecting the course of downstream pathway programs and influencing cell fate decisions [320]. Cells exposed to sustained p53 signaling frequently undergo senescence, whereas cells that experience oscillating p53 dynamics recover from stress. Sustained increases in expression of p53 downstream target genes (*PML*, *YPEL3*, and *CDKN1A*) are required for cellular senescence [320]. The biphasic regulation of p53 protein resulting in fluctuations of the expression of p53 downstream target genes (*PML*, *YPEL3*, and *CDKN1A*) may contribute to an evasion of senescence. The sustained stable expression of *PML*, *YPEL3*, and *CDKN1A* under RNAi-mediated *E6/E7* repression under normoxia might be able to induce senescence in HPV16-positive cancer cells.

3.5.5 Autophagy and metabolism

Depending on the nature and extent of the inducing stress, the p53 tumor suppressor may regulate the same process differently to attain distinct cellular outcomes [114, 115, 209, 321]. As described in chapter 1.3.3 and 1.3.4, many studies indicate the different role for p53 in regulation of autophagy. p53 can positively regulate autophagy and can also inhibit it [115, 142, 206, 322]. The role of autophagy depends on the cell type and the nature of the stress.

3.5.5.1 Role of p53 depletion (at 0-24 h of hypoxia) for the induction of autophagy and metabolic switch

In this study, obvious evidence suggested that autophagy was induced in hypoxic HPV16-positive cancer cells, including the induction of *BNIP3* (**Figure 2.18**), which is critical for mitophagy (see chapter 1.2.3.1), the increase of LC3-II and the reduction of p62 (**Figure 2.19**). As already mentioned in chapter 2.4.1, LC3 and p62 were post-translationally regulated by hypoxia (**Figure 3.10**). The different tendency of LC3-II in hypoxic SiHa (**Figure 2.19A**) and CaSki cells (**Figure 2.19B**) may be due to the different conversion rate of LC3-I to LC3-II and the different degradation rate of LC3-II in autolysosome [111, 323].
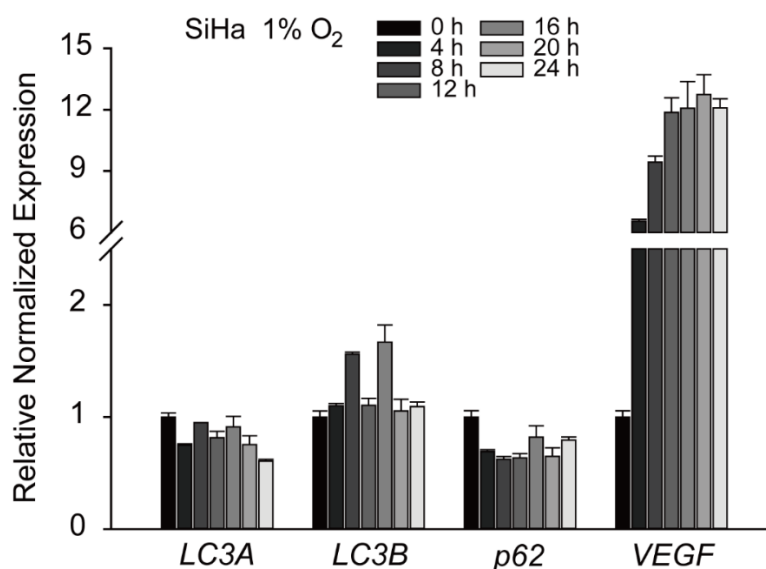
Figure 3.10 | Transcript levels of autophagy-related genes in hypoxic SiHa cells. HPV16-positive SiHa cells were cultured for the indicated time periods at 1% O_2. Total RNA was extracted after respective time intervals. qPCR analyses of *LC3A*, *LC3B*, and *p62* transcripts are shown. Transcript levels of *VEGF* were monitored as marker for hypoxia. *18S* rRNA served as internal control for normalization. Error bars indicate the SD of duplicate wells from one experiment. The 0 h value of gene expression was set as a control (set to 1.0).

In this study, LC3-II and p62 decreased after the reduction of p53 in hypoxic HPV16-positive cells (0-24 h under hypoxia, **Figure 2.19**). Tasdemir *et al.* showed that depletion of p53 activates autophagy in several cell lines, in response to distinct stimuli [206]. Here, overexpression of p53 prevented hypoxia-induced autophagy in HPV16-positive cancer cells (**Figures 2.20** and **3.13**). Thus, the degradation of p53 by hypoxia (0-24 h) might be a strategy of HPV16-positive cancer cells to remove the brake of autophagy, contributing to the survival under energy-limited hypoxic conditions.

As described in chapter 1.2.3.1, hypoxia usually causes dysfunction and reorganization of mitochondria [97] and induces mitophagy [106, 139, 140]. The MTT assay is a colorimetric assay widely used for measuring cell metabolic activity [324]. It is primarily based on the ability of mitochondrial reductase to reduce the water-soluble yellow tetrazolium dye MTT to generate water-insoluble purple-coloured formazan crystals [325, 326] (**Figure 3.11A**). The conversion of MTT to formazan depends on the metabolic rate and number of functional mitochondria. Preliminary results of MTT assay showed that the generation of formazan was decreased in hypoxic SiHa cells (**Figure 3.11B**), negatively correlated with the cell numbers (**Figure 3.1B**). One could speculate that the functional mitochondria and metabolic activity were decreased in hypoxic HPV16-positive cancer cells.

A

3-(4,5-dimethylthiazol-2-yl)-2,5-diphenyltetrazolium bromide
(MTT)

Mitochondrial Reductase

(*E,Z*)-5-(4,5-dimethylthiazol-2-yl)-1,3-diphenylformazan
(Formazan)

B
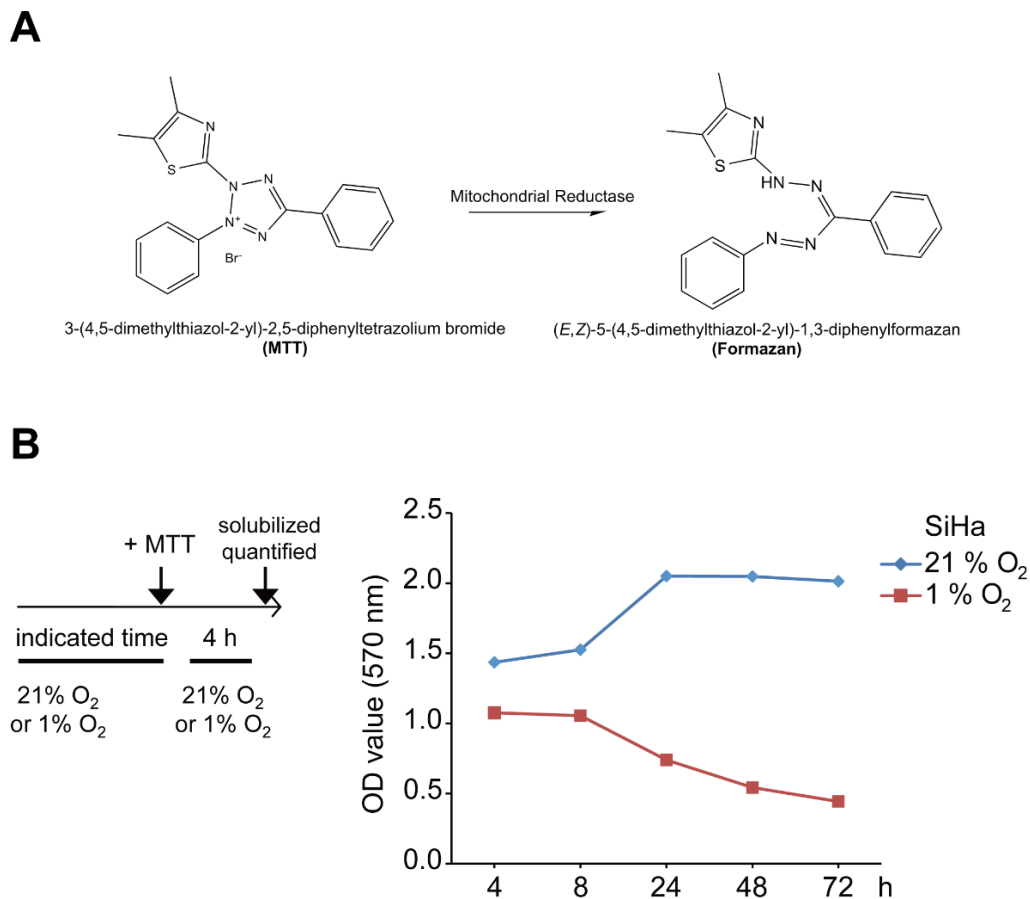
Figure 3.11 | MTT assay in HPV16-positive SiHa cells under normoxia and hypoxia. (A) Mitochondrial reduction of MTT to blue formazan product. [Picture from https://en.wikipedia.org/wiki/MTT_assay (edition of 18.10.2019)] (B) SiHa cells were cultured for the indicated time at 21% O_2 or at 1% O_2. MTT assay was performed after respective time intervals. Scheme *left*: Treatment protocol.

BNIP3 plays a critical role in the induction of mitophagy via several distinct mechanisms, promoting turnover of mitochondria and preventing accumulation of dysfunctional mitochondria, which can lead to oxidative stress and cellular degeneration. Increased expression of *BNIP3* under hypoxia is mainly regulated by the transcription factor HIF-1α [141, 327, 328]. p53 can inhibit the activity of HIF-1 due to competition for co-activators [329-331]. p53 can directly suppress the expression of *BNIP3* [142]. Rapid depletion of p53 under hypoxia (0-24 h) might therefore be a strategy of HPV16-positive cancer cells to remove the competitor of HIF-1 to release the expression of HIF-1 target genes, such as *BNIP3*, that promote cellular adaptation to hypoxic conditions.

As described in chapter 1.2.2 and 3.3, glycolysis is an important altered metabolism for hypoxic cancer cells. TIGAR, induced by p53, can lower fructose-2,6-bisphosphate level to inhibit glycolysis [199]. Decrease of *TIGAR* by hypoxia through p53 depletion (0-24 h, **Figure 2.18**) may facilitate the metabolic switch to glycolysis in HPV16-positive cancer cells.

3.5.5.2 Role of restored p53 after prolonged hypoxia for the maintenance of cellular homeostasis and selection of cell resistant to stress conditions

The preliminary results in **Figure 3.12** show that after prolonged hypoxia (72 h), both p62 and LC3-II were decreased in SiHa cells. Upon treatment with autophagy inhibitor CQ, hypoxic reduction of p62 and LC3-II were blocked. As depicted in **Figure 2.18**, the transcription of *BNIP3* remained induced after prolonged hypoxia (72 h) in HPV16-positive cancer cells. This suggests that autophagy might still take place under prolonged hypoxia.
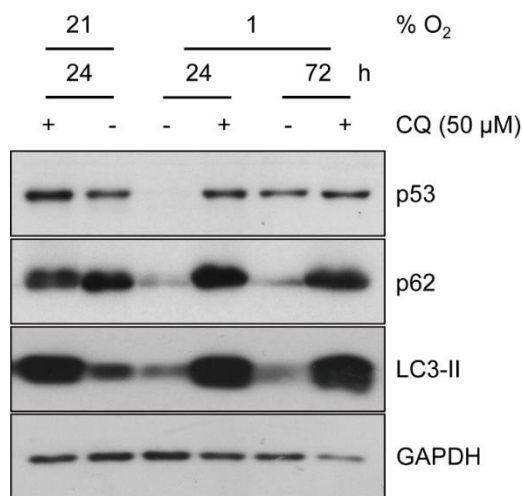
Figure 3.12 | Effect of autophagy inhibitor chloroquine (CQ) on hypoxic reduction of p53, p62 and LC3-II in HPV16-positive SiHa cells. SiHa cells were cultivated for 24 h or 72 h under normoxia or hypoxia in either the absence (-) or the presence (+) of 50 μM chloroquine (CQ). Shown are immunoblots of p53, p62, and LC3-I protein levels. GAPDH served as a loading control.

As discussed in chapter 1.2.3, for tumor cells autophagy is in itself a double-edged sword on cell fates [108, 109]. Scherz-Shouval *et al.* reported that p53 confers increased survival in the face of chronic starvation in many cell types. p53 increases cell fitness by maintaining better autophagic homeostasis, adjusting the rate of autophagy to changing circumstances by post-transcriptionally down-regulating LC3. Loss of p53 in chronically starved cancer cells impairs autophagic flux and causes excessive LC3 accumulation and aberrant autophagosome accumulation, culminating in apoptosis [209]. This implies that a proper autophagic flux is critical for cell survival.

HPV16-positive cancer cells may face a severe condition to survive after prolonged hypoxia. Cells undergoing an extreme amount of stress experience cell death either through necrosis or through apoptosis. Prolonged activation of autophagy leads to a high turnover rate of proteins and organelles. A rate above the survival threshold will kill cancer cells [116, 117]. Continued loss of p53 after prolonged hypoxia might lead to an excessive autophagic flux. Recovery of p53 would enable reduced, yet sustainable/affordable autophagic flux. Restoration of p53 could be another strategy of HPV16-positive cancer cells to increase cell fitness and enhance cell survival by

maintaining better autophagic homeostasis, adjusting the rate of autophagy to changing circumstances under prolonged hypoxia.

Given the role of TIGAR for inhibiting autophagy and protecting cells from oxidative stress, the recovery of *TIGAR* after prolonged hypoxia in HPV16-positive cancer cells (**Figure 2.18**) might help to limit the autophagic flux and reduce the production of ROS, which can be increased in cells after prolonged hypoxia [332].

As depicted in **Figure 2.18**, the transcript levels of *DRAM1* were not strongly induced at the early stage of hypoxia (0-24 h) but increased after prolonged hypoxia (at 48 and 72 h) (**Figure 2.18**). The increased *DRAM1* mRNA levels at 24 h of hypoxia in SiHa cells when p53 was depleted raises the possibility that DRAM1 is regulated by other factors, such as p73 [333], in hypoxic SiHa cells. Although DRAM is essential for p53-induced autophagy, this type of autophagy results in cell death (apoptosis) [253]. Repression of *DRAM1* at the early stage of hypoxia (0-24 h) may avoid cell death in HPV16-positive cancer cells. Its recovery after prolonged hypoxia along with the induction of *BAX* and *PUMA* (**Figure 2.14**, discussed in chapter 3.5.2) may contribute to the selection of cells resistant to cell death.

To summarize, under energy- and nutrient-limited hypoxic conditions, hypoxia and p53 act synergistically to induce cell cycle arrest via regulation of genes like *GADD45A* and *CDKN1A* leading to a temporary halt of proliferation in HPV16-positive cancer cells. The biphasic regulation of p53 might serve as a survival and protective strategy of hypoxic HPV16-positive cancer cells under stress conditions. Under hypoxia (0-24 h), rapid degradation of p53 helps to avoid the pro-apoptotic and pro-senescent functions of p53 and facilitate the induction of autophagy and the metabolic switch to glycolysis. After prolonged hypoxia, the restored p53 might be used to maintain cellular homeostasis and select cells resistant to stress conditions. The biphasic modulation on p53 downstream target genes that coincide with p53 protein dynamics may contribute to enhance cellular adaptation and protect cells from committing to an irreversible fate.

3.6 The evasion of hypoxic HPV16-positive cancer cells from senescence is attributable to the induction of autophagy

3.6.1 p53 overexpression inhibits hypoxia-induced autophagy

It has previously been shown that inhibition of p53 degradation prevented the induction of autophagy [206, 209]. Here, overexpression of p53 indeed diminished hypoxia-induced autophagy

in HPV16-positive cancer cells, as shown by the increased amounts of p62 under hypoxic conditions (**Figures 2.20** and **3.13**).
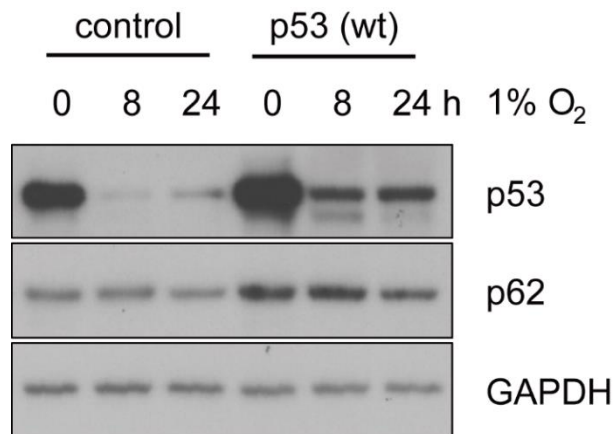
Figure 3.13 | Effect of overexpression of p53 protein on p62. CaSki cells were transfected with an empty vector control (control) or wild-type (wt) p53. 48 h post transfection, the cells were cultured for the indicated time periods at 1% O_2. Total protein was extracted after the respective time intervals. Western Blot analyses using antibodies against p53 and p62. GAPDH served as a loading control.

However, the exact mechanism of inhibition of hypoxia-induced autophagy upon overexpression of p53 in hypoxic HPV16-positive cancer cells is not determined yet.

Autophagy is a highly regulated process in eukaryotic cells, controlled by several kinases including AMPK, which induces autophagy [334], and mTOR, which suppresses autophagy [292]. Tasdemir *et al.* showed that depletion of p53 resulted in AMPK activation and mTOR inhibition in cells. Inhibition of autophagy by p53 was accompanied by reduced activation of AMPK, as well as increased activation of mTOR, underscoring the impact of p53 on the AMPK/mTOR axis [206].

AMP-activated protein kinase (AMPK) is a sensor of cellular energy levels and plays a key role in the regulation of energy homeostasis [335]. The kinase is activated by an elevated AMP/ATP ratio due to cellular and environmental stress, such as heat shock, hypoxia, and ischemia [335]. Preliminary results showed that the cellular ATP levels were decreased under hypoxia in SiHa cells (**Figure 3.1**), suggesting the supply of energy was limited in hypoxic SiHa cells. Demonstrated by Hoppe-Seyler *et al.*, mTOR signaling is impaired under hypoxia in HPV-positive cancer cells [50]. These data suggest that the AMPK/mTOR axis may be involved in the hypoxia-induced autophagy in HPV16-positive cancer cells. It would be interesting to investigate whether inhibition of autophagy by p53 overexpression requires the AMPK/mTOR axis.

p53 can also suppress *BNIP3* expression to inhibit hypoxia-induced autophagy [142]. Overexpression of p53 might impair autophagy by repressing *BNIP3* in hypoxic HPV16-positive cancer cells.

Scherz-Shouval *et al.* described that p53 reduces autophagic flux by post-transcriptionally down-regulating LC3 [209]. Overexpression of p53 may block the decrease of p62 by influencing the autophagic flux in hypoxic HPV16-positive cancer cells.

3.6.2 Inhibition of autophagy induces senescence

Increasing evidence implies that chemotherapeutic agents exert their anticancer effects not only through apoptosis but also by senescence induction in tumor cells [336, 337]. Here, an autophagy inhibitor could be a potent agent to restore senescence induction in HPV16-positive cancer cells (**Figures 2.21** and **3.14**). Although the hypoxic HPV16-positive cancer cells treated with CQ did not stain strongly positive for SA-β-Gal, these cells showed the typical morphology of senescent cells (for example cell enlargement, flattening). Moreover, hypoxic HPV16-positive cancer cells of the control group resumed growth upon reoxygenation (replated in fresh media containing no drug, subsequently cultured under 21% O_2), whereas the hypoxic cancer cells subjected to autophagy inhibitor CQ treatment did not grow after reoxygenation (under the same protocol as the control group) (**Figures 2.21** and **3.14**). These results indicate that inhibition of autophagy prevents the evasion of hypoxic HPV16-positive cancer cells from senescence.
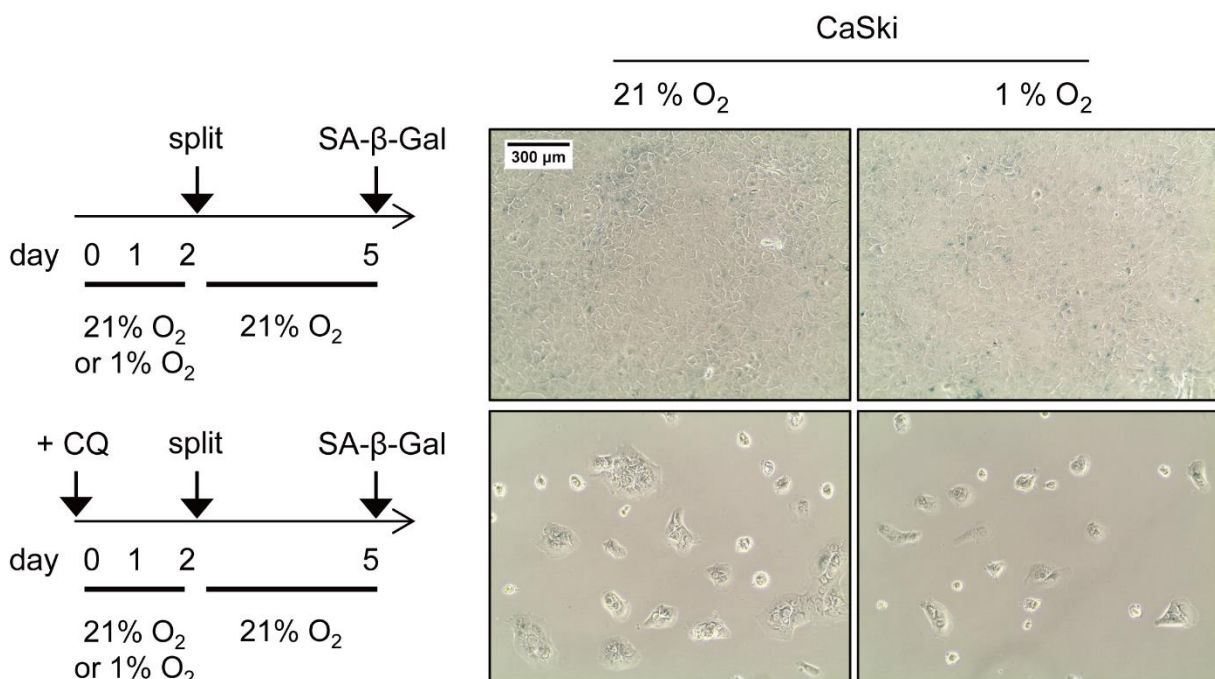
Figure 3.14 | Analyses of cellular senescence upon treatment with autophagy inhibitor CQ in HPV16-positive cancer cells. CaSki cells were cultivated for 48 h under normoxia (21% O_2) or hypoxia (1% O_2), in either the absence (*top*) or the presence (*bottom*) of 50 μM chloroquine (CQ). Cells for senescence assays (SA-β-Gal staining) subsequently cultured under normoxia. Scale bar: 300 μm. Scheme *left*: Treatment protocol.

Treatment with CQ in normoxic SiHa cells led to the emergence of cells staining positive for SA-β-Gal (**Figure 2.21**) and caused a proliferative halt in CaSki cells (**Figure 3.14**). This might be due to the inhibition of autophagy and an unexpected repressive effect of CQ on HPV16 *E6/E7* oncogenes (**Figure 2.8**), which is required for maintaining growth [32].

SA-β-gal is a commonly used biomarker for cellular senescence, which can be detected at pH 6.0 [237]. This is due to a high level of lysosomal β-galactosidase (β-gal) expressed in senescent cells [338–340]. Overexpression of lysosomal β-gal itself is unable to induce senescence [338]. The SA-β-gal staining may be sensitive to the quality of lysosomes [339]. Chloroquine is a lysosomotropic agent, accumulating in the lysosomes and raising their pH [341]. Thus, chloroquine could interfere to some extent with the SA-β-Gal staining assay [339].

Another autophagy inhibitor, Bafilomycin A1, was also used to investigate the effect of inhibition of autophagy on senescence in HPV16-positive cancer cells. Treatment with Bafilomycin A1 strongly decreased viability of HPV16-positive cancer cells, with few attached cells when senescence assays were performed (**Figure 3.15**). Bafilomycin A1 is known as an inhibitor of Vacuolar-type H$^+$-ATPase (V-ATPase), preventing maturation of autophagic vacuoles by inhibiting fusion between autophagosomes and lysosomes [227]. It also functions as a potassium ionophore and inhibits mitochondrial respiration [342]. Nanomolar concentrations of Bafilomycin A1 cause mitochondrial swelling, loss of mitochondrial membrane potential, as well as induction of pyridine nucleotide oxidation. These observations could explain why treatment with Bafilomycin A1 dramatically reduced the viability of HPV16-positive cancer cells.
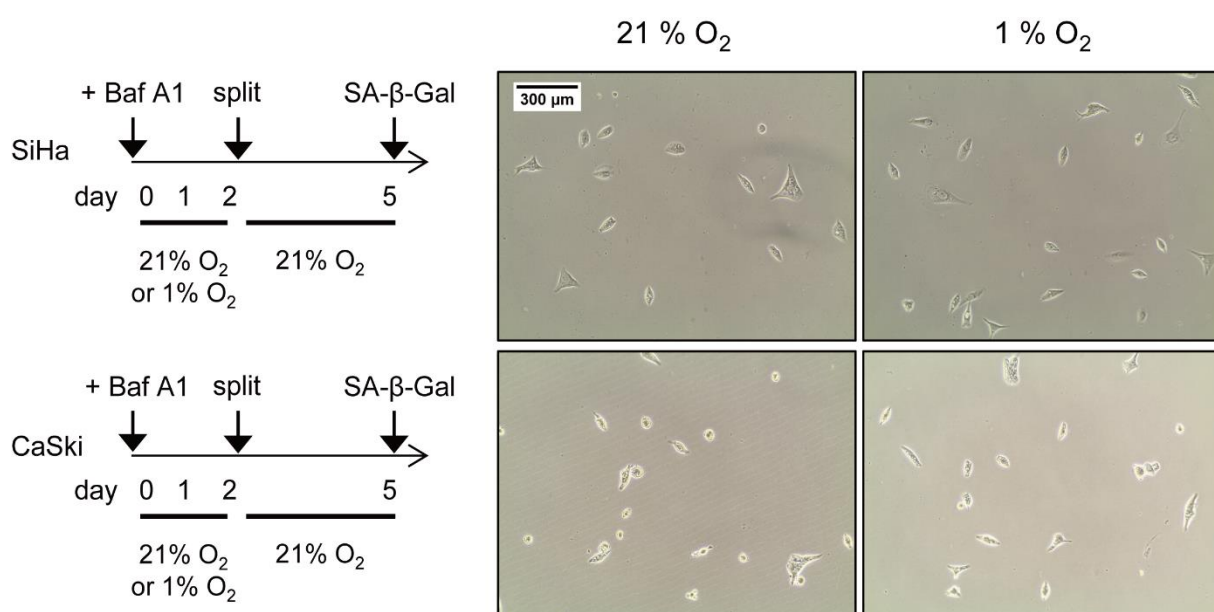
Figure 3.15 | Analyses of cellular senescence upon treatment with Bafilomycin A1 in HPV16-positive cancer cells. SiHa and CaSki cells were cultivated for 48 h under normoxia (21% O$_2$) or hypoxia (1% O$_2$), in either

the absence (*top*) or the presence (*bottom*) of 0.5 µM Bafilomycin A1 (Baf A1). Cells for senescence assays (SA-β-Gal staining) subsequently cultured under normoxia. Scale bar: 300 µm. Scheme *left*: Treatment protocol.

Failure of autophagy causes loss of proteostasis, accumulation of dysfunctional mitochondria and oxidative stress, resulting in entry into cellular senescence [268]. As discussed in chapter 3.5.5, hypoxia-induced autophagy might help to maintain a better cellular homeostasis, clear dysfunctional mitochondria in time, and reduce the production of ROS in cells. Inhibition of autophagy may prevent utilization of autophagy by hypoxic HPV16-positive cancer cells for survival. Thus, the hypoxic HPV16-positive cancer cells treated with autophagy inhibitor cannot recover and eventually enter senescence upon reoxygenation. Targeted perturbation of autophagy may enable novel pharmacological strategies for preventing cancer recurrence in poorly oxygenated regions of HPV-positive tumors.

3.7 Conclusion and perspectives

The p53 tumor suppressor is mutated in a high percentage of tumors. However, many other tumors retain expression of wild-type p53, raising the intriguing possibility that they actually benefit from it. This PhD thesis, for the first time, reveals a new regulation pattern of p53 by hypoxia, a characteristic microenvironment of HPV-positive cervical cancer cells which can increase their resistance to radiation therapy and other cancer treatments and is a negative prognostic marker in patients [49, 58, 61, 99, 343-345]. Hypoxic HPV16-positive cervical cancer cells use the p53 protein by dynamic regulation to reap an advantage to survive stressful conditions.

The dynamics of p53 protein are a critical part of p53 signaling, along with the amplitude of p53 regulation, directly affecting the course of downstream pathway programs and influencing cell fate decisions [320]. Although the effect of hypoxia on p53 tumor suppressor in HPV-positive cancer cells has been studied for decades, the dynamics of p53 during different periods of hypoxic conditions in cervical cancer cells is still not well explored. The hypoxic HPV-positive cancer cells are described entering a dormant state, characterized by an evasion of cellular senescence [50] and resistance to cell death [51], the role of p53 for these cellular outcomes and cellular adaptation under hypoxic conditions remains elusive. Herein, the dynamics of p53 and the mechanism underlying it under hypoxia were explored in HPV16-positive cervical cancer cells. The effect of p53 dynamics on downstream responses (target gene expression and cellular outcomes) in hypoxic HPV16-positive cervical cancer cells was investigated.

Using standard O_2 concentration (1%) and serial duration of hypoxic conditions, a biphasic regulation of p53 protein in hypoxic HPV16-positive cervical cancer cells was identified. Despite a continuous repression of HPV16 *E6/E7* oncogenes, p53 protein was rapidly and strongly depleted via a lysosome-dependent mechanism under hypoxia, whereas after prolonged hypoxia, it was markedly restored in HPV16-positive cervical cancer cells. According to the results provided here, the following model can be hypothesized (**Figure 3.16**). The biphasic regulation of p53 contributes to enhance cellular adaptation, along with its downstream target genes and protect hypoxic HPV16-positive cervical cancer cells from committing to an irreversible fate. The downstream response autophagy is critical for the evasion of senescence by hypoxic HPV16-positive cancer cells. Considering the high resistance of hypoxic tumor cells to therapy, the present findings provide a basis for future studies addressing the development of new treatment strategies.

First, the ability of hypoxic HPV-positive cancer cells to induce a temporary halt of proliferation, reversibly repressing viral oncogenes expression without entering senescence, should be considered in the current development of therapeutic strategies, such as targeted E6/E7 inhibition or immunotherapy. Second, since the reduction of p53 protein is mediated via a lysosome-dependent mechanism, the currently used pharmacological inhibitors, such as Nutlin-3, that are dependent on the proteasomal degradation pathway, will be insufficient to increase p53 levels. The development and usage of anticancer agents targeting p53 should depend on the cell type and the mechanism involved in p53 degradation. Third, the maintenance of cellular homeostasis is required for the resistance of HPV16-positive cervical cancer cells to hypoxia. In this regard, the anticancer drugs targeting metabolism, such as glycolytic inhibitors could be efficient to overcome the hypoxia-induced resistance. In the future, pharmacological strategies such as combination of E6/E7 inhibitors, HIF-target drugs and p53 agonists or glycolytic inhibitors could be used to prevent cancer recurrence in normoxic or hypoxic regions of HPV-positive cancers.
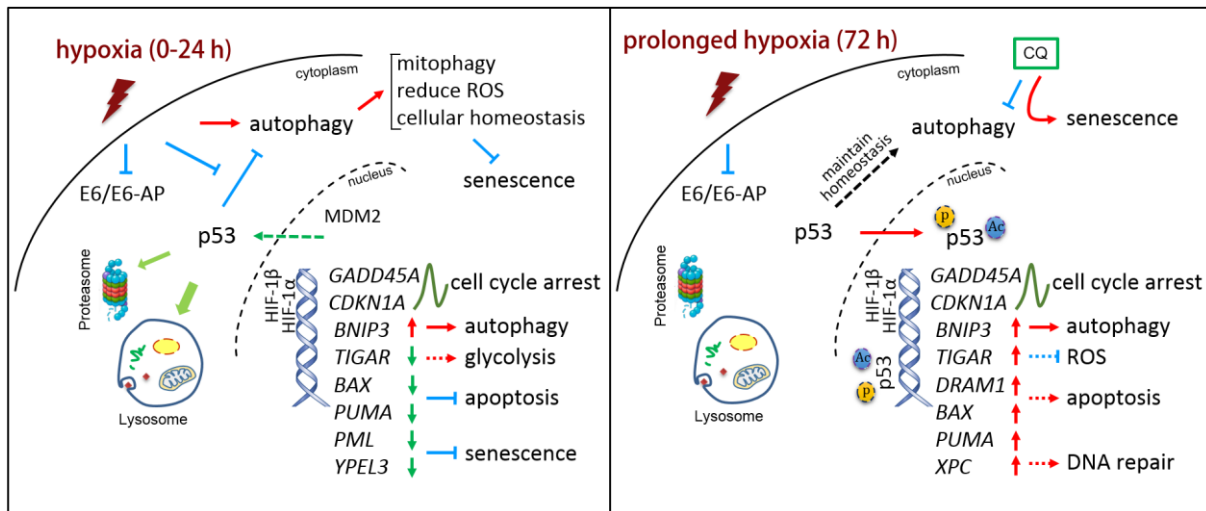
Figure 3.16 | Schematic overview of the biphasic regulation of p53 and its effect on downstream responses and cellular outcomes in hypoxic HPV16-positive cancer cells. Under hypoxic conditions, HPV16 *E6/E7* oncogenes were continuously repressed, whereas p53 protein showed a biphasic regulation in HPV16-positive cancer cells. p53 and hypoxia (such as induction of HIF-1) may act synergistically to induce a temporary cell cycle arrest and to facilitate the metabolic switch to glycolysis. (*Left*) At the early stage of hypoxia (0-24 h), p53 was predominantly degraded via a lysosome-dependent mechanism. Rapid and strong degradation of p53 by hypoxia could avoid the pro-apoptotic or pro-senescent functions of p53 and remove the brake of autophagy, which can be utilized by cancer cells for survival under energy and nutrient-limited conditions. (*Right*) After prolonged hypoxia (72 h), with diminished inhibitory factors and increase in PTMs for protein stabilization, p53 was stably synthesized and transported into the nucleus. Restored p53 might be used by HPV16-positive cancer cells to maintain cellular homeostasis, such as sustainable autophagic flux, and to select cells resistant to stress conditions. The biphasic modulation on p53 downstream target genes that coincide with p53 protein dynamics may contribute to enhance cellular adaptation and protect cells from committing to an irreversible fate. Targeted perturbation of p53 dynamics or autophagy may enable novel pharmacological strategies for preventing cancer recurrence in poorly oxygenated regions of HPV-positive cancers.

4. Materials

4.1 Chemicals and Reagents

2-mercaptoethanol	Carl Roth GmbH, Karlsruhe
2-Propanol	Merck Calbiochem, Darmstadt
6X DNA Loading Dye	Fermentas, St. Leon-Rot
Acetic acid	Merck Calbiochem, Darmstadt
Acrylamide-Bis (29:1), 30% solution	Serva Feinbiochemica, Heidelberg
Agarose	Sigma-Aldrich, Steinheim
Ammonium acetate	Merck Calbiochem, Darmstadt
Ammonium persulfate	Sigma-Aldrich, Steinheim
Aqua ad iniectabilia	Braun, Melsungen
Bovine serum albumin fraction V (BSA)	Biomol, Hamburg
Bradford-Reagent (Bio-rad Protein assay)	Bio-Rad Laboratories, Munich
Bromophenol blue	Serva Feinbiochemica, Heidelberg
Complete Protease Inhibitor Cocktail	Roche, Mannheim
Diethylpyrocarbonate (DEPC)	Sigma-Aldrich, Munich
Dithiothreitol (DTT)	Sigma-Aldrich, Munich
DMSO	Carl Roth GmbH, Karlsruhe
dNTPs Set PCR Grade	Invitrogen, Karlsruhe
EDTA	Carl Roth GmbH, Karlsruhe
EGTA	Sigma-Aldrich, Steinheim
Enhanced Chemiluminescence Substrate (ECL)	PerkinElmer, USA
Ethanol, absolute	Merck Calbiochem, Darmstadt
Ethidium bromide, 1% solution	Fluka, Steinheim
Glycerol	AppliChem, Darmstadt
Glycine	Gerbu, Gaibach
HEPES	Carl Roth GmbH, Karlsruhe
Hydrochloric acid (HCl) 37%	Sigma-Aldrich, Munich
KCl	Merck Calbiochem, Darmstadt
KH_2PO_4	Carl Roth GmbH, Karlsruhe
Methanol	Sigma-Aldrich, Munich
$MgCl_2$	Merck Calbiochem, Darmstadt
$MgSO_4$	Serva Feinbiochemica, Heidelberg

Materials

Milk powder	Carl Roth GmbH, Karlsruhe
MTT	Sigma-Aldrich, Munich
Na_2HPO_4	Carl Roth GmbH, Karlsruhe
NaCl	Sigma-Aldrich, Steinheim
NaF	Merck Calbiochem, Darmstadt
NaOH	Carl Roth GmbH, Karlsruhe
Na_3VO_4 (Sodium ortho-vanadate)	Sigma-Aldrich, Deisenhofen
Nonidet® P-40	Sigma-Aldrich, Steinheim
PIPES	Sigma-Aldrich, Munich
Protease Inhibitor Cocktail Complete, EDTA-free	Roche, Mannheim
RiboLock RNase inhibitor	Thermo Scientific, St. Leon-Rot
Sodium acetate (NaAc)	Merck Calbiochem, Darmstadt
Sodium dodecyl sulfate (SDS), ultra pure	Carl Roth GmbH, Karlsruhe
Sodium deoxycholate	Merck Calbiochem, Darmstadt
Sucrose	Sigma-Aldrich, Munich
TEMED	Sigma-Aldrich, Steinheim
Triton® X-100	Serva Feinbiochemica, Heidelberg
Trizma base (Tris)	AppliChem, Darmstadt
Tween® 20	Gerbu, Gaibach

4.2 Reagents for the Cultivation of Bacteria

Bacto™ Agar	Becton Dickinson, Heidelberg
Bacto™ Trypton	Carl Roth GmbH, Karlsruhe
Yeast extract	GERBU, Wieblingen
Kanamycin	BIOTREND Chemikalien, Cologne
LB Medium	Carl Roth GmbH, Karlsruhe

4.3 Reagents for Cell Culture and Treatment of Human Cells

0.25% Trypsin/EDTA	Invitrogen, Karlsruhe
Bafilomycin A1	Thermo Scientific, St. Leon-Rot
Chloroquine	Sigma-Aldrich, Steinheim
Cycloheximide	Sigma-Aldrich, Steinheim
Dulbecco's Modified Eagle's Medium (DMEM) (Glucose: 1	Sigma-Aldrich, Steinheim

g/L)

Dulbecco's Modified Eagle's (HIGH glucose) Medium (Glucose: 4.5 g/L)	Sigma-Aldrich, Steinheim
Dulbecco's Modified Eagle's (NO glucose) Medium (Glucose: 0 g/L)	Gibco/ Life Technologies, Karlsruhe
Dulbecco's Phosphate Buffered Saline (PBS)	Invitrogen, Karlsruhe
Fetal calf serum (FCS)	Invitrogen, Karlsruhe
InSolution MG132	Merck Calbiochem, Darmstadt
Lipofectamine 2000 Transfection Reagent	Invitrogen, Karlsruhe
Opti-MEM serum-free medium	Invitrogen, Karlsruhe
RPMI 1640 medium (Glucose: 2 g/L)	Sigma-Aldrich, Steinheim
Trypan blue	Biochrom, Berlin
Turbofect in vitro Transfection Reagent	ThermoScientific, St. Leon-Roth

4.4 Consumables

Cell culture flasks (6, 10, 14 cm)	TPP, Trasadingen, Switzerland
Cell culture flasks (25, 75, 175 cm^2)	Greiner, Frickenhausen
Cell culture plates (6-well)	BD Falcon, Heidelberg
Cell culture plates (24-well, 96-well)	Greiner, Frickenhausen
Cell scraper	Corning Sigma, Munich
Gloves (Blossom® Medical Examination gloves)	Mexpo International Inc., Union City, USA
Gloves (Dermatril®)	KCL GmbH, Eichenzell
Needles, sterile, 20G	Needles, sterile, 20G
Nunc® Cryo Tubes	Sigma-Aldrich, Steinheim
PCR SingleCap 8er Soft Strips	Biozym
Pipette Tips	Greiner Frickenhausen
Pipette Tips RAININ LTS (20, 200, 1000 µL)	Mettler-Toledo GmbH, Gießen
Pipette Tips RAININ LTS sterile with filter (20, 200, 1000 µL)	Mettler-Toledo GmbH, Gießen
Polypropylene Tubes 12 mL	BD Falcon, Heidelberg
PVDF membranes Immobilon P (0.2 and 0.45 µm)	Milipore, Schwalbach
Reaction Tubes 0.5 mL blue	Biozym
Reaction Tubes (0.5, 1.5 and 2.0 mL)	Eppendorf, Hamurg

Materials

Reaction Tubes (15 and 50 mL)	Greiner, Frickenhausen
Saran wrap	Toppits, Minden
Scalpels, disposable	Feather Safety Razor, Osaka, Japan
Syringes, single use 1 mL	Th. Geyer GmbH, Renningen
TipOne sterile pipette filter tips	Starlab, Ahrensburg
Whatman 3 MM filter paper	GE Healthcare, Munich
X-ray films Super RX	Fuji, Japan

4.5 Laboratory equipment

Analytical scales AE 160	Mettler-Toledo GmbH, Gießen
Autoradiography cassettes	Kodak, Stuttgart
Bacterial shaker G25	Infors, Bottmingen, CH
Bio-Trap electrophoresis chamber	Renner, Dannstadt
Centrifuge 5415R	Eppendorf, Hamburg
Centrifuge 5417R	Eppendorf, Hamburg
Centrifuge Biofuge pico	Heraeus, Hanau
Centrifuge Biofuge, Varifuge RF	Heraeus, Hanau
Centrifuge Heraeus Minifuge RF	Heraeus, Hanau
Centrifuge Megafuge 1.0R	Heraeus, Hanau
CFX96 Real-Time PCR Detection System	Bio-Rad Laboratories, Munich
Countess® II FL Automated Cell Counter	Life Technologies
Developing machine CURIX 60	AGFA, Cologne
EVOS XL Core Cell Imaging System	Life Technologies, Calsbad, CA, USA
Freezer profi line	Liebherr, Ludwigshafen
Freezer VIP™ Series -86°C	Sanyo, USA
Fridge Premium	Liebherr, Ludwigshafen
Gel documentation system GELSTICK	INTAS Science Imaging Instruments GmbH, Göttingen
Incubator C16	Labotect, Göttingen
Incubator Kelvitron®	Heraeus, Hanau
InvivO$_2$ 400 physiological oxygen workstation	Ruskinn Technology Ltd, Bridgend, UK
Liquid nitrogen tank CHRONOS Biosafe	Messer, Griesheim
Magnetic stirrer MR3000	Heidolph, Rust

Microscope CKX41	Olympus, Hamburg
Microscope Leitz DM RBE	Leica, Bensheim
Microwave	DéLonghi GmbH, Seligenstadt
Mini PROTEAN® Tetra-Cell	Bio-Rad, Munich
Mini-PROTEAN® 3 Cell	Bio-Rad, Munich
Multichannel Pipettes (20-50 µL, 50-200 µL)	Eppendorf, Hamburg
Neubauer hemocytometer	Bender&Hobein, Bruchsal
Overhead shaker REAX2	Heidolph, Rust
Peltier Thermal Cycler PTC-200	MJ Research, St. Bruno, Canada
pH-meter 761 Calimatic	Knick, Berlin
Pipette Boy Acu	Integra Biosciences GmbH, Fernwald
Pipettes RAININ (2, 10, 20, 100, 200, 1000 µL)	Mettler-Toledo GmbH, Gießen
Plate Reader Labsystems Multiskan MS	Thermo Scientific, St. Leon-Rot
Plate reader Synergy 2	BioTek®, Bad Friedrichshall
Polymax 2040	Heidolph, Schwabach
Power supply PHERO-stab 500	Biotech-Fischer, Reiskirchen
Power supply PowerPac™ HC/basic	Bio-Rad, Munich
Rotating wheel	Neolab, Heidelberg
Scales BL610	Sartorius, Göttingen
Semi-dry Transfer unit Hoefer® Semi-Phor™	Pharmacia Biotech, Uppsala, Sweden
Sonifier 250	Branson/Heinemann, Schwäbisch Gmünd
Spectrophotometer NanoDrop® ND-1000	NanoDrop, USA
STERI-CULT 200 Incubator	Forma Scientifc, Marietta, USA
SterilGARD Hood	Baker Company, Sanford, USA
Thermal Cycler C1000™	Bio-Rad, Munich
Thermomixer compact/pico	Eppendorf, Hamburg
UV table N90	Benda Konrad, Wiesloch
Vacuum pump VACUSIP	Integra Biosciences GmbH, Fernwald
Vortexer	Heidolph, Rust
Water bath	GFL - Gesellschaft für Labortechnik mbH, Burgwedel

4.6 Buffers and Solutions

4.6.1 Preparation of cell lysates

CSKI buffer (pH 6.8)	10 mM PIPES 100 mM NaCl 1 mM EDTA 300 mM Sucrose 1 mM $MgCl_2$ 0.5% Triton® X-100 Store in aliquots at –20°C Freshly supplemented with protease and phosphatase inhibitors
Protease and phosphatase inhibitors	Complete Protease Inhibitor Cocktail (Roche), Store at 4°C 0.1 M DTT stock solution, Store at -20°C 20 mM MG132 stock solution (in DMSO), Store at -80°C 500 mM NaF, Store at -20°C 10 mM Na_3VO_4, Store at -20°C
Buffer A	10 mM HEPES pH 7.9 10 mM KCl 0.1 mM EDTA pH 8.0 0.1 mM EGTA pH 7.9 Store at -20°C Freshly supplemented with protease and phosphatase inhibitors
Buffer C	25% (v/v) glycerol 99.5% 20 mM HEPES pH 7.5 400 mM NaCl 1 mM EDTA pH 7.9 Store at -20°C Freshly supplemented with protease and phosphatase inhibitors

4.6.2 Western Blot

Ammonium persulfate (APS)	10% (w/v)
Anode Buffer I	0.3 M Tris 10% Methanol pH 10.4
Anode Buffer II	25 mM Tris 10% Methanol
Cathode Buffer	25 mM Tris 40 mM Glycine 10% Methanol pH 9.4
SDS Loading Dye (5X)	10% (w/v) SDS 0.03% (w/v) bromophenol blue 12.5% (v/v) 2-mercaptoethanol 5 mM EDTA, pH 8.0 50% (v/v) glycerol 0.3 M Tris, pH 6.8

SDS Running Buffer (10X)	1% SDS
	0.25 M Tris
	1.9 M Glycine
TBS (10X)	0.5 M Tris
	1.5 M NaCl
	pH 7.5
TBST (1X)	1X TBS, pH 7.5
	0.1% (v/v) Tween 20
Blocking Buffer (Western Blot)	TBST
	5% (w/v) Milk powder
	Store at 4°C

4.6.3 Agarose gel electrophoresis

DEPC water	0.1%(v/v) DEPC
TAE (50X) pH 7.8	2 M Tris Base
	250 mM NaAc
	50 mM EDTA pH 8.0
	adjust to pH 7.8 with acetic acid

4.6.4 Senescence Assay

Senescence assay fixation buffer	2% formaldehyde
	0.2% glutaraldehyde
	in PBS
Senescence assay staining buffer (pH 6.0)	40 mM citric acid
	150 mM NaCl
	2 mM $MgCl_2$
	adjusted to pH 6.0 with Na_2HPO_4
	5 mM $K_3[Fe(CN)_6]$*
	5 mM $K_4[Fe(CN)_6]$*
	1 mg/mL X-Gal in DMF*
	*freshly added
chromogenic substrate X-Gal	5-bromo-4-chloro-3-indolyl-β-D-galactopyranoside

** All reagents were generously provided by Felix Hoppe-Seyler, DKFZ Heidelberg.

4.7 DNA and protein size markers

GeneRuler™ DNA Ladder Mix	Thermo Scientific, St. Leon-Rot
PageRuler™ Prestained Protein Ladder	Thermo Scientific, St. Leon-Rot

4.8 Universal enzymes

RevertAid Reverse Transcriptase	Thermo Scientific, St. Leon-Rot
Dream Taq™ Green PCR Master Mix (2X)	Thermo Scientific, St. Leon-Rot
iTaq™ Universal SYBR® Green Supermix (2X)	Bio-Rad Laboratories, Munich

4.9 Kits

CellTiter-Glo® Luminescent Cell Viability Assay	Promega, Mannheim
MiniPrep Kit	Qiagen, Hilden
RNase-Free DNase Set	Qiagen, Hilden
RNeasy® Mini Kit	Qiagen, Hilden

4.10 Oligonucleotides

4.10.1 Oligonucleotides for polymerase chain reactions

Table 4.1 | Oligonucleotides (primer) for quantitative real-time polymerase chain reactions (qPCR).

Primer Name	Sequence 5' → 3'	amplicon length (bp)
18S rRNA fw	CATGGCCGTTCTTAGTTGGT	
18S rRNA rev	ATGCCAGAGTCTCGTTCGTT	66
Apaf1 fw	AAGGTGGAGTACCACAGAGG	
Apaf1 rev	TCCATGTATGGTGACCCATCC	116
Bax fw	CCCGAGAGGTCTTTTTCCGAG	
Bax rev	CCAGCCCATGATGGTTCTGAT	155
BNIP3 fw	CAGGGCTCCTGGGTAGAACT	
BNIP3 rev	CTACTCCGTCCAGACTCATGC	131
CDKN1A (p21) fw	TGTCCGTCAGAACCCATGC	
CDKN1A (p21) rev	AAAGTCGAAGTTCCATCGCTC	139
DRAM1 fw	AGTGCTTGGATTGGTGGGATG	
DRAM1 rev	GATGGACTGTAGGAGCGTGTA	136
GADD45 α fw	GAGAGCAGAAGACCGAAAGGA	
GADD45 α rev	CACAACACCACGTTATCGGG	145
HPV16 E6/E7 fw	CAATGTTTCAGGACCCACAGG	
HPV16 E6/E7 rev	CTCACGTCGCAGTAACTGTTG	125
LC3A fw	TCCCGGACCATGTCAACAT	
LC3A rev	ACCATGCTGTGCTGGTTCAC	106
LC3B fw	ACCATGCCGTCGGAGAAG	
LC3B rev	ATCGTTCTATTATCACCGGGATTTT	115
MDM2 fw	GAATCATCGGACTCAGGTACATC	
MDM2 rev	TCTGTCTCACTAATTGCTCTCCT	167

Table 4.1 | Oligonucleotides (primer) for qPCR (continued).

p53 fw	CAGCACATGACGGAGGTTGT	125
p53 rev	TCATCCAAATACTCCACACGC	
p62 fw	AGGCGCACTACCGCGAT	51
p62 rev	CGTCACTGGAAAAGGCAACC	
PML fw	CGCCCTGGATAACGTCTTTTT	127
PML rev	CTCGCACTCAAAGCACCAGA	
ppm1d fw	CTGTACTCGCTGGGAGTGAG	88
ppm1d rev	GTTCGGGCTCCACAACGATT	
Puma fw	GCCAGATTTGTGAGACAAGAGG	136
Puma rev	CAGGCACCTAATTGGGCTC	
TIGAR fw	ACTCAAGACTTCGGGAAAGGA	144
TIGAR rev	CACGCATTTTCACCTGGTCC	
VEGF fw	CACACAGGATGGCTTGAAGA	136
VEGF rev	AGGGCAGAATCATCACGAAG	
XPC fw	CTTCGGAGGGCGATGAAAC	199
XPC rev	TTGAGAGGTAGTAGGTGTCCAC	
YPEL3 fw	GTGCGGATTTCAAAGCCCAAG	170
YPEL3 rev	CCCACGTTCACCACTGAGTT	

4.10.2 Oligonucleotides for RNA interference

Table 4.2 | Oligonucleotides for siRNA-mediated knock-down experiments.

Name		Sequence 5' → 3'	Source
si-16E6/E7 *	si16E6/E7-1	CCGGACAGAGCCCAUUACA	kindly provided by Felix Hoppe-Seyler, DKFZ Heidelberg
	si16E6/E7-2	CACCUACAUUGCAUGAAUA	
	si16E6/E7-3	CAACUGAUCUCUACUGUUA	
Silencer® Select Pre-designed siRNA Atg12		GCAGCUUCCUACUUCAAUUtt	Thermo Scientific, St. Leon-Rot
Silencer® Select Pre-designed siRNA p62/SQSTM1		CUUCCGAAUCUACAUUAAAtt	Thermo Scientific, St. Leon-Rot
si-scramble		Silencer® Negative Control #1 siRNA, Cat#: AM4611	Thermo Scientific, St. Leon-Rot

* Three different siRNAs, each targeting all three HPV16 E6/E7 transcript classes, were pooled at equimolar concentrations (referred to in the text as si-16E6/E7), as detailed in [50].

4.10.3 Oligonucleotides for reverse transcription

Random primers p(dN)$_6$ *	Roche, Mannheim
Oligo dT$_{22}$ primers	DKFZ, Heidelberg

* kindly provided by Daniel Hasche, DKFZ Heidelberg

4.11 Provided plasmids

Table 4.3 | List of protein expression plasmids. CMV: cytomegalovirus. The cryo-conserved bacteria harbouring plasmids were kindly provided by Martina Niebler, DKFZ Heidelberg.

Plasmid Name	Properties	Source
pPK-CMV-E3	empty cloning vector CMV promoter and enhancer C-terminal HA-tag	PromoKine
pPK:p53	expression of wild-type p53 under a CMV promoter	M. Niebler, DKFZ Heidelberg

* Chemically competent bacteria: *E. coli* One Shot® Top 10 DH10B™ (Invitrogen, Karlsruhe)

4.12 Antibodies

Table 4.4 | List of antibodies used for Western Blot analyses. All antibodies were diluted in 5% Milk/TBST (w/v). *: generously provided by Felix Hoppe-Seyler, DKFZ Heidelberg.

Antibody	Distributor	Catalogue number	Work concentration
Anti-Atg12 (D88H11) rabbit monoclonal	Cell Signaling Technology	#4180P	1:1,000
Anti-Actin mouse monoclonal	MP Biomedical	69100	1:10,000
Anti-E6-AP (H-182) rabbit monoclonal	Santa Cruz Biotechnology	sc-25509	1:1,000
Anti-MDM2 (D-7) mouse monoclonal	Santa Cruz Biotechnology	sc-13161	1:1,000
Anti-p53 (DO-1) mouse monoclonal	Santa Cruz Biotechnology	sc-126	1:1,000
Anti-p62/SQSTM1 mouse monoclonal	Abcam	ab56416	1:1,000
Anti-TFIID (TBP) (N-12) rabbit polyclonal	Santa Cruz Biotechnology	sc-204	1:1,000
Anti-α-tubulin (DM1A) * mouse monoclonal	Merk	CP06	1:5,000
Anti-GAPDH (FL-335)* rabbit polyclonal	Santa Cruz Biotechnology	sc-25778	1:4,000
Anti-HIF-1α * mouse monoclonal	BD Pharmingen	610959	1:500
Anti-LC3 * rabbit polyclonal	Novus Biologicals	NB100-2331	1:1,000
Anti-Cleaved PARP (Asp214) (19F4) * mouse monoclonal	Cell Signaling Technology	#9546	1:1,000

Secondary antibodies			
Goat-anti mouse IgG (H+L) HRP	Jackson ImmunoResearch, USA	115-035-003	1:10,000
Goat-anti rabbit IgG (H+L) HRP	Jackson ImmunoResearch, USA	111-035-003	1:10,000

4.13 Human cell lines

Table 4.5 | Human adherent cell lines used throughout the presented thesis.

Cell line	Source	Properties	Reference
CaSki	Cervical carcinoma	tumourigenic HPV16-positive	[346]
SiHa	Cervical carcinoma	tumourigenic HPV16-positive	[347]
HepG2	Hepatocellular carcinoma	non-tumorigenic	[348]

4.14 Software and Databases

Adobe Illustrator CC	Adobe, San Jose, USA
CFX Manager	Bio-Rad Laboratories, USA
Endnote X7	Thomson, Carlsbad, USA
ImageJ 1.51j8	National Institute of Health (NIH), USA
Microsoft Excel 2013	Microsoft, USA
NCBI-Blast (sequence alignment)	https://blast.ncbi.nlm.nih.gov
NCBI-Gene (gene database)	https://www.ncbi.nlm.nih.gov/gene
NCBI-Nucleotide (nucleotide database)	https://www.ncbi.nlm.nih.gov/nucleotide/
NCBI-Pubmed (literature database)	https://www.ncbi.nlm.nih.gov/pubmed/
SigmaPlot 14.0	Systat Software Inc., USA

5. Methods

5.1 Cultivation and treatment of human cells

5.1.1 Cultivation of human cell lines

Cervical cancer cell lines CaSki and SiHa were grown in Dulbecco's Modified Eagle's Medium (DMEM) supplemented with 10% fetal calf serum (FCS). Liver cancer cell line HepG2 was grown in Dulbecco's Modified Eagle's (HIGH glucose) Medium supplemented with 10% fetal calf serum (FCS). Cells were cultivated in cell culture flasks until a confluency of 80-90% was reached and then passaged or seeded for experiments. All cell lines were maintained in an incubator at 37°C, 5% CO_2 and 95% humidity. Cell line integrity was confirmed routinely via semi-quantitative PCR for viral oncogenes as well as for possible contaminations with *Mycoplasma spec*.

5.1.2 Passaging and seeding of cells

In order to detach adherent cells from cell culture vessels, the culture medium was removed and cells were washed once with 1x PBS. 1-2 mL of 0.25% trypsin-EDTA was applied to the cells and distributed evenly to cover the cell monolayer. The cells were then incubated at 37°C until they detached. The trypsin was inactivated by the addition of 5 mL DMEM medium containing 10% FCS and cells were transferred into a 15 mL reaction tube and centrifuged for 10 min at 1000 rpm (room temperature). Cells were washed once in 1x PBS and resuspended in 10 mL of fresh culture medium. For maintenance culture, cells were transferred into culture flasks at a ratio of 1:10 and further incubated at 37°C.

For experimental purpose, 50 μL of the respective cell suspensions were stained with an equal volume of 0.25% trypan blue in 1x PBS and the cell number per mL was determined in a Neubauer hemocytometer or Countess® II FL Automated Cell Counter (Life Technologies). The desired number of cells was transferred into culture vessels and incubated at 37°C.

Unless otherwise mentioned, CaSki cells were seeded at a density of 1.0^*10^6 per 6 cm culture dishes; SiHa and HepG2 cells were seeded at a density of 1.2^*10^6 per 6 cm culture dishes.

5.1.3 Cyroconservation and re-activation of cells

For long-term storage of cell lines, cells were collected as described in the previous paragraph and washed in 1x PBS. Cell pellets of ca. $1-2^*10^6$ cells were resuspended in 1 mL of the respective pre-chilled cryo-medium (60% DMEM, 30% FCS and 10% DMSO) and transferred into cryo tubes

which were quickly wrapped in several layers of tissue paper and transferred to -80°C. After 5-10 days, the cells were transferred into cryo-conservation tanks filled with liquid nitrogen.

To reactivate cells, cryo tubes were placed at room temperature until cells were thawed. The cells were then quickly transferred to 10 mL of cultivation medium. Cells were collected by centrifugation and washed with 1x PBS. Cell pellets were then resuspended in fresh culture medium and transferred to culture flasks.

5.1.4 Experimental oxygen conditions

Generally, cells were grown at 21% O_2 which is termed normoxia and was used as control condition in this study. To monitor the cellular hypoxic reaction, cells were exposed to 1% O_2 in the incubator C16 (Labotect, Göttingen) or in the InvivO$_2$ 400 physiological oxygen workstation (Ruskinn Technology Ltd, Bridgend, UK) two days after seeding. Depending on the experimental approach, the hypoxia treatment lasted from 0-120 h. During that time, the incubator was always closed to prevent reoxygenation of the cells. To ensure a continuous adequate atmosphere, time course experiments were all performed in the InvivO$_2$ workstation.

5.1.5 Experimental glucose conditions

CaSki and SiHa cells were grown in standard glucose conditions of 1 g/L already present in the culture medium; HepG2 cells were grown in glucose conditions of 4.5 g/L already present in the culture medium, unless otherwise mentioned.

Only in the experiment to test the effect of glucose on p53 regulation under hypoxia (described in chapter 3.3), cells were grown in media containing different amounts of glucose (0, 1, 2, 4.5 g/L).

5.1.6 Treatment of cells with chemical compounds

Cells were treated with inhibitors or small molecule compounds (see **Table 5.1**) two days after seeding. The compounds were added directly into the medium and the appropriate volume of the solvent was applied to control cells.

Table 5.1 | Chemical compounds.

Compound	Solvent
Bafilomycin A1	DMSO
Chloroquine	H_2O
Cycloheximide	DMSO
MG132	DMSO

5.1.7 Transfection of siRNA

For siRNA-mediated knock-down of proteins, $0.8*10^6$ cells were seeded in 6 cm cell culture dishes and incubated over night. Cells were transfected using Lipofectamine 2000. Therefore, 20-40 pmoles of specific siRNA or scrambled control siRNA were diluted in 500 μL of Opti-MEM. 6 μL of Lipofectamine were subsequently diluted in 500 μL of Opti-MEM and incubated for 5 min at room temperature. The Lipofectamine suspension was then added to the siRNA solution and mixed by pipetting up and down. The mixture was incubated for 20 min at room temperature, applied to the cells and distributed evenly. 48 h post transfection, the cells were cultured for 0-24 h at 21% O_2 or at 1% O_2. Total protein or total RNA was extracted after this time.

5.1.8 Transfection of expression plasmids

For transfection of plasmid DNA, $1.0*10^6$ cells were seeded in 6 cm cell culture dishes and incubated over night. Cells were transfected using Turbofect *in vitro* Transfection Reagent. Here, the respective plasmid DNA was diluted in 300 μL of Opti-MEM and mixed by vortexing. 4 μL of Turbofect were added to each plasmid solution and the suspension was again mixed by vortexing. The mix was incubated at room temperature for 15 min, added to the culture dishes and distributed evenly. 48 h post transfection, the cells were cultured for 0-24 h at 21% O_2 or at 1% O_2. Total protein was extracted.

5.1.9 Senescence assay

In the experiment to test the effect of hypoxia on cellular senescence, cells were cultured at 21% O_2 or at 1% O_2 for 24 or 72 h.

In the experiment to test the effect of inhibitors on senescence, cells cultured with/without inhibitors for 48 h at 21% O_2 or at 1% O_2. Cells were removed from the normoxic or hypoxic conditions, split into new 6 cm dishes in a ratio of 1:3 and further kept in standard cell culture medium under normoxia for three additional days.

Cells were then washed with PBS and fixed with 1 mL senescence assay fixation buffer for 3 min. After removing the fixation buffer and additional washing with PBS, cells were incubated with 1.5 mL senescence assay staining buffer for 24 h at 37°C in a wet chamber. Senescence assay buffer was then removed and PBS was added to the 6 cm dishes. Images of representative cells were taken with a brightfield microscope (EVOS XL Core Cell Imaging System, Life Technologies, Calsbad, CA, USA).

5.1.10 Cell counts and ATP assay

Cell counts: Cells were cultured for the indicated time periods (4-72 h) at 21% O_2 or at 1% O_2. Viable cell numbers were determined by a standard trypan blue technique, using Countess® II FL Automated Cell Counter (Life Technologies).

ATP assay: Cells were seeded in 96-well plates at a density of $6*10^4$ cells per well in triplicates. Control wells containing medium without cells to obtain a value of background luminescence were included. One plate for each time point. 24 h after seeding, cells were cultured for the indicated time at 21% O_2 or at 1% O_2. ATP assay was performed after respective time intervals (following the protocol of CellTiter-Glo® Luminescent Cell Viability Assay):

1. Equilibrate the plate and its contents at room temperature for approximately 30 minutes.
2. Add a volume of CellTiter-Glo® Reagent equal to the volume of cell culture medium present in each well.
3. Mix contents for 2 minutes on an orbital shaker to induce cell lysis.
4. Allow the plate to incubate at room temperature for 10 minutes to stabilize luminescent signal.
5. Record luminescence (An integration time of 1 second per well).

5.1.11 MTT assay

Cells were seeded in 96-well plates at a density of $6*10^4$ cells per well in quadruplicates. One plate for each time point. 24 h after seeding, cells were cultured for the indicated time at 21% O_2 or at 1% O_2. MTT assay was performed after respective time intervals (using a 10 mg/mL solution in water):

1. Add an equal volume of MTT solution (final concentration 0.5 mg/mL) to the existing media in the culture.
2. Incubate the plates at 37°C for 4 hours at 21% O_2 or at 1% O_2.
3. After incubation, add 100 µL 2-Propanol into each well.
4. Wrap plates in foil and shake on an orbital shaker for 15 min.
5. Read absorbance at OD = 570 nm. Read plate within 1 hour.

5.2 Isolation and analysis of nucleic acids

5.2.1 Isolation of RNA

Cells were washed once with 1x PBS prior to RNA extraction using the RNeasy Mini Kit. RLT lysis buffer was supplemented with 10 µL of 2-mercaptoethanol per mL buffer and 600 µL of buffer were added directly to the washed cells. Cells were dislodged from the cultivation vessel

with a cell scraper and collected in a 2 mL reaction tube. Cell membranes were disrupted by passing the suspension 10 times through a 20G needle. One volume of 70% ethanol (prepared with DEPC water) was added to the suspensions, which were then applied to a spin column and processed according to the manufacturer's protocol. The DNase digestion was performed using the Qiagen RNase-Free DNase Set. RNA was eluted into 35 µL of RNase-free water and its concentration was measured photometrically.

5.2.2 Spectrophotometric determination of nucleic acid concentrations

The concentrations of RNAs and DNAs were determined photometrically using either a Synergy 2 plate reader.

5.2.3 Reverse transcription of RNA

RNA was transcribed into cDNA employing RevertAid Reverse transcriptase with random primers using the following protocol:

In a first step, the following components were pipetted into a 0.5 mL soft reaction tube.

	positive reaction	negative control
RNA	250 ng – 1 µg	250 ng – 1 µg
Primer (20 µM)	1 µL	1 µL
RNase-free water	Add up to final volume 12.5 µL	Add up to final volume 12.5 µL

In order to analyse possible DNA contamination of extracted RNA, reactions without Reverse Transcriptase were prepared in parallel and served as negative controls.

Samples were incubated at 56°C for 5 min in order to allow correct primer annealing to mRNAs. The samples were cooled on ice for 1 min before adding the following reagents:

	positive reaction	negative control
5x RevertAid Buffer	4 µL	4 µL
dNTPS (10mM)	2 µL	2 µL
	1 µL RevertAid Reverse Transcriptase	1.5 µL RNase-free water
	0.5 µL RiboLock	

Samples were incubated at 42°C for 1 h followed by a 10 min incubation step at 72°C.

The generated cDNAs, as well as negative controls, were diluted to a final concentration of 10 ng/µL (assuming that all of the introduced RNA was transcribed). As an internal control, all cDNA samples were analysed for transcripts of human *GAPDH* by semi-quantitative PCR (RT-PCR). Samples showing a signal in the respective negative control were discarded. Samples whose integrity was confirmed were analysed for specific gene transcripts by RT-PCR.

Table 5.2 | Oligonucleotides (primer) for RT-PCR. size: expected size of amplified fragments. T$_A$: annealing temperature of respective primer pairs.

Primer Name	Sequence 5' → 3'	size (bp)	T$_A$ / cycles
GAPDH fw	GCCTTCCGTGTCCCCACTGC	345	65°C/25 cycles
GAPDH rev	GCTCTTGCTGGGGCTGGTGG		

5.2.4 Semi-quantitative polymerase chain reaction

Semi-quantitative polymerase chain reactions (RT-PCRs) were set up according to the following scheme:

Dream Taq Green 2x Master Mix	10 µL
cDNA Template	1 µL
Primer Mix (fw + rev; 20 µM)	1 µL
ddH$_2$O	Add up to final volume 20 µL

Target sequences were amplified in a thermo cycler following the standard amplification protocol:

95°C/3' – [95°C/30'' – X°C/30'' – 72°C/Y] x Z – 72°C/10'

with   X: primer annealing temperature

Y: elongation time, 1 min/1 kb fragment size

Z: cycle number

RT-PCR reactions were subjected to agarose gel electrophoresis and amplified fragments were visualised at 260 nm wavelength in a documentation device or on a UV table.

If unspecific RT-PCR products were detected, 3% DMSO were added to the reactions prior to amplification in order to favour more specific primer binding.

5.2.5 Agarose gel electrophoresis

DNA fragments were separated via gel electrophoresis on agarose gels (1-1.5% agarose in 1x TAE buffer) containing 10 µL ethidium bromide per 100 mL molten agarose. DNA fragments were

visualised under UV light at 260 nm wave-length and their size was determined with the help of a size marker (GeneRuler DNA Ladder Mix) that was applied alongside the DNA samples.

5.2.6 Quantitative polymerase chain reaction

Quantitative real-time PCR (qPCR) was performed using iTaq™ Universal SYBR® Green Supermix. For qPCR, specific primers that yielded fragments of less than 250 bp were employed (see **Table 4.1**)

Reactions were set up as follows:

iTaq™ Universal SYBR® Green Supermix (2X)	7.5 µL
Primer Mix (fw + rev; 10 µM)	0.5 µL
cDNA Template	1 µL
ddH$_2$O	Add up to final volume 15 µL

For every sample, the transcript levels of 18S rRNA was analysed in addition to the respective target gene fragment in order to allow the later normalisation of the obtained signal intensities.

Amplification was performed in CFX96 Real-Time PCR Detection System using the following program:

Step	Temperature	Time	Cycles
Polymerase activation and DNA denaturation	95°C	30 sec	1
Denaturation	95°C	5 sec	40
Annealing/Extension + Plate Read	60°C	30 sec	
Melt curve analysis	65°C, 0.5°C increments 5 sec/step		

The relative transcript content (Fc value) of individual samples was calculated from obtained Ct values, employing the following equation:

$$Fc = 2^{-\Delta\Delta Ct}$$

with
$$\Delta\Delta Ct = (Ct_{target} - Ct_{reference})_{control} - (Ct_{target} - Ct_{reference})_{test}$$

In this study, 18S was used as the reference gene and the control and the test samples were described in figure legends.

5.2.7 Propagation and isolation of expression plasmids

Plasmids were extracted from 2 mL of cell suspensions using a Miniprep Kit (Qiagen) according to the manufacturer's instructions. Isolated plasmids were resuspended in 50-200 μL TE buffer and subsequently used for the transfection of eukaryotic cells.

Suspensions of bacteria harbouring a plasmid of interest were cryo-conserved by mixing 750 μL of suspension with 250 μL of glycerol. These glycerol stocks were stored at -80°C and later used to inoculate fresh LB medium.

5.3 Isolation and analyses of proteins

5.3.1 Extraction of proteins

In order to extract total protein, experimental cells were washed once with ice-cold 1X PBS. 100 μL of CSKI buffer freshly supplemented with protease and phosphatase inhibitors as described in **Table 5.3**.

Table 5.3 | **Protease and phosphatase inhibitors.**

Agent	Function	Final concentration
DTT	Reducing agent	1 mM
Complete protease inhibitor cocktail	Protease inhibitor	1X
MG132	Proteasome inhibitor	1 μM
NaF	Phosphatase inhibitor	1 mM
Na_3VO_4	Phosphatase inhibitor	0.2 mM

The cells were scraped and the cell suspension was transferred into a 1.5 mL reaction tube. The suspensions were incubated on ice for 30 min and mixed every 10 min in order to enhance passive lysis of cells. The lysates were then centrifuged for 30 min at 13000 rpm and 4°C to remove remaining cell debris. Supernatants were then collected in fresh 1.5 mL reaction tubes and stored at -80°C until protein quantification.

5.3.2 Separation of nuclear and cytosolic cell fractions

For protein extractions from different cell fractions, cells were washed once with 1X PBS. 400 μL of pre-chilled buffer A freshly supplemented with protease and phosphatase inhibitors were added to the cells in culture dishes and cells were dislodged using a cell scrapper. The cell suspension was then collected to a 1.5 mL reaction tube and incubated on ice for 15 min. After the hypotonic

swelling of the cells, 25 μL of 10% Nonidet P-40 solution was added to the cell suspension and vortexed for 10 sec. The homogenate was then centrifuged for 1 min at 13000 rpm and 4°C. The supernatant containing cytoplasmic protein was transferred to a fresh 1.5 mL reaction tube and stored at -80°C until protein quantification.

The cell pellet was resuspended in 50 μL of ice-cold buffer C freshly supplemented with protease and phosphatase inhibitors and incubated for 15 min at 4°C, during which the nuclear membrane was lysed. After 5 min of centrifugation at 13000 rpm and 4°C, the supernatant containing the nuclear protein extract was transferred to a fresh 1.5 mL reaction tube and stored at -80°C until protein quantification.

5.3.3 Quantification of protein concentrations

Protein concentrations were determined colorimetrically using Bradford Assay Reagent. 5 μL of a 1:10 dilution of the respective cleared cell lysates were added to 155 μL water in a 96-well plate and mixed with 40 μL of 5x Bradford Reagent. As a standard, a serial dilution of BSA was prepared and measured alongside the respective protein samples, in order to determine the sample's protein content. The absorption of the standard and protein samples was determined photometrically in a plate reader at a wavelength of 595nm and the samples' concentrations were calculated according to the straight calibration line of the standard.

5.3.4 SDS-polyacrylamide gel electrophoresis (SDS-PAGE)

Proteins were separated via SDS-polyacrylamide gel electrophoresis (SDS-PAGE) which employs discontinuous polyacrylamide gels with a stacking and a resolving fraction. The separation of proteins along an electric current is dependent on the proteins' electrophoretic mobility which is determined by protein size and modification. Depending on the expected size of the analysed proteins polyacrylamide gels with 10, 12 or 15% acrylamide in the resolving gel and 6% acrylamide in the stacking gel were cast as follows:

Resolving gels:	Stacking gels:
0.3 M Tris, pH 8.8	0.25 M Tris, pH 6.8
10, 12 or 15% Acrylamide-Bis (29:1)	6% Acrylamide-Bis (29:1)
0.1% SDS	0.1% SDS
0.1% APS	0.1% APS
0.08% TEMED	0.16% TEMED

Cleared protein lysates were supplemented with 5x SDS loading dye and incubated at 99°C for 10 min. 50 µg of denatured protein samples were applied to the acrylamide gel alongside a size marker (PageRuler). SDS-PAGE was carried out in 1x SDS running buffer at 80 V for 20-30 min until the complete sample volume had migrated into the resolving gel. The voltage was then increased to 120 V until the desired size separation according to the marker had taken place.

5.3.5 Immunoblotting and Western blot analyses

Proteins were separated via SDS-PAGE. Size-separated proteins were then transferred to PVDF membranes employing a semi-dry approach. Therefore, acrylamide gels with size-separated proteins were incubated in Cathode Buffer for 10 min. In the meantime, PVDF membranes were activated in methanol for 10-20 sec and washed briefly in water. Activated membranes were equilibrated in Anode Buffer II for 5 min. Together with Whatman papers soaked in Anode Buffer I and II or Cathode Buffer, PVDF membranes and acrylamide gels were placed in a semi-dry blotting chamber according to **Figure 5.1**. The transfer of proteins onto PVDF membranes was performed for 35 min at 0.2 A per membrane.
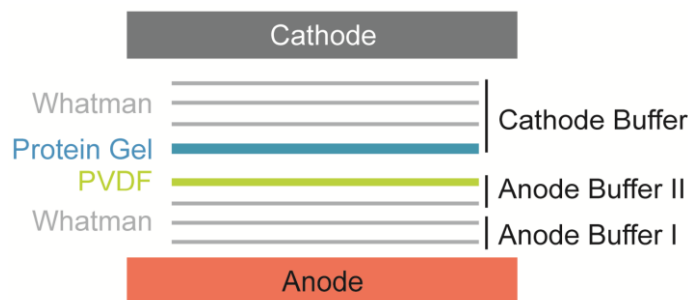
Figure 5.1 | Set-up for immunoblotting via semi-dry transfer of proteins. Whatman filter papers (grey), acrylamide gels with size-separated proteins (blue) and activated PVDF membranes (green) were equilibrated in the indicated transfer buffers. Figure created by Martina Niebler, DKFZ Heidelberg.

After protein transfer, PVDF membranes were blocked with 5% Milk/TBST for 1 h at room temperature. The respective primary antibody (see **Table 4.4**) was diluted in 5% Milk/TBST and applied to the blocked membranes. Membranes were incubated with primary antibodies for 12-18 h on an overhead shaker at 4°C.

For the detection of specific proteins, overnight-incubated membranes were washed four times with 1x TBST. Then the respective HRP-conjugated secondary antibody was added in 5% Milk/TBST and incubated with the membranes for 1 h at room temperature. Membranes were again washed for four times in 1x TBST. 1 mL of ECL was applied to each membrane and incubated for 1 min at room temperature. Proteins were detected via the exposition of medical X-ray films for 3 sec to 40 min, depending on the desired signal intensities.

5.4 Statistical analyses

Microsoft Excel (Microsoft Office 2013) was used for data analysis. Statistical significance was determined by the two-tailed Student's *t* test. P-values of ≤0.05 (*), ≤0.01 (**), or ≤0.001 (***) were considered statistically significant.

For calculation of the half-life of p53 protein in **Figure 2.4**, a linear trendline was added using the trendline function in Excel. The line was generally forced through the origin. Calculate the slope of degradation line for each condition using the slope function in Excel. Use the following formula to determine the half-life: half-life (min) = [log(0.5)]/slope.

6. References

1.   Plummer, M., C. de Martel, J. Vignat, J. Ferlay, F. Bray, and S. Franceschi, *Global burden of cancers attributable to infections in 2012: a synthetic analysis.* Lancet Glob Health, 2016. **4**(9): p. e609-16.

2.   Bray, F., J. Ferlay, I. Soerjomataram, R.L. Siegel, L.A. Torre, and A. Jemal, *Global cancer statistics 2018: GLOBOCAN estimates of incidence and mortality worldwide for 36 cancers in 185 countries.* CA Cancer J Clin, 2018. **68**(6): p. 394-424.

3.   Katzke, V.A., R. Kaaks, and T. Kuhn, *Lifestyle and cancer risk.* Cancer J, 2015. **21**(2): p. 104-10.

4.   Peto, J., *Cancer epidemiology in the last century and the next decade.* Nature, 2001. **411**(6835): p. 390-5.

5.   Walboomers, J.M., M.V. Jacobs, M.M. Manos, F.X. Bosch, J.A. Kummer, K.V. Shah, P.J. Snijders, J. Peto, C.J. Meijer, and N. Munoz, *Human papillomavirus is a necessary cause of invasive cervical cancer worldwide.* J Pathol, 1999. **189**(1): p. 12-9.

6.   Moody, C.A. and L.A. Laimins, *Human papillomavirus oncoproteins: pathways to transformation.* Nat Rev Cancer, 2010. **10**(8): p. 550-60.

7.   Stanley, M.A., M.R. Pett, and N. Coleman, *HPV: from infection to cancer.* Biochem Soc Trans, 2007. **35**(Pt 6): p. 1456-60.

8.   Doorbar, J., N. Egawa, H. Griffin, C. Kranjec, and I. Murakami, *Human papillomavirus molecular biology and disease association.* Rev Med Virol, 2015. **25 Suppl 1**: p. 2-23.

9.   Van Doorslaer, K., Q. Tan, S. Xirasagar, S. Bandaru, V. Gopalan, Y. Mohamoud, Y. Huyen, and A.A. McBride, *The Papillomavirus Episteme: a central resource for papillomavirus sequence data and analysis.* Nucleic Acids Res, 2013. **41**(Database issue): p. D571-8.

10.   Bernard, H.U., R.D. Burk, Z. Chen, K. van Doorslaer, H. zur Hausen, and E.M. de Villiers, *Classification of papillomaviruses (PVs) based on 189 PV types and proposal of taxonomic amendments.* Virology, 2010. **401**(1): p. 70-9.

11.   de Villiers, E.M., C. Fauquet, T.R. Broker, H.U. Bernard, and H. zur Hausen, *Classification of papillomaviruses.* Virology, 2004. **324**(1): p. 17-27.

12.   de Villiers, E.M., *Cross-roads in the classification of papillomaviruses.* Virology, 2013. **445**(1-2): p. 2-10.

13.   Egawa, N. and J. Doorbar, *The low-risk papillomaviruses.* Virus Res, 2017. **231**: p. 119-127.

14.   Chabeda, A., R.J.R. Yanez, R. Lamprecht, A.E. Meyers, E.P. Rybicki, and Hitzeroth, II, *Therapeutic vaccines for high-risk HPV-associated diseases.* Papillomavirus Res, 2018. **5**: p. 46-58.

15.   Van Doorslaer, K., *Evolution of the papillomaviridae.* Virology, 2013. **445**(1-2): p. 11-20.

16.   Stanley, M.A., *Epithelial cell responses to infection with human papillomavirus.* Clin Microbiol Rev, 2012. **25**(2): p. 215-22.

17.   Zheng, Z.M. and C.C. Baker, *Papillomavirus genome structure, expression, and post-transcriptional regulation.* Front Biosci, 2006. **11**: p. 2286-302.

18.   Bravo, I.G. and A. Alonso, *Mucosal human papillomaviruses encode four different E5 proteins whose chemistry and phylogeny correlate with malignant or benign growth.* J Virol, 2004. **78**(24): p. 13613-26.

19.   Wang, X., C. Meyers, H.K. Wang, L.T. Chow, and Z.M. Zheng, *Construction of a full transcription map of human papillomavirus type 18 during productive viral infection.* J Virol, 2011. **85**(16): p. 8080-92.

20.   Kines, R.C., C.D. Thompson, D.R. Lowy, J.T. Schiller, and P.M. Day, *The initial steps leading to papillomavirus infection occur on the basement membrane prior to cell surface binding.* Proc Natl Acad Sci U S A, 2009. **106**(48): p. 20458-63.

21.   Johnson, K.M., R.C. Kines, J.N. Roberts, D.R. Lowy, J.T. Schiller, and P.M. Day, *Role of heparan sulfate in attachment to and infection of the murine female genital tract by human papillomavirus.* J Virol, 2009. **83**(5): p. 2067-74.

22.   Sapp, M. and M. Bienkowska-Haba, *Viral entry mechanisms: human papillomavirus and a long journey from extracellular matrix to the nucleus.* FEBS J, 2009. **276**(24): p. 7206-16.

23.   Sapp, M. and P.M. Day, *Structure, attachment and entry of polyoma- and papillomaviruses.* Virology, 2009. **384**(2): p. 400-9.

24.   Cheng, S., D.C. Schmidt-Grimminger, T. Murant, T.R. Broker, and L.T. Chow, *Differentiation-dependent up-regulation of the human papillomavirus E7 gene reactivates cellular DNA replication in suprabasal differentiated keratinocytes.* Genes Dev, 1995. **9**(19): p. 2335-49.

25.   Scheffner, M., J.M. Huibregtse, R.D. Vierstra, and P.M. Howley, *The HPV-16 E6 and E6-AP complex functions as a ubiquitin-protein ligase in the ubiquitination of p53.* Cell, 1993. **75**(3): p. 495-505.

26. Pim, D. and L. Banks, *Interaction of viral oncoproteins with cellular target molecules: infection with high-risk vs low-risk human papillomaviruses.* APMIS, 2010. **118**(6-7): p. 471-93.

27. Galloway, D.A., L.C. Gewin, H. Myers, W. Luo, C. Grandori, R.A. Katzenellenbogen, and J.K. McDougall, *Regulation of telomerase by human papillomaviruses.* Cold Spring Harb Symp Quant Biol, 2005. **70**: p. 209-15.

28. Buck, C.B., N. Cheng, C.D. Thompson, D.R. Lowy, A.C. Steven, J.T. Schiller, and B.L. Trus, *Arrangement of L2 within the papillomavirus capsid.* J Virol, 2008. **82**(11): p. 5190-7.

29. Day, P.M., R.B. Roden, D.R. Lowy, and J.T. Schiller, *The papillomavirus minor capsid protein, L2, induces localization of the major capsid protein, L1, and the viral transcription/replication protein, E2, to PML oncogenic domains.* J Virol, 1998. **72**(1): p. 142-50.

30. Chung, S.H., S. Franceschi, and P.F. Lambert, *Estrogen and ERalpha: culprits in cervical cancer?* Trends Endocrinol Metab, 2010. **21**(8): p. 504-11.

31. Westrich, J.A., C.J. Warren, and D. Pyeon, *Evasion of host immune defenses by human papillomavirus.* Virus Res, 2017. **231**: p. 21-33.

32. zur Hausen, H., *Papillomaviruses and cancer: from basic studies to clinical application.* Nat Rev Cancer, 2002. **2**(5): p. 342-50.

33. Doorbar, J., *Molecular biology of human papillomavirus infection and cervical cancer.* Clin Sci (Lond), 2006. **110**(5): p. 525-41.

34. Middleton, K., W. Peh, S. Southern, H. Griffin, K. Sotlar, T. Nakahara, A. El-Sherif, L. Morris, R. Seth, M. Hibma, D. Jenkins, P. Lambert, N. Coleman, and J. Doorbar, *Organization of human papillomavirus productive cycle during neoplastic progression provides a basis for selection of diagnostic markers.* J Virol, 2003. **77**(19): p. 10186-201.

35. Jeon, S. and P.F. Lambert, *Integration of human papillomavirus type 16 DNA into the human genome leads to increased stability of E6 and E7 mRNAs: implications for cervical carcinogenesis.* Proc Natl Acad Sci U S A, 1995. **92**(5): p. 1654-8.

36. Schiffman, M. and N. Wentzensen, *Human papillomavirus infection and the multistage carcinogenesis of cervical cancer.* Cancer Epidemiol Biomarkers Prev, 2013. **22**(4): p. 553-60.

37. Wabinga, H.R., S. Nambooze, P.M. Amulen, C. Okello, L. Mbus, and D.M. Parkin, *Trends in the incidence of cancer in Kampala, Uganda 1991-2010.* Int J Cancer, 2014. **135**(2): p. 432-9.

References

38. Chokunonga, E., M.Z. Borok, Z.M. Chirenje, A.M. Nyakabau, and D.M. Parkin, *Trends in the incidence of cancer in the black population of Harare, Zimbabwe 1991-2010.* Int J Cancer, 2013. **133**(3): p. 721-9.

39. Bray, F., J. Lortet-Tieulent, A. Znaor, M. Brotons, M. Poljak, and M. Arbyn, *Patterns and trends in human papillomavirus-related diseases in Central and Eastern Europe and Central Asia.* Vaccine, 2013. **31 Suppl 7**: p. H32-45.

40. in *Comprehensive Cervical Cancer Control: A Guide to Essential Practice*, nd, Editor. 2014: Geneva.

41. Lehtinen, M. and J. Dillner, *Clinical trials of human papillomavirus vaccines and beyond.* Nat Rev Clin Oncol, 2013. **10**(7): p. 400-10.

42. Castle, P.E. and M. Maza, *Prophylactic HPV vaccination: past, present, and future.* Epidemiol Infect, 2016. **144**(3): p. 449-68.

43. Chuang, L.T., S. Temin, R. Camacho, A. Duenas-Gonzalez, S. Feldman, M. Gultekin, V. Gupta, S. Horton, G. Jacob, E.A. Kidd, K. Lishimpi, C. Nakisige, J.H. Nam, H.Y.S. Ngan, W. Small, G. Thomas, and J.S. Berek, *Management and Care of Women With Invasive Cervical Cancer: American Society of Clinical Oncology Resource-Stratified Clinical Practice Guideline.* J Glob Oncol, 2016. **2**(5): p. 311-340.

44. Roden, R.B., M. Ling, and T.C. Wu, *Vaccination to prevent and treat cervical cancer.* Hum Pathol, 2004. **35**(8): p. 971-82.

45. Ke, G., L. Liang, J.M. Yang, X. Huang, D. Han, S. Huang, Y. Zhao, R. Zha, X. He, and X. Wu, *MiR-181a confers resistance of cervical cancer to radiation therapy through targeting the pro-apoptotic PRKCD gene.* Oncogene, 2013. **32**(25): p. 3019-27.

46. Zhu, H., H. Luo, W. Zhang, Z. Shen, X. Hu, and X. Zhu, *Molecular mechanisms of cisplatin resistance in cervical cancer.* Drug Des Devel Ther, 2016. **10**: p. 1885-95.

47. McKeown, S.R., *Defining normoxia, physoxia and hypoxia in tumours-implications for treatment response.* Br J Radiol, 2014. **87**(1035): p. 20130676.

48. Vaupel, P., M. Hockel, and A. Mayer, *Detection and characterization of tumor hypoxia using pO2 histography.* Antioxid Redox Signal, 2007. **9**(8): p. 1221-35.

49. Vaupel, P. and A. Mayer, *Hypoxia in cancer: significance and impact on clinical outcome.* Cancer Metastasis Rev, 2007. **26**(2): p. 225-39.

50. Hoppe-Seyler, K., F. Bossler, C. Lohrey, J. Bulkescher, F. Rosl, L. Jansen, A. Mayer, P. Vaupel, M. Durst, and F. Hoppe-Seyler, *Induction of dormancy in hypoxic human papillomavirus-positive cancer cells.* Proc Natl Acad Sci U S A, 2017. **114**(6): p. E990-E998.

51. Kim, C.Y., M.H. Tsai, C. Osmanian, T.G. Graeber, J.E. Lee, R.G. Giffard, J.A. DiPaolo, D.M. Peehl, and A.J. Giaccia, *Selection of human cervical epithelial cells that possess reduced apoptotic potential to low-oxygen conditions.* Cancer Res, 1997. **57**(19): p. 4200-4.

52. Hockel, M., K. Schlenger, S. Hockel, and P. Vaupel, *Hypoxic cervical cancers with low apoptotic index are highly aggressive.* Cancer Res, 1999. **59**(18): p. 4525-8.

53. Hockel, M., C. Knoop, K. Schlenger, B. Vorndran, E. Baussmann, M. Mitze, P.G. Knapstein, and P. Vaupel, *Intratumoral pO2 predicts survival in advanced cancer of the uterine cervix.* Radiother Oncol, 1993. **26**(1): p. 45-50.

54. Hockel, M., K. Schlenger, B. Aral, M. Mitze, U. Schaffer, and P. Vaupel, *Association between tumor hypoxia and malignant progression in advanced cancer of the uterine cervix.* Cancer Res, 1996. **56**(19): p. 4509-15.

55. Fyles, A.W., M. Milosevic, R. Wong, M.C. Kavanagh, M. Pintilie, A. Sun, W. Chapman, W. Levin, L. Manchul, T.J. Keane, and R.P. Hill, *Oxygenation predicts radiation response and survival in patients with cervix cancer.* Radiother Oncol, 1998. **48**(2): p. 149-56.

56. Bertout, J.A., S.A. Patel, and M.C. Simon, *The impact of O2 availability on human cancer.* Nat Rev Cancer, 2008. **8**(12): p. 967-75.

57. Vaupel, P., *Pathophysiology of solid tumors.* The Impact of Tumor Biology on Cancer Treatment and Multidisciplinary Strategies, ed. M. Molls, Vaupel, P., Nieder, C., Anscher, M.S. 2009, Berlin, Heidelburg: Springer. pp 51–92.

58. Hockel, M. and P. Vaupel, *Tumor hypoxia: definitions and current clinical, biologic, and molecular aspects.* J Natl Cancer Inst, 2001. **93**(4): p. 266-76.

59. Dewhirst, M.W., *Relationships between cycling hypoxia, HIF-1, angiogenesis and oxidative stress.* Radiat Res, 2009. **172**(6): p. 653-65.

60. Jain, R.K., *Tumor angiogenesis and accessibility: role of vascular endothelial growth factor.* Semin Oncol, 2002. **29**(6 Suppl 16): p. 3-9.

61. Vaupel, P. and L. Harrison, *Tumor hypoxia: causative factors, compensatory mechanisms, and cellular response.* Oncologist, 2004. **9 Suppl 5**: p. 4-9.

62. Ritter, S. and M. Durante, *Heavy-ion induced chromosomal aberrations: a review.* Mutat Res, 2010. **701**(1): p. 38-46.

63. Nakano, T., Y. Mitsusada, A.M. Salem, M.I. Shoulkamy, T. Sugimoto, R. Hirayama, A. Uzawa, Y. Furusawa, and H. Ide, *Induction of DNA-protein cross-links by ionizing radiation and their elimination from the genome.* Mutat Res, 2015. **771**: p. 45-50.

64.   Shannon, A.M., D.J. Bouchier-Hayes, C.M. Condron, and D. Toomey, *Tumour hypoxia, chemotherapeutic resistance and hypoxia-related therapies.* Cancer Treat Rev, 2003. **29**(4): p. 297-307.

65.   Minchinton, A.I. and I.F. Tannock, *Drug penetration in solid tumours.* Nat Rev Cancer, 2006. **6**(8): p. 583-92.

66.   Brown, J.M., *Tumor hypoxia in cancer therapy.* Methods Enzymol, 2007. **435**: p. 297-321.

67.   Noman, M.Z., M. Hasmim, Y. Messai, S. Terry, C. Kieda, B. Janji, and S. Chouaib, *Hypoxia: a key player in antitumor immune response. A Review in the Theme: Cellular Responses to Hypoxia.* Am J Physiol Cell Physiol, 2015. **309**(9): p. C569-79.

68.   Wilson, W.R. and M.P. Hay, *Targeting hypoxia in cancer therapy.* Nat Rev Cancer, 2011. **11**(6): p. 393-410.

69.   Hunter, F.W., B.G. Wouters, and W.R. Wilson, *Hypoxia-activated prodrugs: paths forward in the era of personalised medicine.* Br J Cancer, 2016. **114**(10): p. 1071-7.

70.   Semenza, G.L., *Targeting HIF-1 for cancer therapy.* Nat Rev Cancer, 2003. **3**(10): p. 721-32.

71.   Harris, A.L., *Hypoxia--a key regulatory factor in tumour growth.* Nat Rev Cancer, 2002. **2**(1): p. 38-47.

72.   Xu, Q., J. Briggs, S. Park, G. Niu, M. Kortylewski, S. Zhang, T. Gritsko, J. Turkson, H. Kay, G.L. Semenza, J.Q. Cheng, R. Jove, and H. Yu, *Targeting Stat3 blocks both HIF-1 and VEGF expression induced by multiple oncogenic growth signaling pathways.* Oncogene, 2005. **24**(36): p. 5552-60.

73.   van Uden, P., N.S. Kenneth, and S. Rocha, *Regulation of hypoxia-inducible factor-1alpha by NF-kappaB.* Biochem J, 2008. **412**(3): p. 477-84.

74.   Keith, B., R.S. Johnson, and M.C. Simon, *HIF1alpha and HIF2alpha: sibling rivalry in hypoxic tumour growth and progression.* Nat Rev Cancer, 2011. **12**(1): p. 9-22.

75.   Duan, C., *Hypoxia-inducible factor 3 biology: complexities and emerging themes.* Am J Physiol Cell Physiol, 2016. **310**(4): p. C260-9.

76.   Heikkila, M., A. Pasanen, K.I. Kivirikko, and J. Myllyharju, *Roles of the human hypoxia-inducible factor (HIF)-3alpha variants in the hypoxia response.* Cell Mol Life Sci, 2011. **68**(23): p. 3885-901.

77.   Tanaka, T., M. Wiesener, W. Bernhardt, K.U. Eckardt, and C. Warnecke, *The human HIF (hypoxia-inducible factor)-3alpha gene is a HIF-1 target gene and may modulate hypoxic gene induction.* Biochem J, 2009. **424**(1): p. 143-51.

78. Maynard, M.A., A.J. Evans, W. Shi, W.Y. Kim, F.F. Liu, and M. Ohh, *Dominant-negative HIF-3 alpha 4 suppresses VHL-null renal cell carcinoma progression.* Cell Cycle, 2007. **6**(22): p. 2810-6.

79. Ivan, M., K. Kondo, H. Yang, W. Kim, J. Valiando, M. Ohh, A. Salic, J.M. Asara, W.S. Lane, and W.G. Kaelin, Jr., *HIFalpha targeted for VHL-mediated destruction by proline hydroxylation: implications for O2 sensing.* Science, 2001. **292**(5516): p. 464-8.

80. Martin, A.R., C. Ronco, L. Demange, and R. Benhida, *Hypoxia inducible factor down-regulation, cancer and cancer stem cells (CSCs): ongoing success stories.* Medchemcomm, 2017. **8**(1): p. 21-52.

81. Mahon, P.C., K. Hirota, and G.L. Semenza, *FIH-1: a novel protein that interacts with HIF-1alpha and VHL to mediate repression of HIF-1 transcriptional activity.* Genes Dev, 2001. **15**(20): p. 2675-86.

82. Majmundar, A.J., W.J. Wong, and M.C. Simon, *Hypoxia-inducible factors and the response to hypoxic stress.* Mol Cell, 2010. **40**(2): p. 294-309.

83. Peet, D. and S. Linke, *Regulation of HIF: asparaginyl hydroxylation.* Novartis Found Symp, 2006. **272**: p. 37-49; discussion 49-53, 131-40.

84. Nagaraju, G.P., T.E. Long, W. Park, J.C. Landry, L. Taliaferro-Smith, A.B. Farris, R. Diaz, and B.F. El-Rayes, *Heat shock protein 90 promotes epithelial to mesenchymal transition, invasion, and migration in colorectal cancer.* Mol Carcinog, 2015. **54**(10): p. 1147-58.

85. Isaacs, J.S., Y.J. Jung, E.G. Mimnaugh, A. Martinez, F. Cuttitta, and L.M. Neckers, *Hsp90 regulates a von Hippel Lindau-independent hypoxia-inducible factor-1 alpha-degradative pathway.* J Biol Chem, 2002. **277**(33): p. 29936-44.

86. Ravi, R., B. Mookerjee, Z.M. Bhujwalla, C.H. Sutter, D. Artemov, Q. Zeng, L.E. Dillehay, A. Madan, G.L. Semenza, and A. Bedi, *Regulation of tumor angiogenesis by p53-induced degradation of hypoxia-inducible factor 1alpha.* Genes Dev, 2000. **14**(1): p. 34-44.

87. Kamat, C.D., D.E. Green, L. Warnke, J.E. Thorpe, A. Ceriello, and M.A. Ihnat, *Mutant p53 facilitates pro-angiogenic, hyperproliferative phenotype in response to chronic relative hypoxia.* Cancer Lett, 2007. **249**(2): p. 209-19.

88. Warburg, O., *On respiratory impairment in cancer cells.* Science, 1956. **124**(3215): p. 269-70.

89. Vander Heiden, M.G., L.C. Cantley, and C.B. Thompson, *Understanding the Warburg effect: the metabolic requirements of cell proliferation.* Science, 2009. **324**(5930): p. 1029-33.

References

90. Christofk, H.R., M.G. Vander Heiden, M.H. Harris, A. Ramanathan, R.E. Gerszten, R. Wei, M.D. Fleming, S.L. Schreiber, and L.C. Cantley, *The M2 splice isoform of pyruvate kinase is important for cancer metabolism and tumour growth.* Nature, 2008. **452**(7184): p. 230-233.

91. Frauwirth, K.A., J.L. Riley, M.H. Harris, R.V. Parry, J.C. Rathmell, D.R. Plas, R.L. Elstrom, C.H. June, and C.B. Thompson, *The CD28 signaling pathway regulates glucose metabolism.* Immunity, 2002. **16**(6): p. 769-77.

92. Hanahan, D. and R.A. Weinberg, *The hallmarks of cancer.* Cell, 2000. **100**(1): p. 57-70.

93. Ganapathy-Kanniappan, S. and J.F. Geschwind, *Tumor glycolysis as a target for cancer therapy: progress and prospects.* Mol Cancer, 2013. **12**: p. 152.

94. Hu, C.J., L.Y. Wang, L.A. Chodosh, B. Keith, and M.C. Simon, *Differential roles of hypoxia-inducible factor 1alpha (HIF-1alpha) and HIF-2alpha in hypoxic gene regulation.* Mol Cell Biol, 2003. **23**(24): p. 9361-74.

95. Brahimi-Horn, M.C., J. Chiche, and J. Pouyssegur, *Hypoxia signalling controls metabolic demand.* Curr Opin Cell Biol, 2007. **19**(2): p. 223-9.

96. Kim, J.W., I. Tchernyshyov, G.L. Semenza, and C.V. Dang, *HIF-1-mediated expression of pyruvate dehydrogenase kinase: a metabolic switch required for cellular adaptation to hypoxia.* Cell Metab, 2006. **3**(3): p. 177-85.

97. Papandreou, I., R.A. Cairns, L. Fontana, A.L. Lim, and N.C. Denko, *HIF-1 mediates adaptation to hypoxia by actively downregulating mitochondrial oxygen consumption.* Cell Metab, 2006. **3**(3): p. 187-97.

98. Nakazawa, M.S., B. Keith, and M.C. Simon, *Oxygen availability and metabolic adaptations.* Nat Rev Cancer, 2016. **16**(10): p. 663-73.

99. Vaupel, P., O. Thews, and M. Hoeckel, *Treatment resistance of solid tumors: role of hypoxia and anemia.* Med Oncol, 2001. **18**(4): p. 243-59.

100. Yang, Z. and D.J. Klionsky, *An overview of the molecular mechanism of autophagy.* Curr Top Microbiol Immunol, 2009. **335**: p. 1-32.

101. Mizushima, N., *Physiological functions of autophagy.* Curr Top Microbiol Immunol, 2009. **335**: p. 71-84.

102. Rouschop, K.M. and B.G. Wouters, *Regulation of autophagy through multiple independent hypoxic signaling pathways.* Curr Mol Med, 2009. **9**(4): p. 417-24.

103. Rouschop, K.M., T. van den Beucken, L. Dubois, H. Niessen, J. Bussink, K. Savelkouls, T. Keulers, H. Mujcic, W. Landuyt, J.W. Voncken, P. Lambin, A.J. van der Kogel, M.

Koritzinsky, and B.G. Wouters, *The unfolded protein response protects human tumor cells during hypoxia through regulation of the autophagy genes MAP1LC3B and ATG5.* J Clin Invest, 2010. **120**(1): p. 127-41.

104.   Zhang, J. and P.A. Ney, *Role of BNIP3 and NIX in cell death, autophagy, and mitophagy.* Cell Death Differ, 2009. **16**(7): p. 939-46.

105.   Ryter, S.W. and A.M. Choi, *Regulation of autophagy in oxygen-dependent cellular stress.* Curr Pharm Des, 2013. **19**(15): p. 2747-56.

106.   Bellot, G., R. Garcia-Medina, P. Gounon, J. Chiche, D. Roux, J. Pouyssegur, and N.M. Mazure, *Hypoxia-induced autophagy is mediated through hypoxia-inducible factor induction of BNIP3 and BNIP3L via their BH3 domains.* Mol Cell Biol, 2009. **29**(10): p. 2570-81.

107.   Band, M., A. Joel, A. Hernandez, and A. Avivi, *Hypoxia-induced BNIP3 expression and mitophagy: in vivo comparison of the rat and the hypoxia-tolerant mole rat, Spalax ehrenbergi.* FASEB J, 2009. **23**(7): p. 2327-35.

108.   White, E. and R.S. DiPaola, *The double-edged sword of autophagy modulation in cancer.* Clin Cancer Res, 2009. **15**(17): p. 5308-16.

109.   Thorburn, A., *Autophagy and its effects: making sense of double-edged swords.* PLoS Biol, 2014. **12**(10): p. e1001967.

110.   Pimkina, J. and M.E. Murphy, *ARF, autophagy and tumor suppression.* Autophagy, 2009. **5**(3): p. 397-9.

111.   Kabeya, Y., N. Mizushima, A. Yamamoto, S. Oshitani-Okamoto, Y. Ohsumi, and T. Yoshimori, *LC3, GABARAP and GATE16 localize to autophagosomal membrane depending on form-II formation.* J Cell Sci, 2004. **117**(Pt 13): p. 2805-12.

112.   Corcelle, E.A., P. Puustinen, and M. Jaattela, *Apoptosis and autophagy: Targeting autophagy signalling in cancer cells -'trick or treats'?* FEBS J, 2009. **276**(21): p. 6084-96.

113.   Eisenberg-Lerner, A. and A. Kimchi, *The paradox of autophagy and its implication in cancer etiology and therapy.* Apoptosis, 2009. **14**(4): p. 376-91.

114.   Jones, R.G. and C.B. Thompson, *Tumor suppressors and cell metabolism: a recipe for cancer growth.* Genes Dev, 2009. **23**(5): p. 537-48.

115.   Maiuri, M.C., L. Galluzzi, E. Morselli, O. Kepp, S.A. Malik, and G. Kroemer, *Autophagy regulation by p53.* Curr Opin Cell Biol, 2010. **22**(2): p. 181-5.

116.   Yang, Z.J., C.E. Chee, S. Huang, and F.A. Sinicrope, *The role of autophagy in cancer: therapeutic implications.* Mol Cancer Ther, 2011. **10**(9): p. 1533-41.

117. Tavassoly, I., J. Parmar, A.N. Shajahan-Haq, R. Clarke, W.T. Baumann, and J.J. Tyson, *Dynamic Modeling of the Interaction Between Autophagy and Apoptosis in Mammalian Cells.* CPT Pharmacometrics Syst Pharmacol, 2015. **4**(4): p. 263-72.

118. Mazure, N.M. and J. Pouyssegur, *Hypoxia-induced autophagy: cell death or cell survival?* Curr Opin Cell Biol, 2010. **22**(2): p. 177-80.

119. Klionsky, D.J., *Autophagy revisited: a conversation with Christian de Duve.* Autophagy, 2008. **4**(6): p. 740-3.

120. Mizushima, N. and M. Komatsu, *Autophagy: renovation of cells and tissues.* Cell, 2011. **147**(4): p. 728-41.

121. Kobayashi, S., *Choose Delicately and Reuse Adequately: The Newly Revealed Process of Autophagy.* Biol Pharm Bull, 2015. **38**(8): p. 1098-103.

122. Feng, Y., D. He, Z. Yao, and D.J. Klionsky, *The machinery of macroautophagy.* Cell Res, 2014. **24**(1): p. 24-41.

123. Glick, D., S. Barth, and K.F. Macleod, *Autophagy: cellular and molecular mechanisms.* J Pathol, 2010. **221**(1): p. 3-12.

124. Li, W.W., J. Li, and J.K. Bao, *Microautophagy: lesser-known self-eating.* Cell Mol Life Sci, 2012. **69**(7): p. 1125-36.

125. Bandyopadhyay, U., S. Kaushik, L. Varticovski, and A.M. Cuervo, *The chaperone-mediated autophagy receptor organizes in dynamic protein complexes at the lysosomal membrane.* Mol Cell Biol, 2008. **28**(18): p. 5747-63.

126. Saftig, P., W. Beertsen, and E.L. Eskelinen, *LAMP-2: a control step for phagosome and autophagosome maturation.* Autophagy, 2008. **4**(4): p. 510-2.

127. Yu, L., Y. Chen, and S.A. Tooze, *Autophagy pathway: Cellular and molecular mechanisms.* Autophagy, 2018. **14**(2): p. 207-215.

128. Alers, S., A.S. Loffler, S. Wesselborg, and B. Stork, *Role of AMPK-mTOR-Ulk1/2 in the regulation of autophagy: cross talk, shortcuts, and feedbacks.* Mol Cell Biol, 2012. **32**(1): p. 2-11.

129. Mizushima, N., T. Yoshimori, and Y. Ohsumi, *The role of Atg proteins in autophagosome formation.* Annu Rev Cell Dev Biol, 2011. **27**: p. 107-32.

130. Xie, Z. and D.J. Klionsky, *Autophagosome formation: core machinery and adaptations.* Nat Cell Biol, 2007. **9**(10): p. 1102-9.

131. Ichimura, Y., T. Kirisako, T. Takao, Y. Satomi, Y. Shimonishi, N. Ishihara, N. Mizushima, I. Tanida, E. Kominami, M. Ohsumi, T. Noda, and Y. Ohsumi, *A ubiquitin-like system mediates protein lipidation.* Nature, 2000. **408**(6811): p. 488-92.

132. Pankiv, S., T.H. Clausen, T. Lamark, A. Brech, J.A. Bruun, H. Outzen, A. Overvatn, G. Bjorkoy, and T. Johansen, *p62/SQSTM1 binds directly to Atg8/LC3 to facilitate degradation of ubiquitinated protein aggregates by autophagy.* J Biol Chem, 2007. **282**(33): p. 24131-45.

133. Youle, R.J. and D.P. Narendra, *Mechanisms of mitophagy.* Nat Rev Mol Cell Biol, 2011. **12**(1): p. 9-14.

134. Ding, W.X. and X.M. Yin, *Mitophagy: mechanisms, pathophysiological roles, and analysis.* Biol Chem, 2012. **393**(7): p. 547-64.

135. Feng, D., L. Liu, Y. Zhu, and Q. Chen, *Molecular signaling toward mitophagy and its physiological significance.* Exp Cell Res, 2013. **319**(12): p. 1697-705.

136. Hanna, R.A., M.N. Quinsay, A.M. Orogo, K. Giang, S. Rikka, and A.B. Gustafsson, *Microtubule-associated protein 1 light chain 3 (LC3) interacts with Bnip3 protein to selectively remove endoplasmic reticulum and mitochondria via autophagy.* J Biol Chem, 2012. **287**(23): p. 19094-104.

137. Lee, Y., H.Y. Lee, R.A. Hanna, and A.B. Gustafsson, *Mitochondrial autophagy by Bnip3 involves Drp1-mediated mitochondrial fission and recruitment of Parkin in cardiac myocytes.* Am J Physiol Heart Circ Physiol, 2011. **301**(5): p. H1924-31.

138. Fuhrmann, D.C. and B. Brune, *Mitochondrial composition and function under the control of hypoxia.* Redox Biol, 2017. **12**: p. 208-215.

139. Liu, L., D. Feng, G. Chen, M. Chen, Q. Zheng, P. Song, Q. Ma, C. Zhu, R. Wang, W. Qi, L. Huang, P. Xue, B. Li, X. Wang, H. Jin, J. Wang, F. Yang, P. Liu, Y. Zhu, S. Sui, and Q. Chen, *Mitochondrial outer-membrane protein FUNDC1 mediates hypoxia-induced mitophagy in mammalian cells.* Nat Cell Biol, 2012. **14**(2): p. 177-85.

140. Zhang, H., M. Bosch-Marce, L.A. Shimoda, Y.S. Tan, J.H. Baek, J.B. Wesley, F.J. Gonzalez, and G.L. Semenza, *Mitochondrial autophagy is an HIF-1-dependent adaptive metabolic response to hypoxia.* J Biol Chem, 2008. **283**(16): p. 10892-903.

141. Bruick, R.K., *Expression of the gene encoding the proapoptotic Nip3 protein is induced by hypoxia.* Proc Natl Acad Sci U S A, 2000. **97**(16): p. 9082-7.

142. Feng, X., X. Liu, W. Zhang, and W. Xiao, *p53 directly suppresses BNIP3 expression to protect against hypoxia-induced cell death.* EMBO J, 2011. **30**(16): p. 3397-415.

143. Lane, D.P. and L.V. Crawford, *T antigen is bound to a host protein in SV40-transformed cells.* Nature, 1979. **278**(5701): p. 261-3.

144. Linzer, D.I. and A.J. Levine, *Characterization of a 54K dalton cellular SV40 tumor antigen present in SV40-transformed cells and uninfected embryonal carcinoma cells.* Cell, 1979. **17**(1): p. 43-52.

145. Hofseth, L.J., S.P. Hussain, and C.C. Harris, *p53: 25 years after its discovery.* Trends Pharmacol Sci, 2004. **25**(4): p. 177-81.

146. Finlay, C.A., P.W. Hinds, and A.J. Levine, *The p53 proto-oncogene can act as a suppressor of transformation.* Cell, 1989. **57**(7): p. 1083-93.

147. Malkin, D., F.P. Li, L.C. Strong, J.F. Fraumeni, Jr., C.E. Nelson, D.H. Kim, J. Kassel, M.A. Gryka, F.Z. Bischoff, M.A. Tainsky, and et al., *Germ line p53 mutations in a familial syndrome of breast cancer, sarcomas, and other neoplasms.* Science, 1990. **250**(4985): p. 1233-8.

148. Donehower, L.A., M. Harvey, B.L. Slagle, M.J. McArthur, C.A. Montgomery, Jr., J.S. Butel, and A. Bradley, *Mice deficient for p53 are developmentally normal but susceptible to spontaneous tumours.* Nature, 1992. **356**(6366): p. 215-21.

149. Kandoth, C., M.D. McLellan, F. Vandin, K. Ye, B. Niu, C. Lu, M. Xie, Q. Zhang, J.F. McMichael, M.A. Wyczalkowski, M.D.M. Leiserson, C.A. Miller, J.S. Welch, M.J. Walter, M.C. Wendl, T.J. Ley, R.K. Wilson, B.J. Raphael, and L. Ding, *Mutational landscape and significance across 12 major cancer types.* Nature, 2013. **502**(7471): p. 333-339.

150. Lawrence, M.S., P. Stojanov, C.H. Mermel, J.T. Robinson, L.A. Garraway, T.R. Golub, M. Meyerson, S.B. Gabriel, E.S. Lander, and G. Getz, *Discovery and saturation analysis of cancer genes across 21 tumour types.* Nature, 2014. **505**(7484): p. 495-501.

151. Levine, A.J., *p53, the cellular gatekeeper for growth and division.* Cell, 1997. **88**(3): p. 323-31.

152. Lane, D.P., *Cancer. p53, guardian of the genome.* Nature, 1992. **358**(6381): p. 15-6.

153. Kastan, M.B., O. Onyekwere, D. Sidransky, B. Vogelstein, and R.W. Craig, *Participation of p53 protein in the cellular response to DNA damage.* Cancer Res, 1991. **51**(23 Pt 1): p. 6304-11.

154. Matlashewski, G., P. Lamb, D. Pim, J. Peacock, L. Crawford, and S. Benchimol, *Isolation and characterization of a human p53 cDNA clone: expression of the human p53 gene.* EMBO J, 1984. **3**(13): p. 3257-62.

155. Isobe, M., B.S. Emanuel, D. Givol, M. Oren, and C.M. Croce, *Localization of gene for human p53 tumour antigen to band 17p13.* Nature, 1986. **320**(6057): p. 84-5.

156. Lamb, P. and L. Crawford, *Characterization of the human p53 gene.* Mol Cell Biol, 1986. **6**(5): p. 1379-85.

157. Surget, S., M.P. Khoury, and J.C. Bourdon, *Uncovering the role of p53 splice variants in human malignancy: a clinical perspective.* Onco Targets Ther, 2013. **7**: p. 57-68.

158. Ziemer, M.A., A. Mason, and D.M. Carlson, *Cell-free translations of proline-rich protein mRNAs.* J Biol Chem, 1982. **257**(18): p. 11176-80.

159. Itahana, Y., H. Ke, and Y. Zhang, *p53 Oligomerization is essential for its C-terminal lysine acetylation.* J Biol Chem, 2009. **284**(8): p. 5158-64.

160. Gu, W. and R.G. Roeder, *Activation of p53 sequence-specific DNA binding by acetylation of the p53 C-terminal domain.* Cell, 1997. **90**(4): p. 595-606.

161. Chan, W.M., M.C. Mak, T.K. Fung, A. Lau, W.Y. Siu, and R.Y. Poon, *Ubiquitination of p53 at multiple sites in the DNA-binding domain.* Mol Cancer Res, 2006. **4**(1): p. 15-25.

162. Lohrum, M.A., D.B. Woods, R.L. Ludwig, E. Balint, and K.H. Vousden, *C-terminal ubiquitination of p53 contributes to nuclear export.* Mol Cell Biol, 2001. **21**(24): p. 8521-32.

163. Hafner, A., M.L. Bulyk, A. Jambhekar, and G. Lahav, *The multiple mechanisms that regulate p53 activity and cell fate.* Nat Rev Mol Cell Biol, 2019. **20**(4): p. 199-210.

164. Boehme, K.A. and C. Blattner, *Regulation of p53--insights into a complex process.* Crit Rev Biochem Mol Biol, 2009. **44**(6): p. 367-92.

165. Kubbutat, M.H. and K.H. Vousden, *Keeping an old friend under control: regulation of p53 stability.* Mol Med Today, 1998. **4**(6): p. 250-6.

166. Michael, D. and M. Oren, *The p53-Mdm2 module and the ubiquitin system.* Semin Cancer Biol, 2003. **13**(1): p. 49-58.

167. Oliner, J.D., J.A. Pietenpol, S. Thiagalingam, J. Gyuris, K.W. Kinzler, and B. Vogelstein, *Oncoprotein MDM2 conceals the activation domain of tumour suppressor p53.* Nature, 1993. **362**(6423): p. 857-60.

168. Chi, S.W., S.H. Lee, D.H. Kim, M.J. Ahn, J.S. Kim, J.Y. Woo, T. Torizawa, M. Kainosho, and K.H. Han, *Structural details on mdm2-p53 interaction.* J Biol Chem, 2005. **280**(46): p. 38795-802.

169. Barak, Y., T. Juven, R. Haffner, and M. Oren, *mdm2 expression is induced by wild type p53 activity.* EMBO J, 1993. **12**(2): p. 461-8.

References

170. Juven, T., Y. Barak, A. Zauberman, D.L. George, and M. Oren, *Wild type p53 can mediate sequence-specific transactivation of an internal promoter within the mdm2 gene.* Oncogene, 1993. **8**(12): p. 3411-6.

171. Brooks, C.L. and W. Gu, *p53 ubiquitination: Mdm2 and beyond.* Mol Cell, 2006. **21**(3): p. 307-15.

172. Li, M., D. Chen, A. Shiloh, J. Luo, A.Y. Nikolaev, J. Qin, and W. Gu, *Deubiquitination of p53 by HAUSP is an important pathway for p53 stabilization.* Nature, 2002. **416**(6881): p. 648-53.

173. Sheng, Y., V. Saridakis, F. Sarkari, S. Duan, T. Wu, C.H. Arrowsmith, and L. Frappier, *Molecular recognition of p53 and MDM2 by USP7/HAUSP.* Nat Struct Mol Biol, 2006. **13**(3): p. 285-91.

174. Yuan, J., K. Luo, L. Zhang, J.C. Cheville, and Z. Lou, *USP10 regulates p53 localization and stability by deubiquitinating p53.* Cell, 2010. **140**(3): p. 384-96.

175. Hock, A.K., A.M. Vigneron, S. Carter, R.L. Ludwig, and K.H. Vousden, *Regulation of p53 stability and function by the deubiquitinating enzyme USP42.* EMBO J, 2011. **30**(24): p. 4921-30.

176. Shieh, S.Y., M. Ikeda, Y. Taya, and C. Prives, *DNA damage-induced phosphorylation of p53 alleviates inhibition by MDM2.* Cell, 1997. **91**(3): p. 325-34.

177. Polley, S., S. Guha, N.S. Roy, S. Kar, K. Sakaguchi, Y. Chuman, V. Swaminathan, T. Kundu, and S. Roy, *Differential recognition of phosphorylated transactivation domains of p53 by different p300 domains.* J Mol Biol, 2008. **376**(1): p. 8-12.

178. Jenkins, L.M., H. Yamaguchi, R. Hayashi, S. Cherry, J.E. Tropea, M. Miller, A. Wlodawer, E. Appella, and S.J. Mazur, *Two distinct motifs within the p53 transactivation domain bind to the Taz2 domain of p300 and are differentially affected by phosphorylation.* Biochemistry, 2009. **48**(6): p. 1244-55.

179. Vakhrusheva, O., C. Smolka, P. Gajawada, S. Kostin, T. Boettger, T. Kubin, T. Braun, and E. Bober, *Sirt7 increases stress resistance of cardiomyocytes and prevents apoptosis and inflammatory cardiomyopathy in mice.* Circ Res, 2008. **102**(6): p. 703-10.

180. Ito, A., Y. Kawaguchi, C.H. Lai, J.J. Kovacs, Y. Higashimoto, E. Appella, and T.P. Yao, *MDM2-HDAC1-mediated deacetylation of p53 is required for its degradation.* EMBO J, 2002. **21**(22): p. 6236-45.

181. Weber, J.D., L.J. Taylor, M.F. Roussel, C.J. Sherr, and D. Bar-Sagi, *Nucleolar Arf sequesters Mdm2 and activates p53.* Nat Cell Biol, 1999. **1**(1): p. 20-6.

182. Sherr, C.J., *Divorcing ARF and p53: an unsettled case.* Nat Rev Cancer, 2006. **6**(9): p. 663-73.

183. Stommel, J.M. and G.M. Wahl, *Accelerated MDM2 auto-degradation induced by DNA-damage kinases is required for p53 activation.* EMBO J, 2004. **23**(7): p. 1547-56.

184. O'Brate, A. and P. Giannakakou, *The importance of p53 location: nuclear or cytoplasmic zip code?* Drug Resist Updat, 2003. **6**(6): p. 313-22.

185. Jimenez, G.S., S.H. Khan, J.M. Stommel, and G.M. Wahl, *p53 regulation by post-translational modification and nuclear retention in response to diverse stresses.* Oncogene, 1999. **18**(53): p. 7656-65.

186. Stommel, J.M., N.D. Marchenko, G.S. Jimenez, U.M. Moll, T.J. Hope, and G.M. Wahl, *A leucine-rich nuclear export signal in the p53 tetramerization domain: regulation of subcellular localization and p53 activity by NES masking.* EMBO J, 1999. **18**(6): p. 1660-72.

187. Hao, Q. and W.C. Cho, *Battle against cancer: an everlasting saga of p53.* Int J Mol Sci, 2014. **15**(12): p. 22109-27.

188. Bieging, K.T., S.S. Mello, and L.D. Attardi, *Unravelling mechanisms of p53-mediated tumour suppression.* Nature Reviews Cancer, 2014. **14**: p. 359.

189. Fukasawa, K., F. Wiener, G.F. Vande Woude, and S. Mai, *Genomic instability and apoptosis are frequent in p53 deficient young mice.* Oncogene, 1997. **15**(11): p. 1295-302.

190. Hollander, M.C., M.S. Sheikh, D.V. Bulavin, K. Lundgren, L. Augeri-Henmueller, R. Shehee, T.A. Molinaro, K.E. Kim, E. Tolosa, J.D. Ashwell, M.P. Rosenberg, Q. Zhan, P.M. Fernandez-Salguero, W.F. Morgan, C.X. Deng, and A.J. Fornace, Jr., *Genomic instability in Gadd45a-deficient mice.* Nat Genet, 1999. **23**(2): p. 176-84.

191. Mantel, C., S.E. Braun, S. Reid, O. Henegariu, L. Liu, G. Hangoc, and H.E. Broxmeyer, *p21(cip-1/waf-1) deficiency causes deformed nuclear architecture, centriole overduplication, polyploidy, and relaxed microtubule damage checkpoints in human hematopoietic cells.* Blood, 1999. **93**(4): p. 1390-8.

192. Aylon, Y. and M. Oren, *p53: guardian of ploidy.* Mol Oncol, 2011. **5**(4): p. 315-23.

193. Liu, B., Y. Chen, and D.K. St Clair, *ROS and p53: a versatile partnership.* Free Radic Biol Med, 2008. **44**(8): p. 1529-35.

194. Sablina, A.A., A.V. Budanov, G.V. Ilyinskaya, L.S. Agapova, J.E. Kravchenko, and P.M. Chumakov, *The antioxidant function of the p53 tumor suppressor.* Nat Med, 2005. **11**(12): p. 1306-13.

References

195. Riley, T., E. Sontag, P. Chen, and A. Levine, *Transcriptional control of human p53-regulated genes.* Nat Rev Mol Cell Biol, 2008. **9**(5): p. 402-12.

196. Zilfou, J.T. and S.W. Lowe, *Tumor suppressive functions of p53.* Cold Spring Harb Perspect Biol, 2009. **1**(5): p. a001883.

197. Kortlever, R.M., P.J. Higgins, and R. Bernards, *Plasminogen activator inhibitor-1 is a critical downstream target of p53 in the induction of replicative senescence.* Nat Cell Biol, 2006. **8**(8): p. 877-84.

198. Matoba, S., J.G. Kang, W.D. Patino, A. Wragg, M. Boehm, O. Gavrilova, P.J. Hurley, F. Bunz, and P.M. Hwang, *p53 regulates mitochondrial respiration.* Science, 2006. **312**(5780): p. 1650-3.

199. Bensaad, K., A. Tsuruta, M.A. Selak, M.N. Vidal, K. Nakano, R. Bartrons, E. Gottlieb, and K.H. Vousden, *TIGAR, a p53-inducible regulator of glycolysis and apoptosis.* Cell, 2006. **126**(1): p. 107-20.

200. Schwartzenberg-Bar-Yoseph, F., M. Armoni, and E. Karnieli, *The tumor suppressor p53 down-regulates glucose transporters GLUT1 and GLUT4 gene expression.* Cancer Res, 2004. **64**(7): p. 2627-33.

201. Vousden, K.H. and K.M. Ryan, *p53 and metabolism.* Nat Rev Cancer, 2009. **9**(10): p. 691-700.

202. Lohr, K., C. Moritz, A. Contente, and M. Dobbelstein, *p21/CDKN1A mediates negative regulation of transcription by p53.* J Biol Chem, 2003. **278**(35): p. 32507-16.

203. Shats, I., M. Milyavsky, X. Tang, P. Stambolsky, N. Erez, R. Brosh, I. Kogan, I. Braunstein, M. Tzukerman, D. Ginsberg, and V. Rotter, *p53-dependent down-regulation of telomerase is mediated by p21waf1.* J Biol Chem, 2004. **279**(49): p. 50976-85.

204. Mummenbrauer, T., F. Janus, B. Muller, L. Wiesmuller, W. Deppert, and F. Grosse, *p53 Protein exhibits 3'-to-5' exonuclease activity.* Cell, 1996. **85**(7): p. 1089-99.

205. Green, D.R. and G. Kroemer, *Cytoplasmic functions of the tumour suppressor p53.* Nature, 2009. **458**(7242): p. 1127-30.

206. Tasdemir, E., M.C. Maiuri, L. Galluzzi, I. Vitale, M. Djavaheri-Mergny, M. D'Amelio, A. Criollo, E. Morselli, C. Zhu, F. Harper, U. Nannmark, C. Samara, P. Pinton, J.M. Vicencio, R. Carnuccio, U.M. Moll, F. Madeo, P. Paterlini-Brechot, R. Rizzuto, G. Szabadkai, G. Pierron, K. Blomgren, N. Tavernarakis, P. Codogno, F. Cecconi, and G. Kroemer, *Regulation of autophagy by cytoplasmic p53.* Nat Cell Biol, 2008. **10**(6): p. 676-87.

207. Vaseva, A.V. and U.M. Moll, *The mitochondrial p53 pathway.* Biochim Biophys Acta, 2009. **1787**(5): p. 414-20.

208. Marchenko, N.D., A. Zaika, and U.M. Moll, *Death signal-induced localization of p53 protein to mitochondria. A potential role in apoptotic signaling.* J Biol Chem, 2000. **275**(21): p. 16202-12.

209. Scherz-Shouval, R., H. Weidberg, C. Gonen, S. Wilder, Z. Elazar, and M. Oren, *p53-dependent regulation of autophagy protein LC3 supports cancer cell survival under prolonged starvation.* Proc Natl Acad Sci U S A, 2010. **107**(43): p. 18511-6.

210. Graeber, T.G., J.F. Peterson, M. Tsai, K. Monica, A.J. Fornace, Jr., and A.J. Giaccia, *Hypoxia induces accumulation of p53 protein, but activation of a G1-phase checkpoint by low-oxygen conditions is independent of p53 status.* Mol Cell Biol, 1994. **14**(9): p. 6264-77.

211. Chen, B., M.S. Longtine, Y. Sadovsky, and D.M. Nelson, *Hypoxia downregulates p53 but induces apoptosis and enhances expression of BAD in cultures of human syncytiotrophoblasts.* Am J Physiol Cell Physiol, 2010. **299**(5): p. C968-76.

212. Pan, Y., P.R. Oprysko, A.M. Asham, C.J. Koch, and M.C. Simon, *p53 cannot be induced by hypoxia alone but responds to the hypoxic microenvironment.* Oncogene, 2004. **23**(29): p. 4975-83.

213. Alarcon, R., C. Koumenis, R.K. Geyer, C.G. Maki, and A.J. Giaccia, *Hypoxia induces p53 accumulation through MDM2 down-regulation and inhibition of E6-mediated degradation.* Cancer Res, 1999. **59**(24): p. 6046-51.

214. Rodriguez, J., A. Herrero, S. Li, N. Rauch, A. Quintanilla, K. Wynne, A. Krstic, J.C. Acosta, C. Taylor, S. Schlisio, and A. von Kriegsheim, *PHD3 Regulates p53 Protein Stability by Hydroxylating Proline 359.* Cell Rep, 2018. **24**(5): p. 1316-1329.

215. Shweiki, D., A. Itin, D. Soffer, and E. Keshet, *Vascular endothelial growth factor induced by hypoxia may mediate hypoxia-initiated angiogenesis.* Nature, 1992. **359**(6398): p. 843-5.

216. Wang, G.L. and G.L. Semenza, *General involvement of hypoxia-inducible factor 1 in transcriptional response to hypoxia.* Proc Natl Acad Sci U S A, 1993. **90**(9): p. 4304-8.

217. Obrig, T.G., W.J. Culp, W.L. McKeehan, and B. Hardesty, *The mechanism by which cycloheximide and related glutarimide antibiotics inhibit peptide synthesis on reticulocyte ribosomes.* J Biol Chem, 1971. **246**(1): p. 174-81.

218. Lee, D.H. and A.L. Goldberg, *Proteasome inhibitors: valuable new tools for cell biologists.* Trends Cell Biol, 1998. **8**(10): p. 397-403.

References

219. Jackson, M.P. and E.W. Hewitt, *Cellular proteostasis: degradation of misfolded proteins by lysosomes.* Essays Biochem, 2016. **60**(2): p. 173-180.

220. Huber, L.A. and D. Teis, *Lysosomal signaling in control of degradation pathways.* Curr Opin Cell Biol, 2016. **39**: p. 8-14.

221. Tawa, N.E., Jr., R. Odessey, and A.L. Goldberg, *Inhibitors of the proteasome reduce the accelerated proteolysis in atrophying rat skeletal muscles.* J Clin Invest, 1997. **100**(1): p. 197-203.

222. Lee, D.H. and A.L. Goldberg, *Proteasome inhibitors cause induction of heat shock proteins and trehalose, which together confer thermotolerance in Saccharomyces cerevisiae.* Mol Cell Biol, 1998. **18**(1): p. 30-8.

223. Klionsky, D.J., K. Abdelmohsen, A. Abe, M.J. Abedin, H. Abeliovich, A. Acevedo Arozena, H. Adachi, C.M. Adams, P.D. Adams, K. Adeli, et al., *Guidelines for the use and interpretation of assays for monitoring autophagy (3rd edition).* Autophagy, 2016. **12**(1): p. 1-222.

224. Yucel-Lindberg, T., H. Jansson, and H. Glaumann, *Proteolysis in isolated autophagic vacuoles from the rat pancreas. Effects of chloroquine administration.* Virchows Arch B Cell Pathol Incl Mol Pathol, 1991. **61**(2): p. 141-5.

225. Mauvezin, C. and T.P. Neufeld, *Bafilomycin A1 disrupts autophagic flux by inhibiting both V-ATPase-dependent acidification and Ca-P60A/SERCA-dependent autophagosome-lysosome fusion.* Autophagy, 2015. **11**(8): p. 1437-8.

226. Mauvezin, C., P. Nagy, G. Juhasz, and T.P. Neufeld, *Autophagosome-lysosome fusion is independent of V-ATPase-mediated acidification.* Nat Commun, 2015. **6**: p. 7007.

227. Yamamoto, A., Y. Tagawa, T. Yoshimori, Y. Moriyama, R. Masaki, and Y. Tashiro, *Bafilomycin A1 prevents maturation of autophagic vacuoles by inhibiting fusion between autophagosomes and lysosomes in rat hepatoma cell line, H-4-II-E cells.* Cell Struct Funct, 1998. **23**(1): p. 33-42.

228. Bjorkoy, G., T. Lamark, and T. Johansen, *p62/SQSTM1: a missing link between protein aggregates and the autophagy machinery.* Autophagy, 2006. **2**(2): p. 138-9.

229. Bjorkoy, G., T. Lamark, A. Brech, H. Outzen, M. Perander, A. Overvatn, H. Stenmark, and T. Johansen, *p62/SQSTM1 forms protein aggregates degraded by autophagy and has a protective effect on huntingtin-induced cell death.* J Cell Biol, 2005. **171**(4): p. 603-14.

230. Mizushima, N., H. Sugita, T. Yoshimori, and Y. Ohsumi, *A new protein conjugation system in human. The counterpart of the yeast Apg12p conjugation system essential for autophagy.* J Biol Chem, 1998. **273**(51): p. 33889-92.

231. Mizushima, N., T. Noda, T. Yoshimori, Y. Tanaka, T. Ishii, M.D. George, D.J. Klionsky, M. Ohsumi, and Y. Ohsumi, *A protein conjugation system essential for autophagy.* Nature, 1998. **395**(6700): p. 395-8.

232. Suzuki, K., T. Kirisako, Y. Kamada, N. Mizushima, T. Noda, and Y. Ohsumi, *The pre-autophagosomal structure organized by concerted functions of APG genes is essential for autophagosome formation.* EMBO J, 2001. **20**(21): p. 5971-81.

233. Goodwin, E.C., E. Yang, C.J. Lee, H.W. Lee, D. DiMaio, and E.S. Hwang, *Rapid induction of senescence in human cervical carcinoma cells.* Proc Natl Acad Sci U S A, 2000. **97**(20): p. 10978-83.

234. Campisi, J., *Aging, cellular senescence, and cancer.* Annu Rev Physiol, 2013. **75**: p. 685-705.

235. Horner, S.M., R.A. DeFilippis, L. Manuelidis, and D. DiMaio, *Repression of the human papillomavirus E6 gene initiates p53-dependent, telomerase-independent senescence and apoptosis in HeLa cervical carcinoma cells.* J Virol, 2004. **78**(8): p. 4063-73.

236. DeFilippis, R.A., E.C. Goodwin, L. Wu, and D. DiMaio, *Endogenous human papillomavirus E6 and E7 proteins differentially regulate proliferation, senescence, and apoptosis in HeLa cervical carcinoma cells.* J Virol, 2003. **77**(2): p. 1551-63.

237. Dimri, G.P., X. Lee, G. Basile, M. Acosta, G. Scott, C. Roskelley, E.E. Medrano, M. Linskens, I. Rubelj, O. Pereira-Smith, and et al., *A biomarker that identifies senescent human cells in culture and in aging skin in vivo.* Proc Natl Acad Sci U S A, 1995. **92**(20): p. 9363-7.

238. de Stanchina, E., E. Querido, M. Narita, R.V. Davuluri, P.P. Pandolfi, G. Ferbeyre, and S.W. Lowe, *PML is a direct p53 target that modulates p53 effector functions.* Mol Cell, 2004. **13**(4): p. 523-35.

239. Kelley, K.D., K.R. Miller, A. Todd, A.R. Kelley, R. Tuttle, and S.J. Berberich, *YPEL3, a p53-regulated gene that induces cellular senescence.* Cancer Res, 2010. **70**(9): p. 3566-75.

240. Warboys, C.M., A. de Luca, N. Amini, L. Luong, H. Duckles, S. Hsiao, A. White, S. Biswas, R. Khamis, C.K. Chong, W.M. Cheung, S.J. Sherwin, M.R. Bennett, J. Gil, J.C. Mason, D.O. Haskard, and P.C. Evans, *Disturbed flow promotes endothelial senescence via a p53-dependent pathway.* Arterioscler Thromb Vasc Biol, 2014. **34**(5): p. 985-95.

References

241. Ferraro, E., M.G. Pesaresi, D. De Zio, M.T. Cencioni, A. Gortat, M. Cozzolino, L. Berghella, A.M. Salvatore, B. Oettinghaus, L. Scorrano, E. Perez-Paya, and F. Cecconi, *Apaf1 plays a pro-survival role by regulating centrosome morphology and function.* J Cell Sci, 2011. **124**(Pt 20): p. 3450-63.

242. Boulares, A.H., A.G. Yakovlev, V. Ivanova, B.A. Stoica, G. Wang, S. Iyer, and M. Smulson, *Role of poly(ADP-ribose) polymerase (PARP) cleavage in apoptosis. Caspase 3-resistant PARP mutant increases rates of apoptosis in transfected cells.* J Biol Chem, 1999. **274**(33): p. 22932-40.

243. Soldani, C. and A.I. Scovassi, *Poly(ADP-ribose) polymerase-1 cleavage during apoptosis: an update.* Apoptosis, 2002. **7**(4): p. 321-8.

244. Qian, Y. and X. Chen, *Tumor suppression by p53: making cells senescent.* Histol Histopathol, 2010. **25**(4): p. 515-26.

245. Collado, M., J. Gil, A. Efeyan, C. Guerra, A.J. Schuhmacher, M. Barradas, A. Benguria, A. Zaballos, J.M. Flores, M. Barbacid, D. Beach, and M. Serrano, *Tumour biology: senescence in premalignant tumours.* Nature, 2005. **436**(7051): p. 642.

246. Noda, A., Y. Ning, S.F. Venable, O.M. Pereira-Smith, and J.R. Smith, *Cloning of senescent cell-derived inhibitors of DNA synthesis using an expression screen.* Exp Cell Res, 1994. **211**(1): p. 90-8.

247. Pearson, M., R. Carbone, C. Sebastiani, M. Cioce, M. Fagioli, S. Saito, Y. Higashimoto, E. Appella, S. Minucci, P.P. Pandolfi, and P.G. Pelicci, *PML regulates p53 acetylation and premature senescence induced by oncogenic Ras.* Nature, 2000. **406**(6792): p. 207-10.

248. Ferbeyre, G., E. de Stanchina, E. Querido, N. Baptiste, C. Prives, and S.W. Lowe, *PML is induced by oncogenic ras and promotes premature senescence.* Genes Dev, 2000. **14**(16): p. 2015-27.

249. Mu, X.C. and P.J. Higgins, *Differential growth state-dependent regulation of plasminogen activator inhibitor type-1 expression in senescent IMR-90 human diploid fibroblasts.* J Cell Physiol, 1995. **165**(3): p. 647-57.

250. Vernier, M., V. Bourdeau, M.F. Gaumont-Leclerc, O. Moiseeva, V. Begin, F. Saad, A.M. Mes-Masson, and G. Ferbeyre, *Regulation of E2Fs and senescence by PML nuclear bodies.* Genes Dev, 2011. **25**(1): p. 41-50.

251. Kim, Y.Y., H.J. Jee, J.H. Um, Y.M. Kim, S.S. Bae, and J. Yun, *Cooperation between p21 and Akt is required for p53-dependent cellular senescence.* Aging Cell, 2017. **16**(5): p. 1094-1103.

252. Qian, Y. and X. Chen, *Senescence regulation by the p53 protein family.* Methods Mol Biol, 2013. **965**: p. 37-61.

253. Crighton, D., S. Wilkinson, J. O'Prey, N. Syed, P. Smith, P.R. Harrison, M. Gasco, O. Garrone, T. Crook, and K.M. Ryan, *DRAM, a p53-induced modulator of autophagy, is critical for apoptosis.* Cell, 2006. **126**(1): p. 121-34.

254. Boyd, J.M., S. Malstrom, T. Subramanian, L.K. Venkatesh, U. Schaeper, B. Elangovan, C. D'Sa-Eipper, and G. Chinnadurai, *Adenovirus E1B 19 kDa and Bcl-2 proteins interact with a common set of cellular proteins.* Cell, 1994. **79**(2): p. 341-51.

255. Chen, G., R. Ray, D. Dubik, L. Shi, J. Cizeau, R.C. Bleackley, S. Saxena, R.D. Gietz, and A.H. Greenberg, *The E1B 19K/Bcl-2-binding protein Nip3 is a dimeric mitochondrial protein that activates apoptosis.* J Exp Med, 1997. **186**(12): p. 1975-83.

256. Yasuda, M., P. Theodorakis, T. Subramanian, and G. Chinnadurai, *Adenovirus E1B-19K/BCL-2 interacting protein BNIP3 contains a BH3 domain and a mitochondrial targeting sequence.* J Biol Chem, 1998. **273**(20): p. 12415-21.

257. Tracy, K., B.C. Dibling, B.T. Spike, J.R. Knabb, P. Schumacker, and K.F. Macleod, *BNIP3 is an RB/E2F target gene required for hypoxia-induced autophagy.* Mol Cell Biol, 2007. **27**(17): p. 6229-42.

258. Quinsay, M.N., R.L. Thomas, Y. Lee, and A.B. Gustafsson, *Bnip3-mediated mitochondrial autophagy is independent of the mitochondrial permeability transition pore.* Autophagy, 2010. **6**(7): p. 855-62.

259. Jen, K.Y. and V.G. Cheung, *Identification of novel p53 target genes in ionizing radiation response.* Cancer Res, 2005. **65**(17): p. 7666-73.

260. Green, D.R. and J.E. Chipuk, *p53 and metabolism: Inside the TIGAR.* Cell, 2006. **126**(1): p. 30-2.

261. Madan, E., R. Gogna, M. Bhatt, U. Pati, P. Kuppusamy, and A.A. Mahdi, *Regulation of glucose metabolism by p53: emerging new roles for the tumor suppressor.* Oncotarget, 2011. **2**(12): p. 948-57.

262. Lee, P., K.H. Vousden, and E.C. Cheung, *TIGAR, TIGAR, burning bright.* Cancer Metab, 2014. **2**(1): p. 1.

263. Ye, L., X. Zhao, J. Lu, G. Qian, J.C. Zheng, and S. Ge, *Knockdown of TIGAR by RNA interference induces apoptosis and autophagy in HepG2 hepatocellular carcinoma cells.* Biochem Biophys Res Commun, 2013. **437**(2): p. 300-6.

264. Bensaad, K., E.C. Cheung, and K.H. Vousden, *Modulation of intracellular ROS levels by TIGAR controls autophagy.* EMBO J, 2009. **28**(19): p. 3015-26.

265. Wanka, C., J.P. Steinbach, and J. Rieger, *Tp53-induced glycolysis and apoptosis regulator (TIGAR) protects glioma cells from starvation-induced cell death by up-regulating respiration and improving cellular redox homeostasis.* J Biol Chem, 2012. **287**(40): p. 33436-46.

266. Shimizu, T., E. Sugihara, S. Yamaguchi-Iwai, S. Tamaki, Y. Koyama, W. Kamel, A. Ueki, T. Ishikawa, T. Chiyoda, S. Osuka, N. Onishi, H. Ikeda, J. Kamei, K. Matsuo, Y. Fukuchi, T. Nagai, J. Toguchida, Y. Toyama, A. Muto, and H. Saya, *IGF2 preserves osteosarcoma cell survival by creating an autophagic state of dormancy that protects cells against chemotherapeutic stress.* Cancer Res, 2014. **74**(22): p. 6531-41.

267. Chaterjee, M. and K.L. van Golen, *Breast cancer stem cells survive periods of farnesyl-transferase inhibitor-induced dormancy by undergoing autophagy.* Bone Marrow Res, 2011. **2011**: p. 362938.

268. Garcia-Prat, L., M. Martinez-Vicente, E. Perdiguero, L. Ortet, J. Rodriguez-Ubreva, E. Rebollo, V. Ruiz-Bonilla, S. Gutarra, E. Ballestar, A.L. Serrano, M. Sandri, and P. Munoz-Canoves, *Autophagy maintains stemness by preventing senescence.* Nature, 2016. **529**(7584): p. 37-42.

269. Ho, T.T., M.R. Warr, E.R. Adelman, O.M. Lansinger, J. Flach, E.V. Verovskaya, M.E. Figueroa, and E. Passegue, *Autophagy maintains the metabolism and function of young and old stem cells.* Nature, 2017. **543**(7644): p. 205-210.

270. Fu, Z., D. Chen, H. Cheng, and F. Wang, *Hypoxia-inducible factor-1alpha protects cervical carcinoma cells from apoptosis induced by radiation via modulation of vascular endothelial growth factor and p53 under hypoxia.* Med Sci Monit, 2015. **21**: p. 318-25.

271. Brown, J.M., *Evidence for acutely hypoxic cells in mouse tumours, and a possible mechanism of reoxygenation.* Br J Radiol, 1979. **52**(620): p. 650-6.

272. Chaplin, D.J., R.E. Durand, and P.L. Olive, *Acute hypoxia in tumors: implications for modifiers of radiation effects.* Int J Radiat Oncol Biol Phys, 1986. **12**(8): p. 1279-82.

273. Chaplin, D.J., P.L. Olive, and R.E. Durand, *Intermittent blood flow in a murine tumor: radiobiological effects.* Cancer Res, 1987. **47**(2): p. 597-601.

274. Bayer, C., K. Shi, S.T. Astner, C.A. Maftei, and P. Vaupel, *Acute versus chronic hypoxia: why a simplified classification is simply not enough.* Int J Radiat Oncol Biol Phys, 2011. **80**(4): p. 965-8.

275. Bayer, C. and P. Vaupel, *Acute versus chronic hypoxia in tumors: Controversial data concerning time frames and biological consequences.* Strahlenther Onkol, 2012. **188**(7): p. 616-27.

276. Meissner, J.D., *Nucleotide sequences and further characterization of human papillomavirus DNA present in the CaSki, SiHa and HeLa cervical carcinoma cell lines.* J Gen Virol, 1999. **80 (Pt 7)**: p. 1725-33.

277. Van Tine, B.A., J.C. Kappes, N.S. Banerjee, J. Knops, L. Lai, R.D. Steenbergen, C.L. Meijer, P.J. Snijders, P. Chatis, T.R. Broker, P.T. Moen, Jr., and L.T. Chow, *Clonal selection for transcriptionally active viral oncogenes during progression to cancer.* J Virol, 2004. **78**(20): p. 11172-86.

278. Ajiro, M. and Z.M. Zheng, *E6^E7, a novel splice isoform protein of human papillomavirus 16, stabilizes viral E6 and E7 oncoproteins via HSP90 and GRP78.* MBio, 2015. **6**(1): p. e02068-14.

279. Yeung, S.J., J. Pan, and M.H. Lee, *Roles of p53, MYC and HIF-1 in regulating glycolysis - the seventh hallmark of cancer.* Cell Mol Life Sci, 2008. **65**(24): p. 3981-99.

280. Wang, Y., R.I. Pakunlu, W. Tsao, V. Pozharov, and T. Minko, *Bimodal effect of hypoxia in cancer: role of hypoxia inducible factor in apoptosis.* Mol Pharm, 2004. **1**(2): p. 156-65.

281. Galban, S., J.L. Martindale, K. Mazan-Mamczarz, I. Lopez de Silanes, J. Fan, W. Wang, J. Decker, and M. Gorospe, *Influence of the RNA-binding protein HuR in pVHL-regulated p53 expression in renal carcinoma cells.* Mol Cell Biol, 2003. **23**(20): p. 7083-95.

282. Lee, S.G., H. Lee, and H.M. Rho, *Transcriptional repression of the human p53 gene by cobalt chloride mimicking hypoxia.* FEBS Lett, 2001. **507**(3): p. 259-63.

283. Hengstermann, A., L.K. Linares, A. Ciechanover, N.J. Whitaker, and M. Scheffner, *Complete switch from Mdm2 to human papillomavirus E6-mediated degradation of p53 in cervical cancer cells.* Proc Natl Acad Sci U S A, 2001. **98**(3): p. 1218-23.

284. Vassilev, L.T., B.T. Vu, B. Graves, D. Carvajal, F. Podlaski, Z. Filipovic, N. Kong, U. Kammlott, C. Lukacs, C. Klein, N. Fotouhi, and E.A. Liu, *In vivo activation of the p53 pathway by small-molecule antagonists of MDM2.* Science, 2004. **303**(5659): p. 844-8.

285. Vakifahmetoglu-Norberg, H., M. Kim, H.G. Xia, M.P. Iwanicki, D. Ofengeim, J.L. Coloff, L. Pan, T.A. Ince, G. Kroemer, J.S. Brugge, and J. Yuan, *Chaperone-mediated autophagy degrades mutant p53.* Genes Dev, 2013. **27**(15): p. 1718-30.

286.   Talis, A.L., J.M. Huibregtse, and P.M. Howley, *The role of E6AP in the regulation of p53 protein levels in human papillomavirus (HPV)-positive and HPV-negative cells.* J Biol Chem, 1998. **273**(11): p. 6439-45.

287.   Scheffner, M., B.A. Werness, J.M. Huibregtse, A.J. Levine, and P.M. Howley, *The E6 oncoprotein encoded by human papillomavirus types 16 and 18 promotes the degradation of p53.* Cell, 1990. **63**(6): p. 1129-36.

288.   Gogna, R., E. Madan, P. Kuppusamy, and U. Pati, *Chaperoning of mutant p53 protein by wild-type p53 protein causes hypoxic tumor regression.* J Biol Chem, 2012. **287**(4): p. 2907-14.

289.   Puca, R., L. Nardinocchi, D. Givol, and G. D'Orazi, *Regulation of p53 activity by HIPK2: molecular mechanisms and therapeutical implications in human cancer cells.* Oncogene, 2010. **29**(31): p. 4378-87.

290.   Tripathi, V., A. Ali, R. Bhat, and U. Pati, *CHIP chaperones wild type p53 tumor suppressor protein.* J Biol Chem, 2007. **282**(39): p. 28441-54.

291.   Walerych, D., M.B. Olszewski, M. Gutkowska, A. Helwak, M. Zylicz, and A. Zylicz, *Hsp70 molecular chaperones are required to support p53 tumor suppressor activity under stress conditions.* Oncogene, 2009. **28**(48): p. 4284-94.

292.   Faivre, S., G. Kroemer, and E. Raymond, *Current development of mTOR inhibitors as anticancer agents.* Nat Rev Drug Discov, 2006. **5**(8): p. 671-88.

293.   Fabbro, M. and B.R. Henderson, *Regulation of tumor suppressors by nuclear-cytoplasmic shuttling.* Exp Cell Res, 2003. **282**(2): p. 59-69.

294.   Freedman, D.A. and A.J. Levine, *Nuclear export is required for degradation of endogenous p53 by MDM2 and human papillomavirus E6.* Mol Cell Biol, 1998. **18**(12): p. 7288-93.

295.   Chen, D., M. Li, J. Luo, and W. Gu, *Direct interactions between HIF-1 alpha and Mdm2 modulate p53 function.* J Biol Chem, 2003. **278**(16): p. 13595-8.

296.   Koumenis, C., R. Alarcon, E. Hammond, P. Sutphin, W. Hoffman, M. Murphy, J. Derr, Y. Taya, S.W. Lowe, M. Kastan, and A. Giaccia, *Regulation of p53 by hypoxia: dissociation of transcriptional repression and apoptosis from p53-dependent transactivation.* Mol Cell Biol, 2001. **21**(4): p. 1297-310.

297.   Zhu, Y., X.O. Mao, Y. Sun, Z. Xia, and D.A. Greenberg, *p38 Mitogen-activated protein kinase mediates hypoxic regulation of Mdm2 and p53 in neurons.* J Biol Chem, 2002. **277**(25): p. 22909-14.

298.   Hammond, E.M., N.C. Denko, M.J. Dorie, R.T. Abraham, and A.J. Giaccia, *Hypoxia links ATR and p53 through replication arrest.* Mol Cell Biol, 2002. **22**(6): p. 1834-43.

299.   Hammond, E.M., M.J. Dorie, and A.J. Giaccia, *ATR/ATM targets are phosphorylated by ATR in response to hypoxia and ATM in response to reoxygenation.* J Biol Chem, 2003. **278**(14): p. 12207-13.

300.   Porter, J.R., B.E. Fisher, and E. Batchelor, *p53 Pulses Diversify Target Gene Expression Dynamics in an mRNA Half-Life-Dependent Manner and Delineate Co-regulated Target Gene Subnetworks.* Cell Syst, 2016. **2**(4): p. 272-82.

301.   Melanson, B.D., R. Bose, J.D. Hamill, K.A. Marcellus, E.F. Pan, and B.C. McKay, *The role of mRNA decay in p53-induced gene expression.* RNA, 2011. **17**(12): p. 2222-34.

302.   Hammond, E.M., D.J. Mandell, A. Salim, A.J. Krieg, T.M. Johnson, H.A. Shirazi, L.D. Attardi, and A.J. Giaccia, *Genome-wide analysis of p53 under hypoxic conditions.* Mol Cell Biol, 2006. **26**(9): p. 3492-504.

303.   Fei, P., W. Wang, S.H. Kim, S. Wang, T.F. Burns, J.K. Sax, M. Buzzai, D.T. Dicker, W.G. McKenna, E.J. Bernhard, and W.S. El-Deiry, *Bnip3L is induced by p53 under hypoxia, and its knockdown promotes tumor growth.* Cancer Cell, 2004. **6**(6): p. 597-609.

304.   Liu, T., C. Laurell, G. Selivanova, J. Lundeberg, P. Nilsson, and K.G. Wiman, *Hypoxia induces p53-dependent transactivation and Fas/CD95-dependent apoptosis.* Cell Death Differ, 2007. **14**(3): p. 411-21.

305.   Achison, M. and T.R. Hupp, *Hypoxia attenuates the p53 response to cellular damage.* Oncogene, 2003. **22**(22): p. 3431-40.

306.   Fang, S., J.P. Jensen, R.L. Ludwig, K.H. Vousden, and A.M. Weissman, *Mdm2 is a RING finger-dependent ubiquitin protein ligase for itself and p53.* J Biol Chem, 2000. **275**(12): p. 8945-51.

307.   Saletta, F., Y. Suryo Rahmanto, E. Noulsri, and D.R. Richardson, *Iron chelator-mediated alterations in gene expression: identification of novel iron-regulated molecules that are molecular targets of hypoxia-inducible factor-1 alpha and p53.* Mol Pharmacol, 2010. **77**(3): p. 443-58.

308.   Sansome, C., A. Zaika, N.D. Marchenko, and U.M. Moll, *Hypoxia death stimulus induces translocation of p53 protein to mitochondria. Detection by immunofluorescence on whole cells.* FEBS Lett, 2001. **488**(3): p. 110-5.

309. Koshikawa, N., C. Maejima, K. Miyazaki, A. Nakagawara, and K. Takenaga, *Hypoxia selects for high-metastatic Lewis lung carcinoma cells overexpressing Mcl-1 and exhibiting reduced apoptotic potential in solid tumors.* Oncogene, 2006. **25**(6): p. 917-28.

310. Bristow, R.G. and R.P. Hill, *Hypoxia and metabolism. Hypoxia, DNA repair and genetic instability.* Nat Rev Cancer, 2008. **8**(3): p. 180-92.

311. Gardner, L.B., Q. Li, M.S. Park, W.M. Flanagan, G.L. Semenza, and C.V. Dang, *Hypoxia inhibits G1/S transition through regulation of p27 expression.* J Biol Chem, 2001. **276**(11): p. 7919-26.

312. Sermeus, A. and C. Michiels, *Reciprocal influence of the p53 and the hypoxic pathways.* Cell Death Dis, 2011. **2**: p. e164.

313. Bencokova, Z., M.R. Kaufmann, I.M. Pires, P.S. Lecane, A.J. Giaccia, and E.M. Hammond, *ATM activation and signaling under hypoxic conditions.* Mol Cell Biol, 2009. **29**(2): p. 526-37.

314. Jiang, H.Y., L. Jiang, and R.C. Wek, *The eukaryotic initiation factor-2 kinase pathway facilitates differential GADD45a expression in response to environmental stress.* J Biol Chem, 2007. **282**(6): p. 3755-65.

315. Blais, J.D., V. Filipenko, M. Bi, H.P. Harding, D. Ron, C. Koumenis, B.G. Wouters, and J.C. Bell, *Activating transcription factor 4 is translationally regulated by hypoxic stress.* Mol Cell Biol, 2004. **24**(17): p. 7469-82.

316. Rzymski, T., M. Milani, L. Pike, F. Buffa, H.R. Mellor, L. Winchester, I. Pires, E. Hammond, I. Ragoussis, and A.L. Harris, *Regulation of autophagy by ATF4 in response to severe hypoxia.* Oncogene, 2010. **29**(31): p. 4424-35.

317. Goda, N., H.E. Ryan, B. Khadivi, W. McNulty, R.C. Rickert, and R.S. Johnson, *Hypoxia-inducible factor 1alpha is essential for cell cycle arrest during hypoxia.* Mol Cell Biol, 2003. **23**(1): p. 359-69.

318. Hammond, E.M., S.L. Green, and A.J. Giaccia, *Comparison of hypoxia-induced replication arrest with hydroxyurea and aphidicolin-induced arrest.* Mutat Res, 2003. **532**(1-2): p. 205-13.

319. Pires, I.M., Z. Bencokova, M. Milani, L.K. Folkes, J.L. Li, M.R. Stratford, A.L. Harris, and E.M. Hammond, *Effects of acute versus chronic hypoxia on DNA damage responses and genomic instability.* Cancer Res, 2010. **70**(3): p. 925-35.

320. Purvis, J.E., K.W. Karhohs, C. Mock, E. Batchelor, A. Loewer, and G. Lahav, *p53 dynamics control cell fate.* Science, 2012. **336**(6087): p. 1440-4.

321. Feng, Z. and A.J. Levine, *The regulation of energy metabolism and the IGF-1/mTOR pathways by the p53 protein.* Trends Cell Biol, 2010. **20**(7): p. 427-34.

322. Levine, B. and J. Abrams, *p53: The Janus of autophagy?* Nat Cell Biol, 2008. **10**(6): p. 637-9.

323. Kabeya, Y., N. Mizushima, T. Ueno, A. Yamamoto, T. Kirisako, T. Noda, E. Kominami, Y. Ohsumi, and T. Yoshimori, *LC3, a mammalian homologue of yeast Apg8p, is localized in autophagosome membranes after processing.* EMBO J, 2000. **19**(21): p. 5720-8.

324. Stockert, J.C., R.W. Horobin, L.L. Colombo, and A. Blazquez-Castro, *Tetrazolium salts and formazan products in Cell Biology: Viability assessment, fluorescence imaging, and labeling perspectives.* Acta Histochem, 2018. **120**(3): p. 159-167.

325. Mosmann, T., *Rapid colorimetric assay for cellular growth and survival: application to proliferation and cytotoxicity assays.* J Immunol Methods, 1983. **65**(1-2): p. 55-63.

326. Berridge, M.V. and A.S. Tan, *Characterization of the cellular reduction of 3-(4,5-dimethylthiazol-2-yl)-2,5-diphenyltetrazolium bromide (MTT): subcellular localization, substrate dependence, and involvement of mitochondrial electron transport in MTT reduction.* Arch Biochem Biophys, 1993. **303**(2): p. 474-82.

327. Guo, K., G. Searfoss, D. Krolikowski, M. Pagnoni, C. Franks, K. Clark, K.T. Yu, M. Jaye, and Y. Ivashchenko, *Hypoxia induces the expression of the pro-apoptotic gene BNIP3.* Cell Death Differ, 2001. **8**(4): p. 367-76.

328. Sowter, H.M., P.J. Ratcliffe, P. Watson, A.H. Greenberg, and A.L. Harris, *HIF-1-dependent regulation of hypoxic induction of the cell death factors BNIP3 and NIX in human tumors.* Cancer Res, 2001. **61**(18): p. 6669-73.

329. Schmid, T., J. Zhou, R. Kohl, and B. Brune, *p300 relieves p53-evoked transcriptional repression of hypoxia-inducible factor-1 (HIF-1).* Biochem J, 2004. **380**(Pt 1): p. 289-95.

330. Blagosklonny, M.V., W.G. An, L.Y. Romanova, J. Trepel, T. Fojo, and L. Neckers, *p53 inhibits hypoxia-inducible factor-stimulated transcription.* J Biol Chem, 1998. **273**(20): p. 11995-8.

331. Hubert, A., S. Paris, J.P. Piret, N. Ninane, M. Raes, and C. Michiels, *Casein kinase 2 inhibition decreases hypoxia-inducible factor-1 activity under hypoxia through elevated p53 protein level.* J Cell Sci, 2006. **119**(Pt 16): p. 3351-62.

332. Chi, A.Y., G.B. Waypa, P.T. Mungai, and P.T. Schumacker, *Prolonged hypoxia increases ROS signaling and RhoA activation in pulmonary artery smooth muscle and endothelial cells.* Antioxid Redox Signal, 2010. **12**(5): p. 603-10.

333. Crighton, D., S. Wilkinson, and K.M. Ryan, *DRAM links autophagy to p53 and programmed cell death.* Autophagy, 2007. **3**(1): p. 72-4.

334. Meley, D., C. Bauvy, J.H. Houben-Weerts, P.F. Dubbelhuis, M.T. Helmond, P. Codogno, and A.J. Meijer, *AMP-activated protein kinase and the regulation of autophagic proteolysis.* J Biol Chem, 2006. **281**(46): p. 34870-9.

335. Hardie, D.G., *The AMP-activated protein kinase pathway--new players upstream and downstream.* J Cell Sci, 2004. **117**(Pt 23): p. 5479-87.

336. Nardella, C., J.G. Clohessy, A. Alimonti, and P.P. Pandolfi, *Pro-senescence therapy for cancer treatment.* Nat Rev Cancer, 2011. **11**(7): p. 503-11.

337. Ewald, J.A., J.A. Desotelle, G. Wilding, and D.F. Jarrard, *Therapy-induced senescence in cancer.* J Natl Cancer Inst, 2010. **102**(20): p. 1536-46.

338. Lee, B.Y., J.A. Han, J.S. Im, A. Morrone, K. Johung, E.C. Goodwin, W.J. Kleijer, D. DiMaio, and E.S. Hwang, *Senescence-associated beta-galactosidase is lysosomal beta-galactosidase.* Aging Cell, 2006. **5**(2): p. 187-95.

339. Kurz, D.J., S. Decary, Y. Hong, and J.D. Erusalimsky, *Senescence-associated (beta)-galactosidase reflects an increase in lysosomal mass during replicative ageing of human endothelial cells.* J Cell Sci, 2000. **113 (Pt 20)**: p. 3613-22.

340. Le Gall, J.Y., T.D. Khoi, D. Glaise, A. Le treut, P. Brissot, and A. Guillouzo, *Lysosomal enzyme activities during ageing of adult human liver cell lines.* Mech Ageing Dev, 1979. **11**(4): p. 287-93.

341. Poole, B. and S. Ohkuma, *Effect of weak bases on the intralysosomal pH in mouse peritoneal macrophages.* J Cell Biol, 1981. **90**(3): p. 665-9.

342. Teplova, V.V., A.A. Tonshin, P.A. Grigoriev, N.E. Saris, and M.S. Salkinoja-Salonen, *Bafilomycin A1 is a potassium ionophore that impairs mitochondrial functions.* J Bioenerg Biomembr, 2007. **39**(4): p. 321-9.

343. Bachtiary, B., M. Schindl, R. Potter, B. Dreier, T.H. Knocke, J.A. Hainfellner, R. Horvat, and P. Birner, *Overexpression of hypoxia-inducible factor 1alpha indicates diminished response to radiotherapy and unfavorable prognosis in patients receiving radical radiotherapy for cervical cancer.* Clin Cancer Res, 2003. **9**(6): p. 2234-40.

344. Birner, P., M. Schindl, A. Obermair, C. Plank, G. Breitenecker, and G. Oberhuber, *Overexpression of hypoxia-inducible factor 1alpha is a marker for an unfavorable prognosis in early-stage invasive cervical cancer.* Cancer Res, 2000. **60**(17): p. 4693-6.

345.   Sorensen, B.S., M. Busk, N. Olthof, E.J. Speel, M.R. Horsman, J. Alsner, and J. Overgaard, *Radiosensitivity and effect of hypoxia in HPV positive head and neck cancer cells.* Radiother Oncol, 2013. **108**(3): p. 500-5.

346.   Pattillo, R.A., R.O. Hussa, M.T. Story, A.C. Ruckert, M.R. Shalaby, and R.F. Mattingly, *Tumor antigen and human chorionic gonadotropin in CaSki cells: a new epidermoid cervical cancer cell line.* Science, 1977. **196**(4297): p. 1456-8.

347.   Friedl, F., I. Kimura, T. Osato, and Y. Ito, *Studies on a new human cell line (SiHa) derived from carcinoma of uterus. I. Its establishment and morphology.* Proc Soc Exp Biol Med, 1970. **135**(2): p. 543-5.

348.   Knowles, B.B., C.C. Howe, and D.P. Aden, *Human hepatocellular carcinoma cell lines secrete the major plasma proteins and hepatitis B surface antigen.* Science, 1980. **209**(4455): p. 497-9.

7. Appendix

7.1 Abbreviations

v/v	Volume percentage
w/v	Weight/volume
aa	Amino acid
AMPK	AMP activated protein kinase
Apaf1	Apoptotic peptidase activating factor 1
APS	Ammonium persulfate
ARNT	Aryl hydrocarbon receptor nuclear translocator
ATF	Activating transcription factor
Atg	Autophagy-related
ATM	Ataxia telangiectasia mutated
ATP	Adenosine triphosphate
ATR	Ataxia telangiectasia and Rad3-related
Baf A1	Bafilomycin A1
Bax	Bcl-2-associated X protein
bHLH	Basic helix-loop-helix
BLAST	Basic Local Alignment Search Tool
BNIP3	BCL2/adenovirus E1B 19 kDa protein-interacting protein 3
bp	Base pairs
BSA	Bovine serum albumin
ca.	circa
cAMP	cyclic adenosine monophosphate
CBP	CREB-binding protein
Cdk	Cyclin-dependent kinase
CDKN1A	Cyclin dependent kinase inhibitor 1A
cDNA	complementary DNA
CHX	Cycloheximide
CIN	Cervical intraepithelial neoplasia
CMA	Chaperone-mediated autophagy
CmPV1	*Chelonia mydas* papillomavirus type 1
CMV	Cytomegalovirus
CO_2	Carbon dioxide
CPV1	Canine papillomavirus type 1
CQ	Chloroquine
CRE	Calcium/cAMP-responsive element
CTD	Carboxy-terminal domain
Cyto	Cytoplasmic
DBD	DNA-binding domain
ddH_2O	doubly distilled water
DDR	DNA damage response
DEPC	Diethyl-pyrocarbonate
DMEM	Dulbecco's modified Eagle's medium
DMF	Dimethylformamide
DMSO	Dimethyl sulfoxide
DNA	Deoxyribonucleic acid
DNA DSBs/SSBs	DNA double- and single-strand breaks
dNTP	Deoxynucleotide triphosphate
dNTPs	Deoxyribonucleotide triphosphates

DRAM1	DNA damage-regulated autophagy modulator 1
DTT	Dithiothreitol
DUBs	Deubiquitinating enzymes
E. coli	*Escherichia coli*
e.g.	*exempli gratia*
E6-AP	E6-associated protein
ECL	Enhanced Chemiluminescence Substrate
EDTA	Ethylenediaminetetraacetic acid
EGTA	Ethylene glycol tetraacetic acid
Erk	Extracellular signal-regulated kinase
et al.	*et alii*
EtOH	Ethanol
FCS	Fetal calf serum
Fig.	Figure
FIH	Factor inhibiting HIF
fw	Forward
GADD45 α	Growth arrest and DNA damage inducible alpha
GAPDH	Glycerinaldehyde 3-phosphate dehydrogenase
Glut 1-4	Glucose transporter types 1-4
HDAC1	Histone deacetylase
HEPES	4-(2-hydroxyethyl)-1-piperazine-ethanesulfonicacid
HIF	Hypoxia-inducible factor
HIPK2	Homeodomain-interacting protein kinase 2
HPV(s)	Human papillomavirus(es)
HRE	Hypoxia response element
HRP	Horseradish peroxidase
HSP	Heat Shock Protein
IgG	Immunoglobuline G
IP	Immunoprecipitation
JNK	c-Jun terminal kinase
K	Lysine
kb	Kilobases
KCl	Potassium chloride
KH_2PO_4	Potassium dihydrogen phosphate
LB	Lysogeny broth
lncRNAs	large intergenic non-coding RNAs
mA	Miliampère
MAP	Mitogen-activated protein
MAPK	Mitogen-activated protein kinase
MDM2	Mouse double minute 2 homolog
$MgCl_2$	Magnesium chloride
$MgSO_4$	Magnesium sulfate
MMP	Matrix Metalloproteinase
MOMP	Mitochondrial outer membrane permeabilization
mRNA	Messenger RNA
mTOR	Mammalian target of rapamycin
n.s.	Not significant
Na_2HPO_4	Sodium dihydrogen phosphate
NaCl	Sodium chloride
NaOH	Sodium hydroxide
NER	Nucleotide excision repair
NES	Nuclear export signal

NF-κB	Nuclear factor kappa B
NLS	Nuclear localization signal
NP-40	Nonidet P-40
Nucl	Nuclear
O_2	Oxygen
ODD	Oxygen-dependent degradation domain
ORF(s)	Open reading frame(s)
ORI	Origin of replication
OXPHOS	Mitochondrial oxidative phosphorylation
p	Probability
pAE	Early polyadenylation site
PAGE	Polyacrylamide gel electrophoresis
pAL	Late polyadenylation site
PARP	Poly (ADP-ribose) polymerase
PBS	Phosphate-buffered saline
PCR	Polymerase chain reaction
PDK	Pyruvate dehydrogenase kinase
PFK	Phosphofructokinase
pg	Picogram
PHD	Prolyl hydroxylase
PI3K	Phosphoinositide 3-kinase
PIPES	Piperazine-N,N'-bis(2-ethanesulfonic acid)
PML	Promyelocytic leukemia protein
PML-NBs	PML nuclear bodies
pmoles	Picomoles
pO_2	Oxygen partial pressure
Poly A	Polyadenylation
ppm1d (WIP1)	Protein phosphatase magnesium-dependent 1 delta (wild-type p53 induced phosphatase 1)
pRb	Retinoblastoma protein
PRD	Proline-rich domain
PTM	Post-translational modification
Puma	p53 upregulated modulator of apoptosis
PV	Papillomavirus
PVDF	Polyvinylidene fluoride
pVHL	Von Hippel Lindau protein
qPCR	Quantitative polymerase chain reaction
rev	Reverse
RNA	Ribonucleic acid
RNAi	RNA interference
ROS	Reactive oxygen species
rpm	rounds per minute
rRNA	ribosomal RNA
RT	Reverse transcription
SA-β-Gal	Senescence-Associated β-Galactosidase
SD	Standard deviations
SDS	Sodium dodecyl sulfate
Ser	Serine
si-16E6/E7	Small interfering RNA against HPV16 E6/E7
si-Atg12	Small interfering RNA against Atg12
si-p62	Small interfering RNA against p62
siRNA	Small interfering RNA

SMYD2	SET and MYND domain-containing protein 2
SUMO	Small Ubiquitin-related Modifier
SV40	Simian Virus 40
T_A	Annealing temperature
Tab.	Table
TAD	Transcriptional activation domain
TAE	Tris acetate EDTA
Taq	*Thermus aquaticus*
TBP	TATA-binding protein
TBS	Tris-buffered saline
TBST	Tris-buffered saline/Tween20
TEMED	Tetramethylethylenediamine
TERT	Telomerase reverse transcriptase
TIGAR	TP53 induced glycolysis regulatory phosphatase
Tris	Tris(hydroxymethyl)-aminomethane
URR	Upstream regulatory region
USP	Ubiquitin specific peptidase
UV	Ultraviolet
VEGF	Vascular endothelial growth factor
VLPs	Virus-like particles
WB	Western Blot
YPEL3	Yippee-like-3

Units

°C	degree Celsius
Da	Dalton
g	gram
h	hour(s)
L	liter
M	molar (mole/L)
m	meter
min	minute(s)
mol	mole
sec	second(s)
V	volt
%	percent

Prefixes

Symbol	Prefix	Factor
k	kilo	10^3
c	centi	10^{-2}
m	milli	10^{-3}
μ	micro	10^{-6}
n	nano	10^{-9}

7.2 Publications and presentations

L. Zhuang, F. Roesl, M. Niebler, *Biphasic regulation of p53 in hypoxic HPV16-positive cancer cells.* manuscript in preparation.

L. Zhuang, F. Roesl, M. Niebler, *Biphasic regulation of p53 in hypoxic HPV16-positive cervical cancer cells.* The N² Event 2019 – From Research to Application, 13-15th November 2019, Berlin, Germany. Poster Presentation.

L. Zhuang, F. Roesl, M. Niebler, *Evasion of hypoxic HPV16-positive cervical cancer cells from senescence via p53 depletion.* Retreat of the DKFZ Research Program "Infection, Inflammation and Cancer", 25-27th March 2019, Schöntal, Germany. Oral Presentation.

L. Zhuang, F. Roesl, M. Niebler, *Regulation of p53 by hypoxia in HPV16-positive cervical cancer cells.* Helmholtz International Graduate School for Cancer Research PhD Poster Presentation, 12-16th November 2018, Heidelberg, Germany. Poster Presentation.

L. Zhuang, F. Roesl, M. Niebler, *Regulation of p53 by hypoxia in HPV16-positive cervical cancer cells.* Helmholtz International Graduate School for Cancer Research PhD Retreat, 18-20th July 2018, Weil der Stadt, Germany. Poster Presentation.

Acknowledgments